THE UNIVERSITY OF CHICAGO

BRIDGING MICRO- AND MACROEVOLUTION IN NEOTROPICAL ARMY ANTS

A DISSERTATION SUBMITTED TO
THE FACULTY OF THE DIVISION OF THE BIOLOGICAL SCIENCES
AND THE PRITZKER SCHOOL OF MEDICINE
IN CANDIDACY FOR THE DEGREE OF
DOCTOR OF PHILOSOPHY

COMMITTEE ON EVOLUTIONARY BIOLOGY

BY
MAX E. WINSTON

CHICAGO, ILLINOIS
JUNE 2017

The decay of familial connection is not why we play the game. We play the game because it suits us, because our developing minds crave the collective knowledge of foreign intellect. We may be island folk, but that cannot prevent our rafts from shoring on fertile soil. We must fight entropy and ignorance with consilience.

Anonymous

Wherever they move, the whole animal world is set in commotion, and every creature tries to get out of their way.

The Naturalist on the River Amazons
Henry Walter Bates

Contents

List of Figures

List of Tables

1 Introduction

Continuity of evolutionary processes across hierarchy and scale is by no means a given, and discordance may be expected, informative, and critical in understanding the scale and reach of different evolutionary mechanisms (Jablonski, 2007). For example, trait variation and covariation are known to impact the response of populations to natural selection on microevolutionary time scales, but their role in shaping long-term macroevolutionary divergence is still unclear (Hunt, 2007). Grasping how and under what circumstances genetic variances and covariances constrain evolution can illustrate the extent to which the classic microevolutionary framework is congruent with macroevolutionary change (Schluter, 1996). Furthermore, exploration of macroevolutionary discontinuities uncoupled from standard microevolutionary variation can inform our knowledge of other important processes, such as the role of hybridization in evolutionary innovation (Abbott et al., 2013; Seehausen, 2004).

Geographic barriers and landscape change have been viewed as the primary drivers of biological diversification to date (Coyne & Orr, 2004; Smith et al., 2014). The accumulation of prezygotic and postzygotic barriers via reproductive isolation during the speciation process is a well-established phenomenon that links the micro- and macroevolutionary paradigms (Coyne & Orr, 2004). Yet, spatiotemporal variation in geographic barriers and uncertainty or low resolution in geological data over broad scales allows for the possibility of alternative driving mechanisms of speciation (Rundle & Nosil, 2005; Stone, 2013). Although the burden of proof for alternative drivers of diversification is often higher, several study systems have demonstrated that ecology can be extremely influential in the generation of new species (Losos & Mahler, 2010; Grant & Grant, 2011; Rundle & Nosil, 2005; McGee et al., 2013; Seehausen, 2006; Schluter & McPhail, 1992). Furthermore, a plethora of work has suggested that developmental plasticity within organisms could be critical to the origin of species differences (West-Eberhard, 2003; West-Eberhard, 2005). This possibility is particularly relevant to the continuity of micro- and macroevolutionary processes, since it implies an important connection between variation at the two scales. Although Neotropical army

ants are a useful study system for all of these mechanisms, the maintenance of adaptive developmental plasticity across species makes them particularly ideal for understanding the contribution of developmental plasticity to macroevolutionary change.

High-throughput sequencing is increasingly being used in both phylogenetic (Cruaud et al., 2013; Eaton & Ree, 2013) and population genetic (Hohenlohe et al., 2011; Novembre et al., 2008) contexts, greatly increasing genetic resolution to answer diverse questions. Although the basic frameworks for understanding these disciplines remain distinct, the increase in new sequencing methods and analyses has provided an analytic bridge to address questions at the nexus of these two evolutionary scales (Eaton, 2014; Pease & Hahn, 2013). Concurrently, morphological variation is central to uniting micro- and macroevolutionary work, as morphology is used heavily in both neontological and paleontological disciplines, with extensive variation and information content across evolutionary scales. Recent advances in the quantification of morphological variation by landmark-based geometric morphometrics have demonstrated the increased power of this higher resolution data (Selz et al., 2013). Utilizing these new methods, my dissertation aims to address four questions regarding the evolution of complex morphological traits at different hierarchical scales in Neotropical army ants:

- What factors have driven diversification in Neotropical army ants?
- Is the structure of morphological variation stable across subspecific and specific lineages?
- How is change in this structure associated with phylogenetic or ecological divergence?
- Does macroevolutionary morphological change occur more frequently in the direction of maximum heritable and/or phenotypic variation of extant lineages?

As heritable morphological variation is the raw material on which natural selection acts, understanding its structure and lability can directly inform the extent to which microevolutionary forces may extend into macroevolutionary time. Over the course of this dissertation,

my work has focused on addressing questions central to both micro- and macroevolutionary paradigms, by exploiting the unique biology of Neotropical army ants with modern scientific methods. Through investigating the cross-section of genomics, geography, and developmental plasticity in Neotropical army ants, my work has aimed at bridging our understanding of evolutionary processes across broad spatial and temporal scales.

2 Background

Study System

Neotropical army ants are keystone predators with broad geographic ranges and hundreds of vertebrate and invertebrate associates (Franks & Fletcher, 1973; Boswell et al., 1998; Schneirla, 1971). Although all *Eciton* species are invertebrate predators, the diet preferences range from strict ant specialists to leaf litter generalists (Powell & Franks, 2006; Schneirla, 1971; Burton & Franks, 1985). An *Eciton* colony is composed of hundreds of thousands of sterile workers, all produced by a single queen, mated multiply to several males (Kronauer, 2009). Within the sterile workers, *Eciton* species contain multiple morphological worker subcastes, which are critical to their efficacy as predators (Franks, 2001). These behaviorally, morphologically, and physiologically distinct subcastes are the result of a conserved, developmentally plastic pathway across ants, which have also been shaped by dietary ecology (Abouheif & Wray, 2002; Powell & Franks, 2006). The documented differences in diet between *Eciton* species define the interactions with their biotic environment and their role in the Neotropical ecosystem, illustrating a diverse clade of ecologically distinct species (Powell & Franks, 2006).

Bridging Micro- and Macroevolutionary Frameworks

Although the dispute concerning punctuated equilibrium and gradualism is a canonical example of the debate between micro- and macroevolution, it is only a kernel in the larger debate of the extent and continuity of evolutionary processes across micro- and macroevolutionary levels (Gould, 2002; Erwin, 2000; Simons, 2002; Jablonski, 2000). The recent acknowledgment that separate processes may be expected across hierarchical scale has focused research efforts and stimulated a plethora of questions about the nature of these processes (Jablonski, 2007). Despite the potential for elucidating the nexus of micro- and macroevolution, much of the continuing work has been divided among disciplines and tended

to focus on the processes at a single scale. While this work is foundational in understanding the different processes, it does not necessarily contribute to understanding their extent, and how they interact, which is especially important when considering documented constraints on microevolutionary selection (Brakefield, 2006).

Studies that have managed to bridge the broad spatial and temporal scales necessary to address the interaction between these evolutionary processes have produced results critical for understanding evolution. Schluter (1996) provided an early link between micro- and macroevolution in demonstrating the repeated tendency for morphological differentiation between species to be biased in the multivariate direction of greatest additive genetic variance (G_{max}). This effect was shown to decay over evolutionary time, but persisted despite the presence of natural selection for millions of years. Renaud et al. (2006) revealed within rodent lineages that the direction of high phenotypic variation was important, but could be overwhelmed by a strong selection regime, making the case that the persistence of genetic constraints may depend greatly on ecological context. Alternative roles of ecology could also be an important consideration in this work, as work in shrew mandibles has suggested evolutionary divergence along axes of stress-induced variation (Badyaev & Foresman, 2000).

In other cases, it is not so clear that influence between evolutionary scales exists at all. For example, studies such as Eroukhmanoff & Svensson (2008) have detected significant evolutionary movement against directions of high phenotypic variation in exceedingly short timescales. Similarly, although the focal scale was limited in scope, population divergence and morphometric integration in the green finch was demonstrated to be against lines of evolutionary least resistance (Merila & Bjorklund, 1999). Despite these contradictory studies, the majority of work has found macroevolutionary change preferentially in the direction of maximal variation (Bégin & Roff, 2004; Marriog & Cheverud, 2001). Negative findings may reflect particular contexts, as several of the studies demonstrating this pattern also showed an important interaction of organismal ecology (Marriog & Cheverud, 2001; Renaud et al., 2006). In perhaps the most rigorous attempt to address this question, Hunt (2007) used a

paleontological approach to examine the directions of high phenotypic variation through deep time. His seminal work demonstrated that phenotypic variation on the microevolutionary scale had a significant influence on macroevolutionary change—fitting Schluter's model of genetic constraints—but that the influence weakened with increasing phylogenetic distance (Schluter, 1996; Hunt, 2007). Despite this rigor, the study was unable to generate molecular data, making the study incapable of testing heritable morphological variation directly.

3 Early and dynamic colonization of Central America drives speciation in Neotropical army ants

Abstract

The emergence of the Isthmus of Panama is one of the most important events in recent geological history, yet its timing and role in fundamental evolutionary processes remain controversial. While the formation of the isthmus was complete around 3 million years ago (Ma), recent studies have suggested prior intercontinental biotic exchange. In particular, the possibility of early intermittent land bridges facilitating colonization constitutes a potential mechanism for speciation and colonization before full closure of the isthmus. To test this hypothesis, we employed genomic methods to study the biogeography of the army ant genus *Eciton*, a group of keystone arthropod predators in Neotropical rainforests. Army ant colonies are unable to disperse across water and are therefore ideally suited to study the biogeographic impact of land bridge formation. Using a reduced representation genome sequencing approach, we show that all strictly Central American lineages of *Eciton* diverged from their respective South American sister lineage between 4 and 7 Ma, significantly prior to the complete closure of the isthmus. Furthermore, three of the lineage pairs form extensive and coincident secondary contact zones in Costa Rica and Nicaragua, with no evidence of gene flow. Such a discrete and repeated biogeographic pattern indicates at least two waves of army ant dispersal into Central America that were separated by significant genetic divergence times. Thus, by integrating phylogenomic, population genomic and geographic evidence, we show that early colonization of Central America across the emerging Isthmus of Panama drove parallel speciation in *Eciton* army ants.

Introduction

Revealing historic change in geographic distributions is critical to understanding the origins and evolutionary dynamics of biodiversity (Jablonski et al., 2006). Range expansion can be

as essential to the origins of regional biota as the speciation process itself, and therefore, proper models testing established biogeographic patterns should consider dispersal along with speciation and extinction (Rull, 2011). Simultaneously, as landscape change has been viewed as the primary driver of biological diversification to date, it is important to recognize that paleogeographic events likely affect evolutionary dynamics in several ways (Coyne & Orr, 2004; Smith et al., 2014). For example, the uplift of the Isthmus of Panama (IP) and consequent closure of the Central American Seaway (CAS) had an unparalleled impact on biodiversity (Simpson, 1980), oceanic currents, and global climate (Haug et al., 2005). Most notably, the IP provided a land bridge between two previously disconnected landmasses, prompting the Great American Biotic Interchange (GABI) (Stehli & Webb, 1985).

As one of the most significant episodes of biological migration, the GABI is integral to decoding evolutionary dynamics of Neotropical and Nearctic biota (Bagley & Johnson, 2014), yet many aspects of the timing and process of isthmus closure remain contentious (Stone, 2013). For example, major differences in salinity and benthic carbon between the Pacific Ocean and the Caribbean Sea arising from 4.2 to 4.7 Ma (millions of years ago) suggest the end of deep water exchange and the CAS (Haug et al., 2001), and the measured shifts in oceanic currents and global climate suggest a full closure of the IP by 3.0—2.5 Ma (Bartoli et al., 2005). Conversely, recent geological discoveries of Panamanian fluvial deposits in South America argue for a closure of the CAS as early as c. 13—15 Ma (Montes et al., 2015). To add to this debate, the most thorough tectonic reconstructions of the region demonstrate the extant volcanic arc beginning to form at c. 12 Ma, with a series of islands clearly above sea level by 6 Ma (Coates et al., 1992). Evidence even shows that the corridors surrounding the Chorotega volcanic front in modern-day Nicaragua and Costa Rica emerged far before full closure, only to be submerged again for millions of years (Gutiérrez-García & Vázquez-Domínguez, 2013). Although there is wide variation in the specific interpretations of this collective body of geological scholarship, the complexity of the emergence of the IP cannot be debated.

Interpretation of the biotic evidence and its relation to the complex geological substrate is perhaps more varied than the geological evidence of the emergence itself. Traditionally, the IP was considered a relatively simplistic land bridge that initiated the GABI after its emergence c. 3 Ma (Marshall et al., 1982). In this view, the isthmus provided the first overland corridor, designating taxa exchanged previous to this date as heralds or island hoppers (Stehli & Webb, 1985). Although the original publications were faunally biased towards mammals, a thorough analysis of Caribbean and Pacific strata containing a multitude of near-shore marine fauna by Coates et al. (1992) strongly bolstered this argument with evidence suggesting a 3.5 Ma divergence date. Yet, the more recent treatment of the GABI in the literature has acknowledged spatial heterogeneity and temporal dynamics inherent to a complex rise of the IP. In fact, several clades–including predatory mammal families such as the Felidae, Mustelidae, and Procyonidae–show early colonization of South America easily pre-dating the traditional timing of the rise of Panama (Woodburne, 2010; Eizirik, 2012). Furthermore, rather than treating the isthmus as a simple land bridge, a few recent studies have increasingly acknowledged the propensity of a complex geological substrate to generate diversity *in situ* through both dispersal and vicariant mechanisms via transient formation and disappearance of land bridges and islands during a transitional period of IP formation (Woodburne, 2010; Bagley & Johnson, 2014). Lastly, and perhaps most strikingly, a reanalysis of hundreds of previous studies assuming a closure of 3 Ma showed that the most significant increase in intercontinental migration was around 8 Ma for several terrestrial clades (Bacon et al., 2015), suggesting that the traditional date of 3 Ma for the first land connection may be too late even for species that can disperse across aquatic barriers. Although these studies highlight variation in the inferred timing of species exchange across the IP, none of them explicitly consider dispersal strategies, which can have a profound effect on migration potential (Ree & Sanmartín, 2009). Taxa that cannot disperse over water are particularly suitable for understanding the biogeographic history of land bridges as they produce fewer false positives for vicariant events (Cowie & Holland, 2006), and are better

indicators for evaluating landscape-driven speciation. We therefore chose a clade of Neotropical army ants to study the temporal and spatial dynamics of speciation across the IP, and to elucidate its complex geographic history.

Army ants of the genus *Eciton* are keystone arthropod predators exerting strong top-down trophic effects in terrestrial ecosystems (Kaspari & O'Donnell, 2003; Kronauer, 2009). Colonies of hundreds of thousands of individuals collectively hunt, kill and transport their prey (Kaspari & Vargo, 1995). Due to this foraging strategy, new colonies can only form through fission, where a mature colony splits into two with each containing a single wingless queen (Kronauer, 2009). Probably because of their massive colony sizes and predatory lifestyle, *Eciton* species have adapted a nomadic life history strategy to avoid local resource depletion (Willson et al., 2011). Although Neotropical army ant colonies cannot disperse over aquatic barriers due to wingless queens and workers that cannot swim or raft, gene flow is maintained by the dispersal of winged males across existing barriers (Berghoff et al., 2008). While male dispersal outperforms that of the queen and the rest of the colony, this male-biased dispersal also has its limits: genetic evidence for landscape effects on dispersal has been found in *Eciton burchellii* (Pérez-Espona et al., 2012; Soare et al., 2014), and simulations have suggested that extinction may occur far before the habitat is fully fragmented (Boswell et al., 1998).

Despite limitations in dispersal capability and range expansion, *Eciton* species assert their ecological dominance across broad geographic ranges in Neotropical rainforests, from Mexico to Argentina (Schneirla, 1971; Watkins, 1976). Previous work on the biogeographic origins of the multiple genera of army ants, including *Eciton*, suggests a Gondwanan origin followed by vicariant speciation resulting from the split of Gondwana into the South American and African continents (Brady, 2003). Given this model and additional geographic evidence, *Eciton* species likely originated in the Amazon (Brady, 2003; Scotese, 2014) and colonized Central America during GABI following the closure of the IP (Stehli & Webb 1985; Hoorn et al., 2010). To tease apart the nature of this colonization process, we present two alternative

models of colonization with explicit predictions, representing alternative interpretations of the geological and biological evidence on the emergence of the IP: The traditional Full Closure Colonization (FCC) model posits a simpler colonization of Central America beginning at full closure of the IP (c. 3 Ma), while the Early Dynamic Colonization (EDC) model posits a much earlier colonization (>3 Ma) across the spatiotemporally complex substrate of the emerging IP. Due to the weak dispersal capability of army ants (Schneirla, 1971; Kronauer, 2009), it is unlikely that colonization occurred before the completion of a single or a series of connected land bridges. This assumption is supported by the absence of Neotropical army ants from all noncontinental Caribbean islands, despite the ample ecological opportunity presented by these habitats (Dunn et al., 2007). Moreover, even with a rich and abundant fossil record in the Dominican amber deposits, no fossil *Eciton* have been found on the islands (Wilson, 1985).

To test these alternative models of colonization across the IP, we generated a large, robust data set using a reduced representation genome sequencing approach, genotyping by sequencing (GBS). From these data, we infer the phylogeny of the genus *Eciton* and elucidate its biogeographic history. In addition to providing increased phylogenomic resolution compared with traditional gene-based methods (Eaton & Ree, 2013), GBS facilitates population genomic analyses, which we leverage here to assess gene flow between distinct army ant lineages to test possible parallel, cryptic speciation. By collecting a large set of geographically distinct specimens for each species, we are able to test the predictions of two distinct colonization models–the FCC and the EDC–in generating observed Neotropical biodiversity.

Materials & Methods

Taxon Sampling

Taxa were selected for sequencing based on three main criteria: (i) broad taxonomic coverage within the New World army ants was required to assess congruence with previous phylogenetic work on Dorylinae (Moreau & Bell, 2013; Brady et al., 2014); (ii) all nine *Eciton* species

that are known from queens and workers were included to account for full taxonomic coverage; and (iii) extensive geographic coverage for all *Eciton* species–many of which (six of nine species) have cosmopolitan Neotropical distributions extending from Mexico to Argentina–was required to study biogeographic patterns and to infer species boundaries. Comprehensive sampling of specimens across the geographic range was particularly important given the many taxonomically recognized and morphologically distinguishable subspecies (Watkins, 1976) (Appendix C1: Table S3). All voucher specimens have been deposited at the Field Museum of Natural History.

GBS library preparation and locus assembly

DNA from all specimens was extracted following a standard protocol for ants (Moreau, 2014). Library preparation for GBS followed a published protocol with a modified size-selection step (Elshire et al., 2011). The restriction enzyme *ApeK1* was chosen for genome digestion based on *in silico* digests of the eight published ant genomes available at the time of study design (Appendix C1: 1, Supporting information), and was later confirmed by an in silico digest and analysis (Appendix C1: SI. 2) on a draft genome of *E. burchellii*. All libraries were size-selected for fragment sizes between 300 and 800 bp to maximize coverage and number of loci (Appendix C1: SI. 1). Finally, three libraries with 50 barcoded samples each were prepared for GBS by this protocol, totalling 150 specimens sent for single-end sequencing on three lanes of the Illumina HiSeq 2000. All sequences have been deposited in GenBank (SRA Accession: SRP072129). *De novo* locus assembly was accomplished using the data pipeline pyRAD (Eaton, 2014). *De novo* locus assembly was a multistep computational process where sequencing reads were sorted and filtered for quality, and then clustered by sequence similarity within and between samples to form genomic loci with a minimum of 10 coverage [$\mu = 20.1x$] (Appendix C1: SI. 3). The final set of genomic loci was then subset by (i) the minimum number of samples for which a locus genotype was available, (ii) the maximum number of individuals with a shared allele in the locus and (iii) the exclusion of

specific taxa, depending on the particular analysis.

Phylogenomic inference

Following quality filtering of the assembled GBS loci, all parsimony-informative loci were concatenated into a single data matrix with pyRAD for phylogenetic inference (Eaton, 2014). This matrix included 135 *Eciton* samples and 11 samples from outgroup genera. Based on previous phylogenetic work in *Dorylinae* (Brady, 2003; Brady et al., 2014), the three *Neivamyrmex* specimens in the data set were set as outgroups for rooting the tree in both maximum likelihood (ML) and Bayesian inference (BI). ML inference was implemented in a Randomized Axelerated Maximum Likelihood with High Performance Computing (RAxML-HPC) pipeline with a GTR-GAMMA model and 100 rapid bootstrap trees (Appendix C1: SI. 4) (Stamatakis, 2006). BI was accomplished using an Exabayes MCMC approach with a GTR-GAMMA model of evolution and a Dirichlet prior (Appendix C1: SI. 4) (Aberer et al., 2014).

Population genomic inference

Because large genomic data sets generated by GBS can lend strong phylogenetic support to populations that may not be truly distinct lineages due to gene flow, we chose to test our findings with population genomic inference. Specifically, gene flow between monophyletic groups as recovered by phylogenetic analyses was tested on a locus-by-locus basis. To manage the variable sample coverage between loci, we chose a modified Wright's F_{ST} estimator (Appendix C1: SI. 5) weighted by sample size that could provide comparable F_{ST} estimates across our loci as defined in Chen et al. (2015).

As nucleotide diversity (π) and sample coverage (n) offer important evidence towards understanding potential gene flow, these statistics were also calculated and incorporated into the analyses, along with allele class, HardyWeinberg chi-squared statistic and minor allele frequency (Chen et al., 2015). As loci with singleton mutations are uninformative with

respect to evaluating gene flow between two putative populations, they were removed from the analysis. Presence of large numbers of fixed loci, especially in loci with high nucleotide diversity and sample coverage, is a strong indicator that there is little to no gene flow between distinct lineages, despite geographic overlap in parapatric ranges. Loci with low nucleotide diversity may show reduced F_{ST} even in fully differentiated species if a novel allele has not spread through one of the species. Due to wide geographic sampling and population structure within the divergent parapatric lineages, distribution of F_{ST} in tested loci may deviate from normal two-population F_{ST} expectations. However, as the deviations would only reduce the sensitivity of our analysis by reducing F_{ST} values, no corrections are necessary to reduce type I error.

Tree dating

Conversion to an ultrametric tree and dating of the Bayesian inference (BI) phylogeny using node calibration was accomplished using the r package *ape* (Paradis et al., 2004; Paradis, 2013). We implemented the chronos function (Paradis et al. 2004), which uses a penalized likelihood approach for estimating absolute rates of molecular evolution, known as nonparametric rate smoothing (NPRS) (Sanderson, 2002). To choose the optimal value for the rate smoothing parameter (λ), we used a twofold cross-validation step using the CV functionality in chronos, first cross-validating with a broad range of rate smoothing parameters ($10^{-6} < \lambda < 10^{6}$), followed by finer resolution cross-validation ($0.1 < \lambda < 2.0$). Once the optimal value was achieved, we leveraged the recent fossil-calibrated phylogeny for all Dorylinae using the 95% confidence interval for the marginal posterior probabilities of several generic nodes to date our tree (Appendix C1: SI. 6) (Brady et al., 2014). Specifically, to test congruence between our inferred phylogeny and that of Brady et al. (2014), we used the marginal posterior probability distribution of the most recent common ancestor (MRCA) of *Eciton* and *Neivamyrmex* for calibration, and marginal posterior probability distributions of the MRCA of *Eciton* and *Nomamyrmex*, *Labidus* and *Cheliomyrmex* for validation (Brady

et al., 2014). To ensure robustness in our results to differing calibrations, we followed the same procedure for the recent family-level dated phylogeny by Moreau & Bell (2013).

Results

Locus assembly

Strict filtering of the demultiplexed Illumina reads for Phred quality, read length and adapter sequence resulted in 441.3 million utilizable reads for clustering across 147 samples, with a mean 3.0 million reads per individual specimen (Appendix C1: SI. 3). Several steps of clustering and quality filtering, including a step for a minimum 10 coverage for each locus at each individual, resulted in a mean of 58,095 loci per specimen. As is expected in reduced representation sequencing, the number of final loci was highly variable among specimens (Appendix C1: SI. 3), which we modelled effectively with several linear models using processing statistics and phylogenetic distance (Appendix C1: SI. 7).

Phylogenomic inference

Maximum likelihood (ML) and Bayesian inference (BI) resulted in congruent phylogenies with perfect statistical support for all but one species-level node within the genus *Eciton*, resolving these relationships within the genus with high confidence (Fig. 1; Appendix C1: SI. 4). Both phylogenies included 135 *Eciton* samples and 11 samples from outgroup genera. The generic-level topology of the tree (*Neivamyrmex*, (*Cheliomyrmex*, (*Labidus*, (*Nomamyrmex*, *Eciton*)))) confirms recent molecular phylogenetic work on Neotropical army ants (Brady, 2003; Brady et al., 2014). Furthermore, all of the nine recognized *Eciton* species (Watkins, 1976) were reciprocally monophyletic, validating current taxonomy (Fig. 1).

Biogeographic inference

Within each *Eciton species*, the phylogenetic signal was completely concordant with biogeography, in that each major monophyletic lineage occupied a distinct geographic area

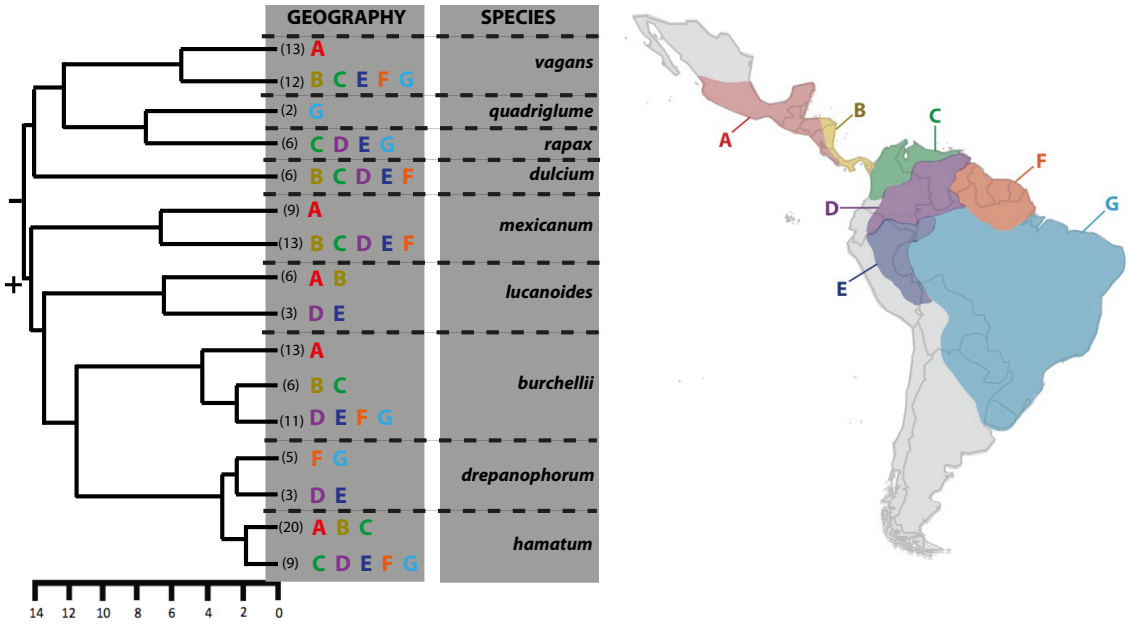

Figure 1: The phylogeny of *Eciton* army ants and the biogeographic areas occupied by distinct lineages. Phylogeny inferred from 146 specimens and 419,804 loci with 6,700,494 distinct nucleotide sites. All nodes on the phylogeny had maximum support from ML bootstrap (BS) and Bayesian posterior probability (BPP) analyses, with one exception (+ = 95/100 BS, + = 0.98 BPP). Numbers in parentheses give the number of samples contained within each monophyletic group, and letters illustrate the biogeographic regions occupied by that group. Scale bar (bottom left) gives absolute timing of divergences in millions of years ago (Ma). Biogeographic areas are adapted from Morrone (2006).

with minimal overlap with the areas of the other major monophyletic lineages from that species (Fig. 1; Fig. 3). Biogeographic areas were adapted from Morrone (2006), where any areas that lacked substantial occurrence data were merged into broader biogeographic areas of a more appropriate resolution. Mapping the occupied biogeographic areas for each sample onto the phylogeny, we found a remarkable amount of geographically coincidental, deep phylogenetic divergence across taxa, particularly around the Isthmus of Panama (Fig. 1; Fig. 3; Appendix C1: SI. 4, SI. 8). Three of the six species that have colonized Central America during the GABI had coincident geographic boundaries between their respective oldest phylogenetically distinct lineages across the Chorotega volcanic front of Costa Rica into Nicaragua and Panama (Fig. 1; Fig. 3). In each case, the Central American lineage corresponded to a previously recognized subspecies (Watkins, 1976). These three species with tightly coincident geographic boundaries–*E. burchellii*, *E. mexicanum* and *E. vagans*– are all known to have extensive secondary contact zones where their respective subspecies occur in parapatry (Fig. 3). The available biogeographic data suggest that this zone, which stretches throughout Costa Rica, Nicaragua and Panama, is 500 miles long and up to 100 miles wide (Dunn et al., 2007). For the fourth species (*E. lucanoides*) that has migrated into Central America, the two oldest lineages also meet at a geographic boundary along the Isthmus of Panama (Fig. 1; Appendix C1: 8, Supporting information). In the fifth species, *E. hamatum*, the two phylogenetically most distinct lineages meet along a geographic break near the junction of the isthmus and South America (Fig. 1; Appendix C1: SI. 8). Lastly, *E. dulcium*, the sixth species that has colonized Central America, lacked distinct and deeply divergent intraspecific lineages (Fig. 1). However, it should be noted that our geographic sampling for this species was limited. In particular, we were not able to include samples from north of the Chorotega volcanic front, although the species is known to extend into this region (Watkins, 1976).

Population genomic inference

To further assess the hypothesis that the three discrete lineages of Central American *Eciton* army ants constitute distinct biological species, we gathered several locus-specific population genetic statistics (Appendix C1: SI. 5). Nucleotide diversity (π), F_{ST} (test and randomized pseudo-null) and sample coverage were calculated for a mean of 29,370 variable loci ($\sigma = 11,327$) from five pairs of distinct lineages associated with the IP, three of which were known to have extensive secondary contact zones in the Chorotega region (Appendix C1: SI. 5). All five lineage pairs had several thousand loci ($\mu = 11,505, \sigma = 5,164$) with the maximum fixation index value ($F_{ST} = 1$) throughout the genome (Appendix C1: 5, Supporting information). Limiting the analysis to variable loci with high nucleotide diversity ($\pi > 0.8$) and high sample coverage ($n > 9$) only increased this proportion, resulting in a mean of 55.0% ($\mu = 4,620, \sigma = 2,015$) that were fixed (Fig. 4; Appendix C1: SI. 5). Finally, genotype assignments were randomized to create a pseudo-null distribution of F_{ST} values to compare to the results for each lineage pair. On average, less than three of the conservative loci were fixed for each lineage pair in the pseudo-null distribution. Therefore, the number of false positives expected by chance is orders of magnitude lower than the observed mean of 4,620 fixed conservative loci across sister lineages, showing that the observed large number of fixed loci cannot be attributed to chance (Appendix C1: SI. 5).

Tree dating

We used a penalized likelihood approach with a twofold cross-validation step for divergence dating (Sanderson, 2002; Paradis et al., 2004), calibrating with the marginal posterior probability for generic nodes from Brady et al. (2014). Specifically, using the most recent common ancestor (MRCA) of Neotropical army ants from Brady et al. (2014) as our fixed prior calibration, we estimated distributions for the MRCA of *Eciton* and the other Neotropical army ant genera for comparison with the remaining prior distributions from the same paper (Appendix C1: SI. 6) (Brady et al., 2014). All of our estimated MRCA ages were within the

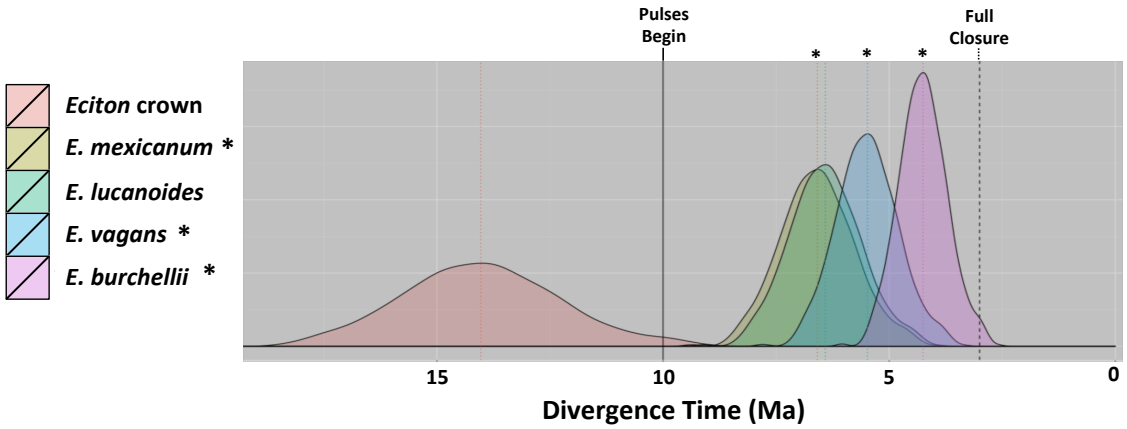

Figure 2: Divergence times for *Eciton* sister lineages across the Isthmus of Panama. Asterisks indicate lineages with geographically coincident species boundaries across Costa Rica, Nicaragua and Panama. Pulses of dispersal across the isthmus might have begun as early as 10 Ma (solid line) according to Bacon et al. (2015), while full closure of the Isthmus of Panama occurred around 3 Ma (black dashed line). All coloured dashed lines and areas represent the mean divergence times and divergence time density distributions estimated for the sister lineage of that colour, respectively.

original confidence intervals of Brady et al. (2014), suggesting general concordance across studies (Brady et al., 2014). Divergence date distributions were estimated for all five pairs of sister lineages across the IP (Fig. 2; Appendix C1: SI. 6). Four of these lineage pairs had divergence dates significantly prior to the full formation of the isthmus and closure of the CAS (*E. burchellii*: 4.3 Ma [98.6% CI $>$ 3 Ma]; *E. lucanoides*: 6.4 Ma [100.0% CI $>$ 3 Ma]; *E. mexicanum*: 6.6 Ma [100.0% CI $>$ 3 Ma]; *E. vagans*: 5.5 Ma [99.9% CI $>$ 3 Ma]). The fifth parapatric lineage pair (*E. hamatum*) diverged 2.3 Ma, shortly after the full formation of the isthmus [98.6% PD $<$ 3 Ma]. Calibration of our phylogeny with the date estimated by Moreau & Bell (2013) for the MRCA of Neotropical army ants yielded similar results, demonstrating that our findings are robust with respect to the precise date chosen for calibration (Appendix C1: SI. 6) (Moreau & Bell, 2013).

Testing alternative colonization models

Testable predictions of colonization models rely heavily on the geological model of isthmus emergence considered. Here, we offer a null (FCC) model and an alternative (EDC) model, including their predictions based on the current state of the controversy in the literature and

its implications for biological diversity. These models and their predictions are described below and summarized in Table 1.

First, we offer the Full Closure Colonization (FCC) model as our null model: traditionally, timing of the full formation of the Isthmus of Panama and closure of the CAS is dated at 3 Ma (Simpson, 1980), and would represent the earliest date for a strictly over land dispersal into Central America. Under this model, we would expect dispersal of Neotropical army ant lineages into Central America to be within the last 3 Ma, with no particular expectation on where geographic range breaks may fall within Central America. Depending on the diversity within a given species group, we would also expect the earliest branching army ant lineages to be South American, and in situ diversification in Central America to be no older than 3 Ma (Table 1).

Second, we test our Early Dynamic Colonization (EDC) model, a model where the complex emergence of Panama acts as a mechanism for speciation on dispersing lineages: more recently, extensive biotic (Woodburne, 2010; Bacon et al., 2015) and abiotic (Gutiérrez-García & Vázquez-Domínguez, 2013; Montes et al., 2015) evidence has suggested that isthmus formation was far more sophisticated than originally proposed and that the emergence of suitable habitat and connective land mass may have predated the full closure of the CAS by several million years (Bagley & Johnson, 2014). Under this model, dispersal into Central America presents both a novel ecological opportunity for colonization and an opportunity for clade diversification across a spatiotemporally complex landscape. Specifically, rather than a single migration across a suitable corridor into Central America, the complex landscape provided a series of patches of suitable habitat analogous to stepping stones with respect to the eventual colonization of Central America (Gutiérrez-García & Vázquez-Domínguez, 2013). In this model, we would likely infer *in situ* diversification/speciation before full formation of the isthmus (c. 3 Ma) as a result of dispersing across a complex geological substrate. Lastly, secondary contact zones between parapatric sister-lineage pairs may be expected to coincide for species that diversified on the isthmus. Specifically, if these sister-lineage pairs shared the

Evidence	FCC prediction	EDC prediction	Results	Model Support
Diversification	No effect	Increase	Increase	EDC
Divergence times	Less than 3 Ma	3—8 Ma	4—7 Ma	EDC
Parapatry	Random	Yes[†]	Yes[‡]	EDC

Table 1: Predictions made by the Full Closure Colonization (FCC) model and the Early Dynamic Colonization (EDC) model for various lines of evidence with model support from observed results. Evidence labels are as follows: Diversification is relative amount of speciation events associated with the IP compared to the remainder of the geographic range in the same time period. Divergence times refers to the divergence times of parapatric sister lineages with secondary contact zones in Central America, where we would expect younger ages for *in situ* diversification in FCC than EDC. Parapatry coincidence refers to the geographic coincidence of the secondary contact zones across parapatric sister lineage pairs, where we would potentially expect zone coincidence under EDC with a shared mechanism of diversification (†), and we see coincidence in our results for three lineages (‡)

same geological mechanism of diversification—such as a large change in landscape providing a vicariance boundary—it is possible that the secondary contact zones would have remained coincident following the second wave of dispersal. On the other hand, given no known ecological differences between the respective members of each sister-lineage pair, there would be no reason to expect coincidence of secondary contact zones across species without a shared mechanism of diversification.

Overall, our results provide strong support for the predictions of the EDC model and reject the FCC model (Table 1). Specifically, we find that the majority of the diversification not associated with the early burst at the crown of *Eciton* occurs in the Central American region (Fig. 1), which is consistent with EDC, but not expected under FCC. In addition, for the three lineages that we can confirm as coincident and parapatric across the Chorotega volcanic range (*E. burchellii*, *E. mexicanum*, and *E. vagans*), their divergence times are all significantly older than 3 Ma [E. burchellii: 4.27; E. vagans: 5.50; E. mexicanum: 6.61] (Fig. 2; Fig. 3; Appendix C1: SI. 6). The temporal and spatial congruence in the parapatric divergence of these lineages provides strong evidence supporting the EDC model. While *E. lucanoides* also has a deep phylogenetic break across the isthmus, this lineage is less abundant than the others, and thus, range parapatry cannot be ascertained at this point. *E. hamatum* also has a phylogenetic break near the Isthmus of Panama in Colombia. However, this divergence is younger than 3 Ma and requires increased geographic sampling to assess

the extent of parapatry, as there are no subspecific designations in the literature setting the precedent for this break.

Discussion

Understanding the factors that drive speciation is critical to revealing the origins of biodiversity and ecosystem assembly. Remarkably, we find strong evidence across multiple species for speciation associated with the complex emergence of Panama. In four of the six taxonomically recognized *Eciton* species with geographic ranges extending into Central America, our phylogenomic and population genomic data support the Early Dynamic Colonization model. In each case, the northernmost populations constitute a distinct lineage that is sister to the respective southern counterpart. In three of these cases—*E. burchellii*, *E. mexicanum* and *E. vagans*—we have identified coincident parapatric zones on the isthmus between the sister lineages that demonstrate evolutionary divergence and speciation far before the full closure of the isthmus (Figs 1-4; Appendix C1: SI. 5, SI. 6).

Recent work on the uplift of Panama and the associated faunal exchange has continued to depart from the more simplistic view of a single event that provided a corridor for the GABI. Geologically, the tectonic reconstructions of volcanic island arcs (Coates et al., 2004), evidence for shoaling (Haug & Tiedemann, 1998; Haug et al., 2001) and changes in sea level (Haug et al., 2005) provide an ample palette of mechanisms for speciation via dispersal and vicariance. For groups such as Neotropical army ants that cannot disperse across water, it is likely that the continued exchange of shallow waters between the Pacific and Atlantic oceans sufficiently segmented the landscape during this time to create several holding pens for evolutionary divergence (Woodburne, 2010; Bacon et al., 2015). Under this scenario, colonization of the Central American landmass may have been an extremely slow process, with several local extinctions of isolated island populations dispersing across the landscape, which may explain the deep divergence we find for all of the Central American lineages. Moreover, the high dietary demands and small population sizes of a top predator would

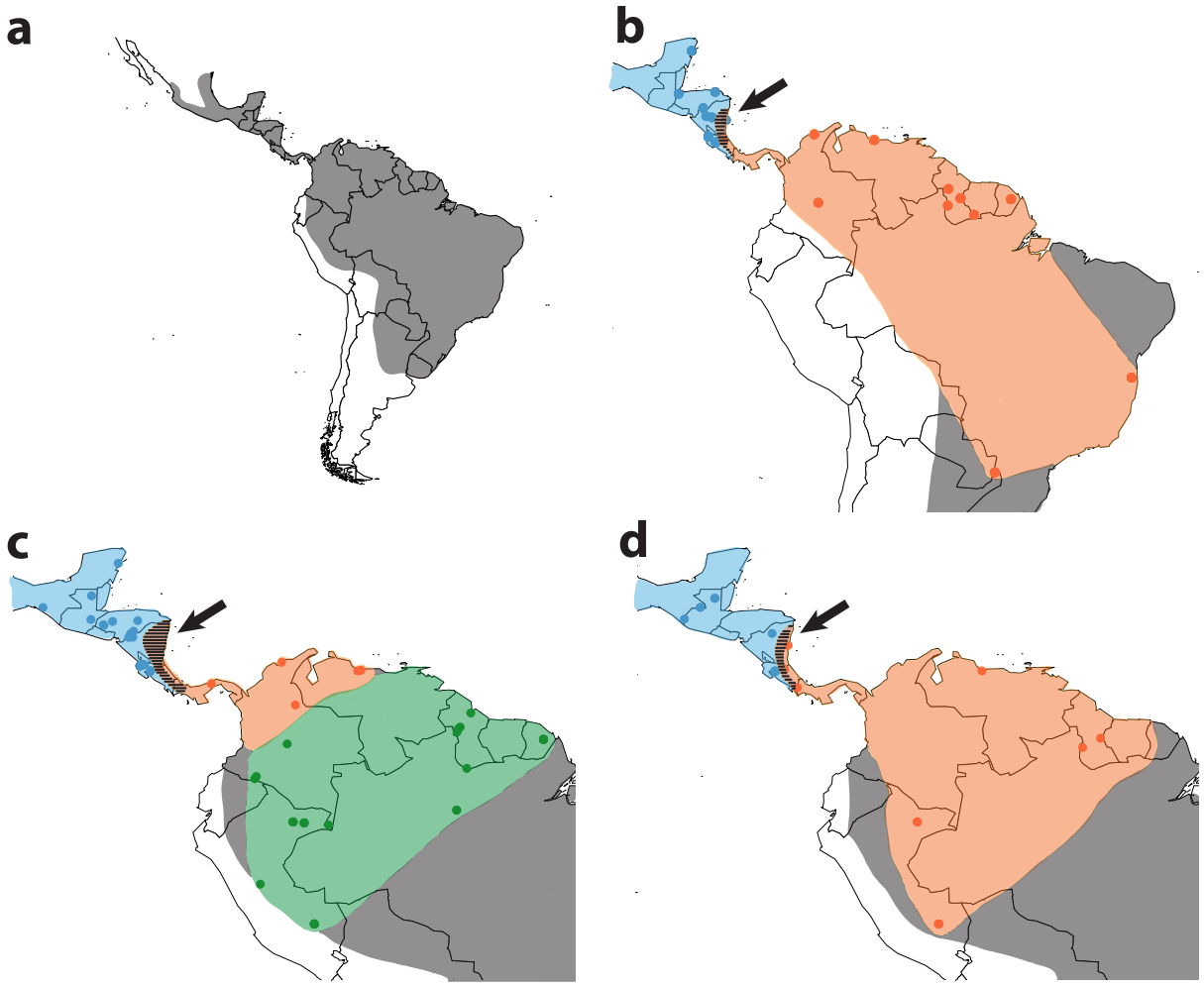

Figure 3: Geographic range for *Eciton* army ants with ranges and sampling for three species showing parallel speciation and coincidence of secondary contact zones. (a) The genus-level geographic range of *Eciton* is indicated by the grey shaded area, with most of the species in the genus occupying this cosmopolitan Neotropical distribution. Maps for each of the three species with distinct, overlapping lineages in Central America (b) *E. vagans*, (c) *E. burchellii* and (d) *E. mexicanum* with points representing the geographic coordinates of the specimens sequenced in this study. Colours indicate the assignment to a distinct phylogenetic lineage within each currently defined species, and black arrows indicate the secondary contact zones (hashed black lines) between the distinct lineages in northern Central America (blue) and southern Central America (orange) for each species. Although *E. burchellii* (c) also has a third distinct lineage (green), there are no data to suggest a secondary contact zone in South America. Estimated range areas (coloured by clade assignment) are based on our genomic data and geographic data associated with relevant, validated subspecies (Watkins, 1976). Grey areas represent areas of the geographic range for that species that could not be assigned to a clade using genomic or geographic data. Note that many of the points represent multiple samples and some sites are obscured by the large scale of the map. For sample sizes, refer to Fig. 1.

only have exacerbated the propensity for local extinction, further impeding the colonization process (Reznick & Ricklefs, 2009). Most importantly, geological reconstructions of the formation of the Central American volcanic archipelago reinforce our findings in both timing and specific path of dispersal, providing precise landscape features for colonization, as well as subsequent aquatic barriers for speciation (Appendix C1: SI. 8) (Coates et al., 2004; Gutiérrez-García & Vázquez-Domínguez, 2013).

When considering this evidence in the light of our alternative colonization models, we find clear support for the Early Dynamic Colonization (EDC) model over the Full Closure Colonization (FCC) model. Specifically, we find that the age of parapatric lineages found on the isthmus itself—all significantly older than 3.0 Ma—as strong evidence (Fig. 2), given that any assertion against in situ diversification would require an unspecified mechanism of speciation that acted upon all of these lineages in parallel. Furthermore, any competing assertion would then require the migration of these boundaries hundreds of miles from South America into Central America in four independent lineage pairs, with three lineage pairs emerging as completely coincident along the Nicaraguan depression and Chorotega volcanic range (Fig. 3). As this scenario is highly unlikely, we thus reject the prospect of *ex situ* diversification. Additionally, it is clear that the majority of recent divergences (4 out of 7) are associated with the complex emergence of the IP, supporting the EDC model and indicating a clear increase in diversification around the IP in comparison with the much larger sampled geographic area in South America (Fig. 1; Fig. 3; Table 1; Appendix C1: SI. 8). Although this support is not a formal statistical test, the concentration of divergences along the IP compared with the overall geographic area under study is striking.

As revealed by our population genomic data, the lack of gene flow in the extensive secondary contact zones of recently diverged lineages reinforces our argument for speciation (Fig. 4). More precisely, the fact that the majority of the loci in these lineage pairs demonstrate the maximum F_{ST} value ($\mu = 11,505, \sigma = 5,164$) despite our wide geographic sampling (Figs 1 and 3; Appendix C1: SI. 8) would only be expected without gene flow (Appendix

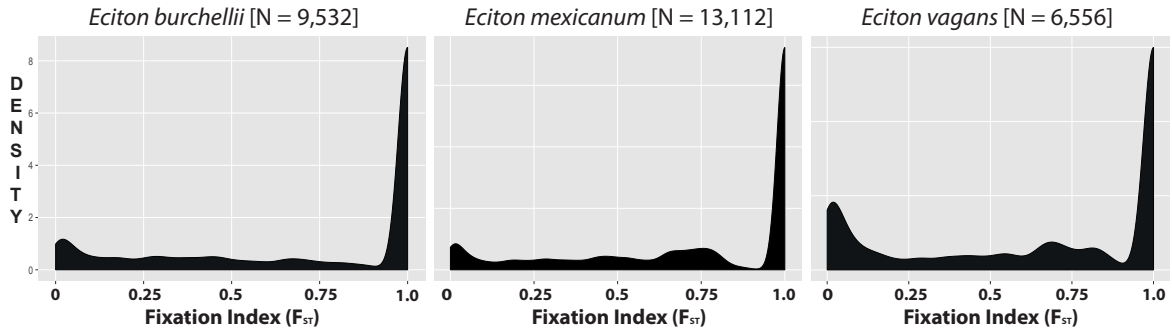

Figure 4: Distribution of F_{ST} values for conservative sets of loci for the three distinct lineage pairs with coincident secondary contact zones. Density distributions for *Eciton burchellii* (left), *E. mexicanum* (center) and *E. vagans* (right). The number of loci tested for each species is indicated to the right of the species name above each plot. Note that the majority of loci for all three lineage pairs have the maximum F_{ST} values (1.0), as well as many other loci with elevated F_{ST} values (>0).

C1: SI. 5). As the secondary contact zones between these lineages are large areas with ample opportunity for mating—on the order of thousands of square miles—these distributions of high F_{ST} values constitute one of the main lines of evidence for speciation. Combined with the comparison against our permutation-based pseudo-null that generated four orders of magnitude fewer loci with such extreme F_{ST} values ($\mu = 2.6, \sigma = 3.8$), we present strong evidence that these three co-occurring lineages are in fact distinct species (Appendix C1: SI. 5).

Considering our EDC model for in situ diversification implicates large-scale abiotic processes associated with the rise of the isthmus rather than ecological specialization, competition among these species may be particularly strong in these regions (Price & Kirkpatrick, 2009). Invading, ecologically similar lineages may thus have experienced competitive exclusion from closely related incumbent lineages, in addition to strong selective forces on premating isolation mechanisms to avoid costly hybridization (Coyne & Orr, 2004). This perspective is particularly relevant in Neotropical army ants, where competitive exclusion seems to frequently occur between closely related sister lineages and niche partitioning appears common between more distantly related lineages: as demonstrated in the current study (Fig. 1), no ecologically similar sister lineages regularly co-occur in any part of their ranges. On the other hand, despite all species being top predators, more distantly related lineages

partition niches in a number of ways—such as daily activity rhythms and food spectra—which may allow for co-occurrence without direct competition (Powell & Franks, 2006).

The repeated pattern of deep divergences among Central American army ant lineages provides important new insights into the GABI and the closure of the IP. Aside from an independent source of validation for the mounting geological and biological evidence asserting an earlier and more complex emergence of the IP (Gutiérrez-García & Vázquez-Domínguez, 2013; Stone, 2013; Bagley & Johnson, 2014; Bacon et al., 2015), our study shows this pattern in a clade without the ability to colonize land across aquatic barriers. As the early timing (4—7 Ma) of Central American colonization by Neotropical army ants was robust to multiple calibrations, this provides strong evidence for ephemeral land bridges prior to the full closure of the IP. We suggest that these early, intercontinental land connections played an important role in the dispersal of many taxa during the GABI (Gutiérrez-García & Vázquez-Domínguez, 2013; Bacon et al., 2015), and likely functioned as a mechanism of speciation through alternating bouts of dispersal and vicariance. Considering that the majority of lineages in lower Central America exhibit genetic structure in this region (Bagley & Johnson, 2014)—including other Neotropical army ant genera (Barth et al., 2015)—we predict that support for cryptic diversification and the EDC model will only increase as more research is conducted on weakly dispersing Central American species. Lastly, our research suggests that the spatial and temporal complexity of the emerging isthmus needs to be seriously evaluated when invoking the commonly used biogeographic phenomenon of sweepstakes dispersal.

4 Novel approach to heritability detection suggests robustness to paternal genotype in a complex morphological trait

Abstract

Heritable variation is essential for evolution by natural selection. In Neotropical army ants, the ecological role of a given species is linked intimately to the morphological variation within the sterile worker caste. Furthermore, the army ant *Eciton burchellii* is highly polyandrous, presenting a unique opportunity to explore heritability of morphological traits among related workers sharing the same colonial environment. In order to exploit the features of this organismal system we generated a large genetic and morphological dataset and applied our new method that employs geometric morphometrics (GM) to detect the heritability of complex morphological traits. After validating our approach with an existing dataset of known heritability, we simulated our ability to detect heritable variation given our sampled genotypes, demonstrating the method can robustly recover heritable variation of small effect size. Using this method, we tested for genetic caste determination and heritable morphological variation using genetic and morphological data on 216 individuals of *Eciton burchellii*. Results reveal this ant lineage (1) has the highest mating frequency known in ants, (2) demonstrates no paternal genetic caste determination, and (3) suggests a lack of heritable morphological variation in this complex trait associated with paternal genotype. We recommend this method for leveraging the increased resolution of GM data to explore and understand heritable morphological variation in non-model organisms.

Introduction

Complex quantitative traits are ubiquitous in natural populations, and often mediate important aspects of organismal niche. Morphological traits tend to be more heritable than physiological and life history traits (Roff & Mousseau, 1987; Visscher et al., 2008), with sev-

eral well-documented patterns of highly heritable craniofacial characteristics in vertebrates (Adams, 2011; Johannsdottir et al., 2005; Carson, 2006; Postma, 2014), as well as numerous traits in insects (Schwander et al., 2005; Roff, 1986). Geometric morphometrics (GM) are commonly used for the quantification of morphological variation because they provide better resolution than linear measurements, especially in exploratory analyses (Webster & Sheets, 2010; Zelditch et al., 2012). Although analytical solutions exist for applying quantitative genetics to linear measurements—such as the calculation of detectable effect size—these solutions do not generalize to GM due to the interdependence of shape data and the use of Procrustes transformation in shape analysis (Falconer & Mackay, 1996; Lande, 1979). Thus, researchers interested in the heritable component of morphological traits in non-model organisms would greatly benefit from new methods for heritability detection that harness the quantitative resolution of GM.

Neotropical army ants are obligate social predators where cooperation between hundreds of thousands of sterile workers is critical to the success of the colony (Franks, 1986). The Neotropical army ant *Eciton burchellii* is the premier example of this cooperation, containing colonies with several behaviorally, morphologically, and physiologically distinct sterile worker subcastes (Berghoff, 2003; Franks et al., 2001; Westwood, 1842) generated from known developmentally-plastic pathways (Abouheif & Wray, 2012; Libbrecht et al., 2013). Although morphologically distinct, the worker subcastes demonstrate continuous variation in size, and are delimited by size thresholds along this range (Franks, 1985). *Eciton burchellii* is highly polyandrous, with a single queen who mates multiply in a single interval and can produce millions of individuals over her lifespan from the stored sperm (Kronauer et al., 2006; Barth et al., 2014). Despite the fact studies have documented the role of developmental plasticity in generating the morphological diversity observed among worker subcastes (Abouheif & Wray, 2012; Jaffé et al., 2007) it is unknown whether there is genotypic bias in the production of morphological traits. This question is critical to understanding the evolution of the ecologically important trait of head shape in workers of *Eciton burchellii*

(Powell & Franks, 2006), since heritable variation is the primary material used by natural selection (Falconer, 1960). Furthermore, the mating system presents a unique opportunity to explore heritability of morphological traits among related workers in half-sibling families that all share the same colonial environment.

The high rate of polyandry found in army ant lineages contributes to increased genetic diversity within a colony (Barth et al., 2014; Jaffé et al., 2007; Jaffé et al., 2009; Kronauer et al., 2007; Kronauer et al., 2006). Several leading hypotheses to explain the large number of multiple matings revolve around the advantages of genetic diversity, which, for example, may increase resistance to a large variety of parasites (Kronauer et al., 2006; Hughes & Boomsma, 2006; Van Baalen & Beekman, 2006). Polyandry may also facilitate the evolution of task specialization, promoting division of labor within a colony by increasing morphological diversity among workers (Oldroyd & Fewell, 2007). This hypothesis is often considered in studies demonstrating a significant genetic basis to worker caste determination (Jaffé et al., 2007; Hughes et al., 2003; Keller et al., 1997), and suggests that morphological traits themselves may be heritable. Thus, not only does the unique mating system of *Eciton burchellii* provide a unique opportunity to learn about heritability within a plastic system, but studies also suggest that the high mating frequency could be driven by natural selection on increased morphological diversity (Jaffé et al., 2007; Kronauer et al., 2006).

Existing quantitative genetic and GM methods offer an important foundation for exploring heritability in non-model organisms (Adams, 2011; Klingenberg et al., 2004; Falconer & Mackay, 1996). By pairing existing methods with simulations based on empirical data, our approach provides a standardized procedure for guiding experimental design and understanding detectable effect size in exploratory empirical work for non-model organisms. Furthermore, the use of dimensionality reduction in our likelihood framework improves detection of heritable variation along shared axes of variation, which may be expected in many organismal systems (McGuigan et al., 2010; Aubin-Horth & Renn, 2009). For example, sensitivity to hormonal signaling during development—such as juvenile hormone in developing

insects—may produce shared heritable variation between different genotypes (Zera, 2006; Nijhout, 2003; Nijhout & Wheeler, 1982).

Here, we present a new method employing a relatedness matrix and high-dimensional GM data that can robustly recover heritable morphological variation among several half-sibling groups and in the presence of strong non-heritable variation. The method generalizes to any system of related individuals, and can be applied with any set of landmarks that are appropriate for GM analysis. Our method is novel in that it provides a simulation-based solution for applying quantitative genetics to GM data, using a dimensionality reduction approach that explicitly searches for concerted heritable variation among half-sibling groups. We demonstrate how the application of our method can be used in a non-model organism to address fundamental questions of evolution by investigating the mating frequency and heritability of morphological traits seen in the worker caste of *Eciton burchellii*.

Methods

Sample collection

Samples for the study were collected in June 2012 from the Area de Conservación Guanacaste (ACG), in northwestern Costa Rica. In total, we collected 216 individual sterile workers from three different colonies, which were sampled for genetic and morphological analyses. The 216 individuals were sampled by colony in the following breakdown: 48 from Colony 1 (C1), 72 from Colony 2 (C2), and 96 from Colony 3 (C3). Voucher specimens have been deposited in the biological collections of the Field Museum of Natural History (FMNH), Chicago, IL, USA.

Genotyping

Two sets of microsatellites were used for genotyping. First, we used three of eight highly polymorphic microsatellites previously isolated from *Eciton burchellii foreli* (Denny et al., 2004; Winston et al., 2017). The chosen highly polymorphic microsatellites were chosen due

to amplification performance, in order to reduce the prevalence of null alleles. Second, we used 10 of 45 conserved microsatellite loci identified from a study of eight phylogenetically-dispersed ant genomes (Butler et al., 2014). Conserved microsatellite loci were selected in order to maximize polymorphism among the samples. In order to preserve individuals for morphological analysis, we extracted DNA from the 3 right legs of each specimen. We then homogenized the legs with a Qiagen Tissue Lyser, and used a DNeasy Blood & Tissue Animal tissue spin column protocol to extract and purify the DNA following the protocols outlined by Moreau (2014). The Polymerase chain reaction (PCR) master mix was comprised of the following: 4 μL H_2O, 2 μL BSA (100X), 0.875 μL $MgCl_2$ (25 mM), 1 μL buffer with $MgCl_2$ (10X), 0.6 dNTPs, 0.4 μL forward and reverse primers (10 μM), 0.15 μL Taq polymerase (5 U/ μL), and 1μL DNA template for a total reaction volume of 10.4 μL. We ran the reaction in a Bio-Rad Peltier Thermal Cycler with the following parameters: An initial denaturation of 4 minutes at 95° C, then thirty-five cycles of 30 seconds at 95° C, 30 seconds at 55° C, 45 sec at 72° C, and a final extension at 72° C for 7 minutes. We genotyped the PCR reactions using an Applied Biosystems 3730xl DNA Analyzer sequencer. Allele calling and fragment sizing of chromatograms were performed using Geneious R7 software (Kearse et al., 2012). We then added a quality control step by having an independent party call alleles and cross-validating these results.

Parentage inference

Parentage inference in *Eciton burchellii* is facilitated by haplodiploidy and the presence of only one queen in each colony (Rettenmeyer & Watkins, 1978). We assigned queen and male genotypes using COLONY (Jones & Wang, 2010), which implements full-pedigree likelihood methods to simultaneously infer sibship and parentage. Unlike many other parentage inference programs, COLONY can accommodate and estimate genotyping error at each locus. For robust parentage inference, we created several subsetted datasets by subsampling both individuals and loci, and compared inferred parentage across the datasets. Genotyping error

and paternal genotype mismatches were minimal (Appendix C2: SI. 1-3), thus the paternal genotypes used in our analysis were inferred from the maximum likelihood estimation from the full dataset.

Workflow for Detection of Heritable Morphological Variation

In order to estimate whether there is heritable morphological variation in the castes of *Eciton burchellii* and the effect size of heritable variation we could detect given our data, we created a workflow linking simulated and empirical genotypic and GM data to a likelihood-based method. This workflow is outlined in Table 2.

Morphometrics

We took both linear and geometric morphometric measurements on different body parts of sterile workers from all worker subcastes. Because back leg length (BLL) has been used in previous studies on *Eciton burchellii* as a proxy for body size (Powell & Franks, 2006), we included this measurement in our analysis. The rest of the measurements were taken on images of the head of the sterile workers using landmark-based, geometric morphometrics (GM), which are a set of methods for quantifying multidimensional shape data. Landmarks were chosen on the heads of the sterile workers for three reasons: (1) The heads demonstrate the most inter- and intraspecific morphological variation in comparison to other body parts, (2) head shape has been strongly associated with the behavioral ecology of the sterile workers (Powell & Franks, 2005), and (3) morphological variation in the head of the sterile workers has a strong link to the ecological dominance and niche of different *Eciton* species (Powell & Franks, 2006). Each specimen has 14 landmarks assigned to homologous points on the head case (Table 2: Step 1), as illustrated in Figure 5. Standard traditional morphometric measures such as head length (HL) and head width (HW) can also be calculated from distances between landmarks (Watkins, 1976; Ward & Downie, 2005).

We took images for GM analysis on the Photo Montage Leica Imaging Suite ver. 4.2

Step 1. Landmark selection
Homologous landmarks are chosen to capture the variation associated with trait(s) of interest, [Morphometrics section].
Step 2. Preliminary data collection
A geometric morphometric dataset of the selected landmarks is collected to estimate and parameterize variation [Data Simulation section, Fig. 2]. It is critical that within-sample measurement error in selected landmarks is negligible in comparison to between-sample variation, and that the samples included in the preliminary data collection encompass the phenotypic variation observed in the organism.
Step 3. Simulations of heritable variation
Simulations are parameterized with the morphological variation estimated from the preliminary dataset (Data Simulation section, Fig. 7), and are specific to the set of homologous landmarks chosen in Step 1. The nature of the heritable variation (i.e. number of landmarks affected, covariance of morphological variation of distinct genotypes) should be based on assumptions determined from the relevant literature (Data Simulation section). Several effect sizes of heritable variation should be chosen to find the edge of the detectable range by iteratively using the likelihood test defined in this paper (Data Simulation section, Tables 2—3). Investigator will determine a range of attainable sample sizes for data collection, and will also need to define a relatedness matrix for the tested individuals based on the organismal system (Maximum Likelihood Method for Detecting Morphological Variation section).
Step 4. Data collection for heritability estimation
Given the detectable effect sizes of heritable morphological variation for the range of sample sizes used in the simulations (Step 3), the investigator should collect GM data for a sample size that matches the desired effect size (Testing Empirical Data section).
Step 5. Testing data for heritable variation
Once GM data for all samples have been collected, this data can be used to assess heritable variation with our likelihood-based method. This involves constructing a relatedness matrix in a similar fashion to Step 3, except based on the relationships attained from empirical genetic data. See R script for running code for the method in Supplementary Information (Appendix C2: SI.6) and available on GitHub.

Table 2: A workflow for detecting heritable morphological variation with GM data.

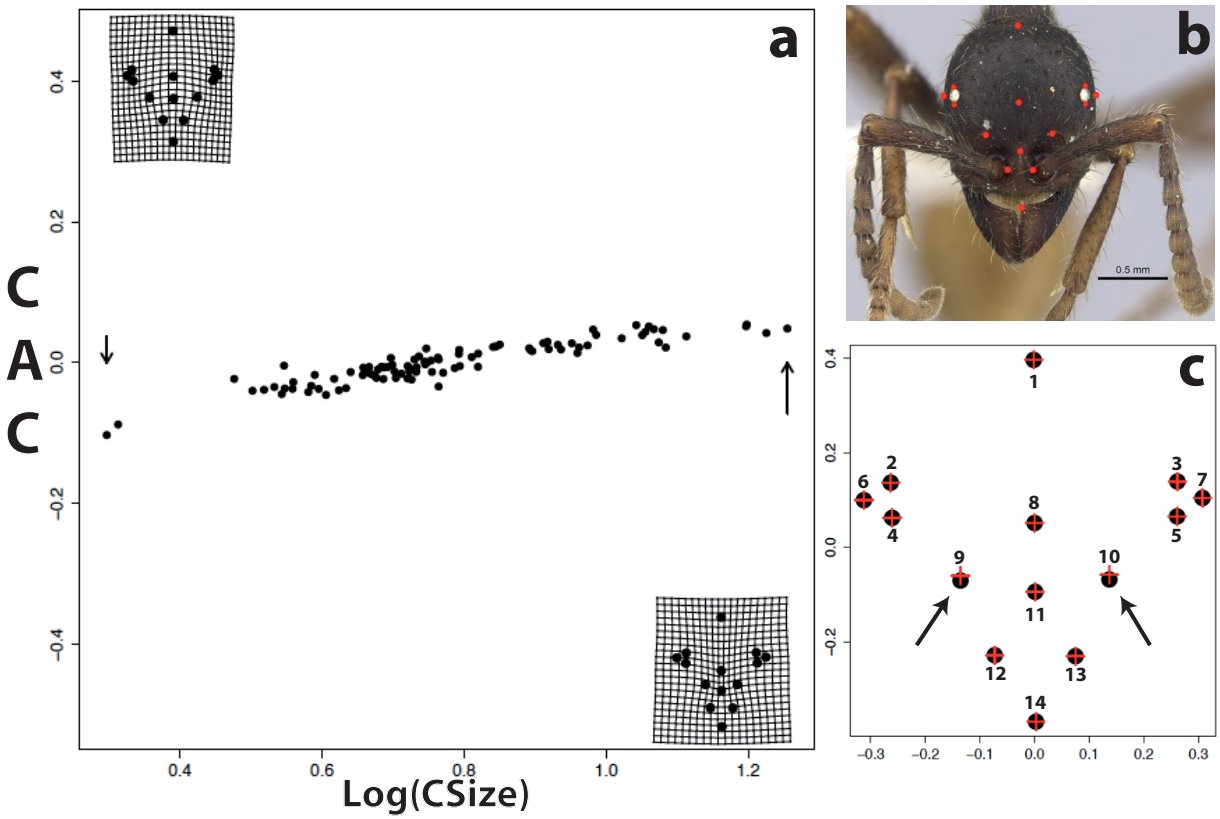

Figure 5: Visualizations of geometric morphometric landmarks, allometric deformation, and standard heritable deformation. (a) The allometric deformation (AD) is derived from the common allometric component (CAC) from 48 individuals, and is visualized using thin-plate splines in the top-left and bottom-right corners of the plot (arrowed individuals). (b) The 14 landmarks employed for this study demonstrated on a worker head case seen in red. (c) Reference form landmarks plotted with black dots, landmarks showing standard heritable deformation (HD1) plotted with red crosses to visualize effect size. Note that all landmarks (red crosses and black dots) are the same except for the two indicated with black arrows (landmarks 9 and 10), where the difference between the red crosses and black dots represents the effect size for HD1.

in the Collaborative Invertebrate Laboratory in the Field Museum of Natural History in Chicago, IL. We standardized orientation of the head so that the bilaterally-symmetric plane between the clypeus and the occiput was orthogonal to the imaging direction in all specimens. The auto-montage synthesized between 8-50 images for a single composite image for each specimen. We processed and digitized all images in ImageJ (Schneider, Rasband, & Eliceiri, 2012).

Morphometric analysis was primarily performed using the geomorph and shapes packages in R, as well as the IMP7 package (Webster & Sheets, 2010; Adams & Otarola-Castillo, 2013; Dryden & Mardia, 1998). Analyses consisted of principal components analysis (PCA), modeling of static allometric curves, and calculation of morphological disparity. As generalized Procrustes analysis removes difference in sizes by scaling the landmark configurations by centroid size—the square root of the summed distances of all the landmarks to the centroidthe Procrustes-fit shape variation can then be modeled against centroid size to model static allometry. Since Custom R scripts for each analysis mentioned above can be found in the supplementary information (Appendix C2: SI.6–7, and on GitHub: https://github.com/mewinsto).

Data simulation

In order to evaluate our ability to detect heritable morphological variation in a system with abundant non-heritable variation (Jaffé et al., 2007), we took an empirically-based simulation approach by using morphological data from 48 specimens to define traits from the measurements, and the static allometry (Table 2: Step 2). Detection of the heritable variation would take place within this parameterized, allometric variation with additional noise to simulate measurement error (Appendix C2: SI.8).

Specifically, after applying Procrustes Analysis using the geomorph package to the set of 48 specimens, the plotAllometry function was then applied to the Procrustes-fitted individuals, generating a multidimensional set of allometry curves known as the common allometric

Data Simulation 1

Treatment	Heritable Deformation	Noise Deformation
T1	Standard (HD1)	Standard (ND1)
T2	Double (HD2)	Standard (ND1)
T3	Standard (HD1)	Double (ND2)
T4	Half (HD3)	Standard (ND1)

Table 3: Treatment definitions for first data simulation.

component (CAC) (Adams & Otarola-Castillo, 2013). Using the predicted shapes from the generated allometry curves and the known centroid sizes of the individuals, linear models were then constructed for each individual landmark with the stats package, effectively parameterizing the static allometry for data simulations. This is defined as the Allometric Deformation (AD).

Because data collection of morphological characters will always introduce measurement error, a necessary component of modeling detection of heritable variation is noise. As determined by previous empirical error analysis of technical replicates, there is no evidence within our morphological measurements of anisotropic error (Appendix C2: SI. 13). Thus we modeled our noise using the rnorm function from the stats package, with a mean of zero and a landmark-specific standard deviation from the allometry-removed empirical dataset. In the following work, this is defined as the standard Noise Deformation (ND1).

Parameterizing the heritable morphological variation is difficult since there are many different interpretations and models for heritable morphological traits (Aubin-Horth & Renn, 2009; Nijhout & German, 2012; Nijhout & Wheeler, 1996). In order to keep the simulations to a manageable number of treatments, we ran two separate data simulations, the first of which aimed at understanding the necessary effect size of the heritable morphological variation for detection, and the second of which aimed at assessing our ability to detect different types of heritable variation within a sample of a greater number of patrilines.

In our first data simulation (Table 3; Table 2: Step 3), the treatment was a simple deformation of a given effect size applied to two landmarks for those individuals sharing one patriline, while the remaining individuals fathered with a second patriline were designated

the reference form (Fig. 5). We defined this as the standard Heritable Deformation (HD1). In order to assess our ability to detect this heritable variation, we ran this simulation under four treatments: Treatment 1 (T1) was the standard treatment, Treatment 2 (T2) was the same noise (ND1) and allometric (AD) deformations but with double the effect size of the heritable variation (HD2), Treatment 3 (T3) was HD1 and AD, but with double the noise (ND2), and Treatment 4 was ND1 and AD, but with half the heritable variation (HD3). Finally, each treatment was put in Procrustes superimposition using the *gpagen* function from the *geomorph* package, followed by principal components analysis of this shape variation with the *plotTangentSpace* from the *geomorph* package (Adams & Otarola-Castillo, 2013).

In our second data simulation (Table 4; Table 2: Step 3), we focused on the robustness of the model to higher mating frequencies and different deformation types. To accomplish this we implemented two types of heritable morphological variation at two different strengths, across four mating frequencies (3, 5, 10, 20). First, the most straightforward treatment was a simple deformation of a given effect size applied to two landmarks, where the strength of the maximum effect size was independent of the mating frequency, defined as the independent Heritable Deformation (HD5). Second, the effect size of the variation was slightly increased with increases in mating frequency, defined as the non-independent Heritable Deformation (HD6). These treatments can then be applied to the two landmarks in different directions, orthogonal (o) and parallel (p), creating four total treatments for the data simulations (T5o, T5p, T6o, T6p). Matching our first set of simulations, each treatment was then put in Procrustes superimposition using the *gpagen* function from the *geomorph* package, followed by principal components analysis of this shape variation with the *plotTangentSpace* from the *geomorph* package (Adams & Otarola-Castillo, 2013).

In summary, for any randomly generated set of n individualswhere centroid sizes are parameterized by the empirical set of 48 individualsdata can be simulated by simply adding the three types of deformation (AD, ND, HD) to the mean shape for each individual (Appendix C2: SI.8). The custom R script written to perform the data simulation is in-

Data Simulation 2

Treatment	Heritable Deformation	Noise Deformation	Orientation
T5o	Independent (HD5)	Standard (ND1)	Orthogonal
T5p	Independent (HD5)	Standard (ND1)	Orthogonal
T6o	Non-independent (HD6)	Standard (ND1)	Parallel
T6p	Non-independent (HD6)	Standard (ND1)	Parallel

Table 4: Treatment definitions for second data simulation.

cluded in the Supplementary Information (Appendix C2: SI. 6 and available on GitHub: https://github.com/mewinsto). All datasets were created for 100 individuals to match given sample sizes of the empirical dataset, and then replicated under all treatments 100 times to test statistical power.

Maximum likelihood method for detecting heritable morphological variation

In order to detect significant heritable morphological variation in both simulated and empirical datasets, we created and utilized a maximum-likelihood (ML) approach (Table 2: Step 5) based on the probability model defined in Equations 2-4:

$$PC \sim MVN(\mu_A, [VCV]\sigma^2) \qquad \text{(Eq. 2)}$$

$$\mu_A = \beta(size) + \mu_0 \qquad \text{(Eq. 3)}$$

$$[VCV] = [K]h^2 + [I](1 - h^2) \qquad \text{(Eq. 4)}$$

Where the principal component scores (PCs) are distributed as a multivariate normal (MVN) with vector of means equal to an allometric model of mu (μ_A) and variance equal to an among-observation variance-covariance matrix ($[VCV]$) multiplied by a variance coefficient (Eq. 2). The allometric model (μ_A) is detailed in Equation 3, defined simply as the centroid size scaled by an allometric coefficient (β) with a mean value of mu (μ_0). Lastly, the expected variance-covariance matrix ($[VCV]$) under a heritable trait can be modeled as the propor-

tion of variance expected to covary by a relatedness matrix ($[K]$), times the heritability (h^2), added to the non-heritable proportion of variance ($1-h^2$) expected to vary independently as defined by the identity matrix ($[I]$). The partitioning of the variance-covariance matrix follows the common mixed-model analysis in quantitative genetics (Speed et al., 2012; Falconer & Mackay, 1996), and further notes on derivation can be found in the supplementary information (Appendix C2: SI. 12). Due to the facts that *Eciton burchellii* are haplodiploid, have a single mated queen (Kronauer et al., 2006), and tested individuals were sterile workers, the relatedness matrix ($[K]$) was constructed using relatedness coefficients of 0.75 for individuals with the same father, 0.25 for individuals with different fathers, and 0 for individuals from different colonies.

To evaluate our ability to detect heritable morphological variation, we applied a likelihood ratio test (LRT) using the R package *bbmle* (Bolker, 2016), with a null hypothesis that the complex trait was not heritable at all ($H_0 : h^2 = 0$), and an alternative that there was some heritable component to the variation ($H_A : h^2 > 0$). Specifically, the LRT is illustrated in Equation 5, where the null hypothesis maximizes over all nuisance parameters (η) and constrains heritability to zero, whereas the alternative hypothesis maximizes both the nuisance parameters (η) and the heritability parameter (h^2):

$$L_0 = max[\eta]L(h^2 = 0, \eta) \qquad \text{(Eq. 5)}$$

$$L_A = max[\eta, h^2]L(h^2, \eta) \qquad \text{(Eq. 6)}$$

Standard to the LRT, the test statistic (λ) is then calculated, and should be distributed as a chi-squared with a mixture of one degree of freedom ($\lambda \sim X_1^2$) and zero degrees of freedom ($\lambda \sim X_0^2$) since the heritability statistic cannot be negative (Pinhero & Bates, 2000; Self & Liang, 1987). Following this, because the LRT was applied to the top four PC scores, the Bonferroni-corrected significance value (α) is 0.0125. Although we chose to test four PCs due to the nature of our empirical dataset–in particular the distribution of our eigenvalues–any

number of PCs can be used for our approach, so long as the significance value (α) is adjusted accordingly. However, investigators should avoid using all the PCs, as it reduces the relative power of this method. The custom R script employed the R package *mvtnorm* for generation of null data.

Testing empirical data

Testing the generated genotypic and morphological data for genotypic bias and heritable variation in caste was accomplished using a number of methods. We stress that the application of our approach in *Eciton burchellii* leverages the known genetic variation within a single colonial environment (C3) due to high rates of polyandry (Barth et al., 2014; Jaffé et al., 2007; Jaffé et al., 2009; Kronauer, Johnson, & Boomsma, 2007; Kronauer et al., 2006)—not between colonies—creating ideal conditions for testing for heritable variation (Falconer & Mackay, 1996). First, tests of genotypic bias in caste determination with two proxies for body size (BLL and centroid size) used an ANOVA among half sibling families of related workers. Second, testing for heritable variation followed the tests from the simulations for greater interpretability, which included permutational significance tests of canonical correlation analysis (CCA) and the ML approach on the top four PCs. Furthermore, to confirm the efficacy of our novel method, a published GM dataset of Plethodon salamander hatchlings with verified heritable morphological variation (Adams, 2011) was tested with our ML approach.

Results

Mating frequency

Mating frequency for all three *Eciton burchellii* colonies was estimated using COLONY. Despite continued accumulation of patrilines with increased sampling (Fig. 6), the inferred number of patrilines was steady across colonies with increased number of microsatellite loci (SI.1). This finding is consistent with the fact that COLONY is conservative in parentage

assignment by accounting for genotyping errors (Jones & Wang, 2010). Mean estimated error rates and standard deviation (σ) from parentage inference across all microsatellites and COLONY runs were 0.0371 for C2 (σ = 0.0268), 0.0388 for C3 (σ = 0.0165), and 0.0539 for C1 (σ = 0.0295). Generally, mean error rates were higher in COLONY runs using a larger number of microsatellites, however increases in error rates remain relatively low (SI.2). Across all COLONY runs, the mean error rate for all thirteen microsatellites were under 5% [$\mu = 0.045, \sigma = 0.015, N = 13$]. Distributions for estimated error rates by microsatellite can be found in SI.3.

Generally, increased sampling of individuals led to an increase in observed mating frequency, suggesting that estimates of the true mating frequency are conservative (Fig. 2). Nonetheless, the estimates for observed mating frequency in *Eciton burchellii parvispinum* [31 for C2 (n = 72), 25 for C3 (n = 96), and 17 for C1 (n = 48)] are higher than previous estimates of 13 25 matings (Jaffé et al., 2007). Less conservative estimates based on rarefaction of individuals and a Chao1 estimator range from 46 for C2, to 39 for C3, to 31 for C1.

Morphological variation

Due to the multidimensionality of the GM data, PCA is an appropriate ordination method to explore morphological variation (Mitteroecker & Gunz, 2009). For example, the static allometry resulting from a developmentally-plastic pathway is easily demonstrated by plotting centroid size against the first principal component (Appendix C2: SI.9). Since PCA of Procrustes-fit GM data contains no information of centroid size, this relationship shows that the majority of variation among individuals (55.1%) results from static allometry associated with morphological plasticity. The static allometry produced by this morphological plasticity defines the differences between worker subcastes, and is likely mediated by developmental pathways involving hormonal morphogens (Abouheif & Wray, 2002). For a more direct estimation of allometry, the CAC can be calculated using the geomorph package (Fig.

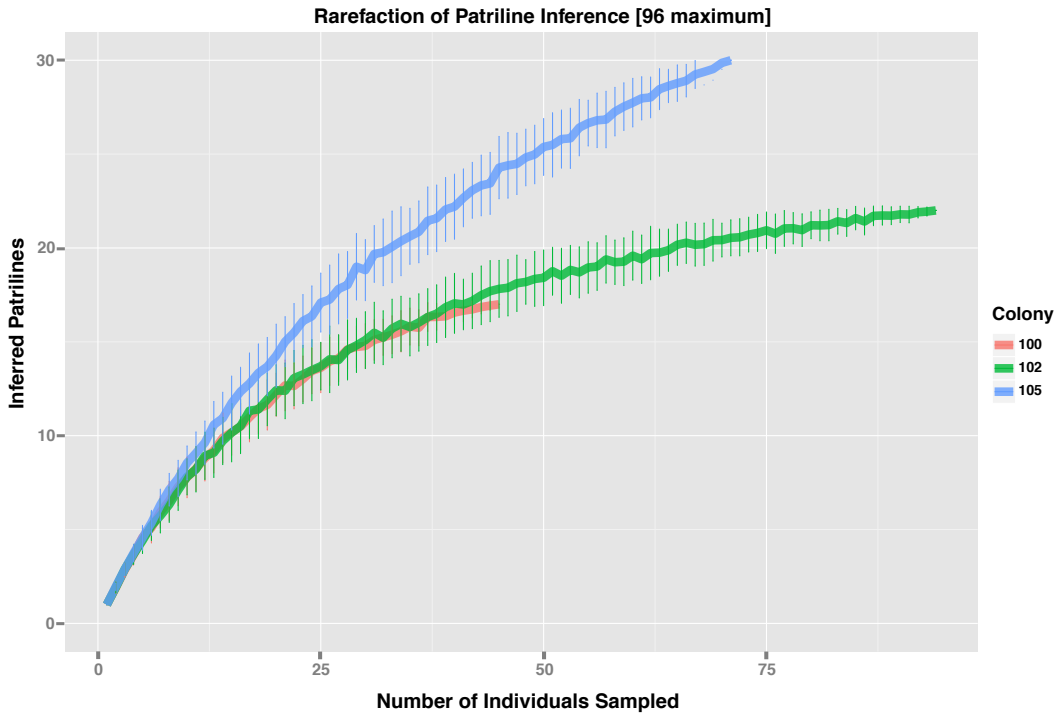

Figure 6: Patriline accumulation curves for all 216 genotyped individuals. Rarefaction accomplished using standard bootstrapping procedures for all three colonies, each of different sample size: 48 individuals genotyped for C1 (red), 72 individuals genotyped for C2 (blue), 96 individuals genotyped for C3 (green).

5a), which explicitly models the variation by worker size (Mitteroecker et al., 2004).

Data simulation I

Using the common allometric component (CAC) derived from centroid size and from empirical morphological data (Fig. 5a), we parameterized the static allometry and replicated this deformation (AD) for 100 individuals over 100 replicates. For each of these replicates, the plastic static allometry could be represented on a single PC axis (Appendix C2: SI.10). Combining the allometric deformation (AD) with noise deformation (ND) and heritable deformation (HD) as described by our four treatments (T1, T2, T3, T4), we generated four datasets with 100 replicates each. Performing PCA on the replicates from each of the treatments demonstrated visible segregation for some of the treatments (Fig. 7), and allowed for the construction of test statistics (Eq. 2-4) for assessing detection power.

Assessing statistical power of detecting heritable variation was accomplished by recording

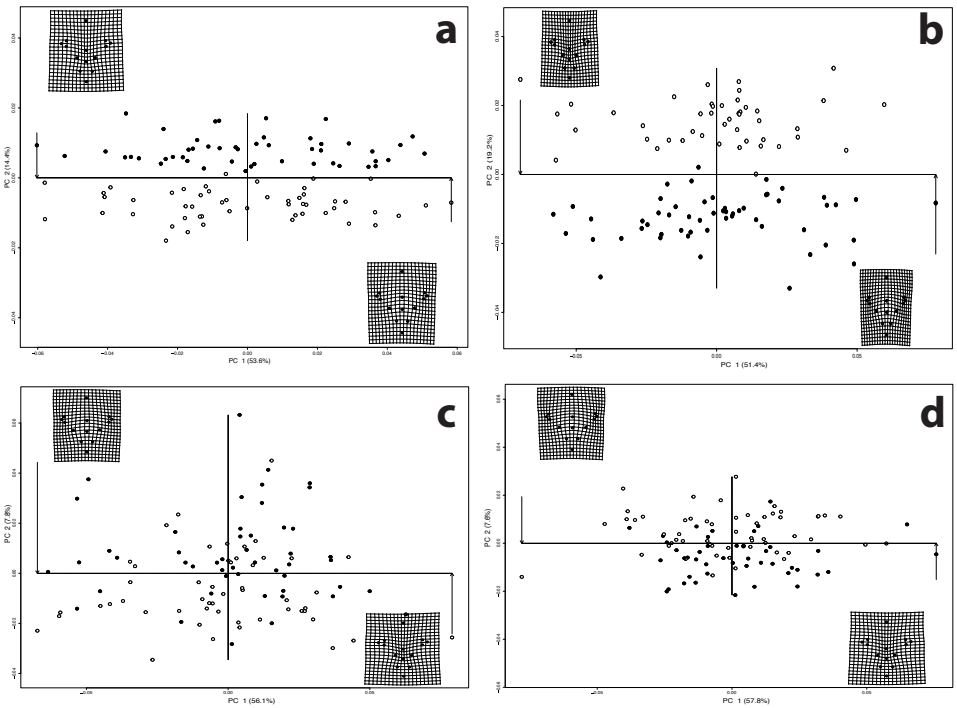

Figure 7: Principal component plots for each treatment from data simulation 1. Treatments are labeled as following: T1 (a), T2 (b), T3 (c), T4 (d). Black and white dots denote individuals of the two different patrilines, which separate on PC2 to different degrees among the different treatments. See Figure 8 for detection capability based on these scores. Scores on PC1 are highly correlated with AD shape change, with the most extreme values on PC1 illustrated in the two thin plate splines for each plot.

the fraction of replicates able to recover a significant, Bonferroni-corrected LRT value (Fig. 8). Generally, PC2 offered the highest statistical power for detection (T1 = 1.0 [SE = 0.0], T2 = 0.992 [SE = 0.004], T3 = 0.692 [SE = 0.017], T4 = 0.072 [SE = 0.013]), with PC1 offering statistical power only under the treatment (T2) with double effect size (T1 = 0.067 [SE = 0.017], T2 = 0.906 [SE = 0.017], T3 = 0.05 [SE = 0.007], T4 = 0.004 [SE = 0.002]). Statistical power of detection using PC3 (T1 = 0.002 [SE $<$ 0.001], T2 = 0 [SE = 0.0], T3 = 0.476 [SE = 0.021], T4 = 0.196 [SE = 0.020]) and PC4 (T1 = 0 [SE = 0.0], T2 = 0 [SE = 0.0], T3 = 0.160 [SE = 0.012], T4 = 0.194 [SE = 0.020]) for varied with treatment, but never reached higher than 50%.

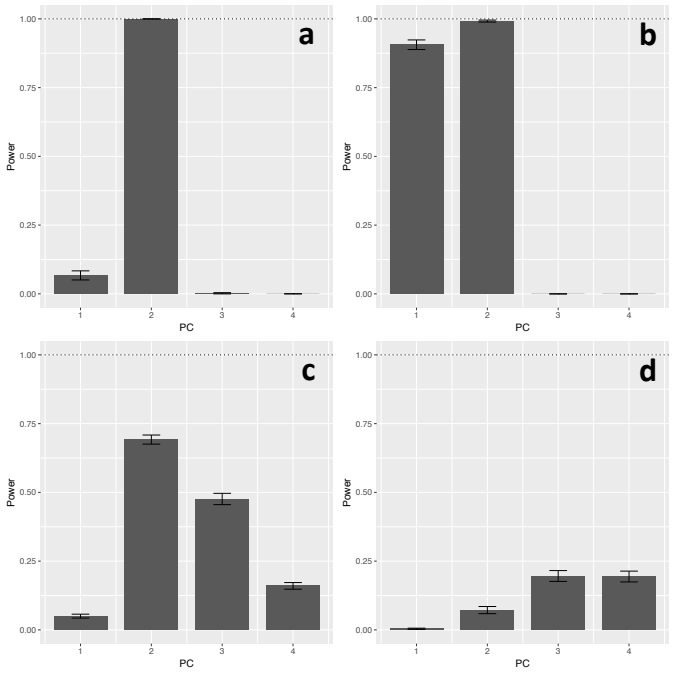

Figure 8: Statistical power for detection of heritable variation in data simulation 1. Plots demonstrate the number of 100 replicates recovered as statistically significant using each of the four principal components (PC1—PC4) for each treatment from data simulation 1. Error bars represent standard error. Treatments are labeled as following: T1 (a), T2 (b), T3 (c), T4 (d). Note the strong statistical power for detection of heritable variation with PC2 for T1 and T2, with the dotted line as the maximum statistical power (100%).

Data simulation II

Creation of replicates for the second data simulation matched the first simulation, except that there were four treatments (T5o, T5p, T6o, T6p) and four mating frequencies (3, 5, 10, 20), resulting in a total of 16 datasets, each with 100 replicates of 100 individuals. Performing PCA on the replicates from each of the treatments demonstrated visible segregation for some of the treatments (Appendix C2: SI.11), and allowed for the computation of test statistics (Eq. 2-4) for assessing detection power.

Assessment of statistical power in the second data simulation was performed in the same manner as the first. For all 16 datasets, detection of heritable variation using PC2 was 1.0 or 0.99. Conversely, detection of PC1, PC3 and PC4 was 0 or below 0.02. In order to understand the rate at which statistical power to detect heritable variation decreased, we utilized a ten-increment step-wise decrease in the variation, with the mean effect between

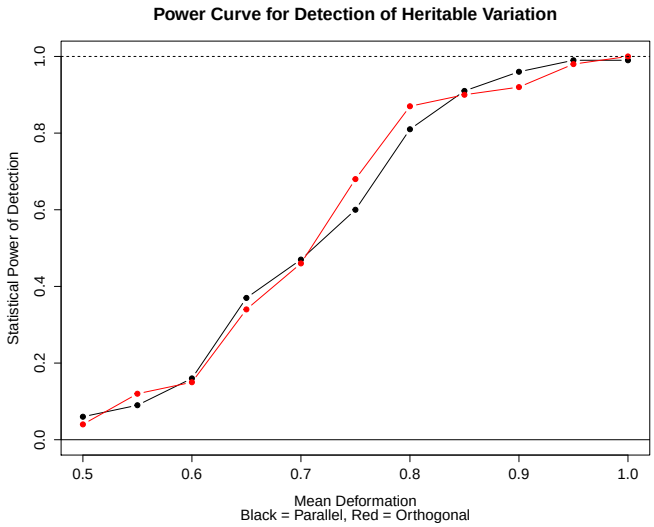

Figure 9: Statistical power for detection of heritable variation using PC2 in data simulation 2. Plot demonstrates the number of 100 replicates recovered as statistically significant using PC2, with the dotted line as the maximum (100/100). X-axis is the mean deformation used in each set of simulations (replicate), with the standard effect size (HD1) as the largest value of 1.0. Detection of PC1, PC3, and PC4 for all treatments was 0 or below 0.02.

the standard heritable variation (HD5), and half this value with the same noise deformation (ND1). Results demonstrate that statistical power to detect heritable variation decays between values of less than the standard heritable variation (HD5), but greater than half the standard heritable variation (Fig. 9).

Method validation on *Plethodon* hatchling dataset

A dataset containing 282 hatchlings from 44 families of *Plethodon cinereus* salamander hatchlings with verified heritability (Adams, 2011) was tested with our heritability detection method. To mirror testing of our own data, we used the first four PCs of the Procrustes-fit GM data for heritability detection, finding three of the four PCs as demonstrating highly significant heritable variation (PC1: p = 5.39e-11, PC2: p = 2.65e-05, PC3: p = 0.814, PC4: p = 0.005) at a Bonferroni-corrected significance threshold ($\alpha = 0.0125$). Estimated heritability values of morphological variation described by the three significant PCs ranged between 0.41 and 0.72 (PC1: $h^2 = 0.72$, PC2: $h^2 = 0.41$, PC4: $h^2 = 0.56$).

Testing for genotypic bias in army ant caste determination

Because our study took measurements on two independent proxies for body size, tests for genotypic bias in caste determination used each of the proxies separately. First, for the 96 individuals that had GM measurements, we used centroid size as a proxy for caste. Under an ANOVA among patrilines, we found no significant effect of patriline on centroid size (F = 0.997, p = 0.32), with the mean ML estimate for effect size being 0.009. Second, with the measurements of back leg length from all 216 individuals genotyped (Fig. 10), we found no significant effect of patriline (F = 0.949; p = 0.58), with the mean ML estimate for effect size being 1.19mm. Simulations of detectable effect size for the ANOVA analysis of centroid size (Appendix C2: SI. 4) show a mean effect centroid size of 0.018 necessary for likely detection (>50% replicates) given our sample size (n = 96) and centroid size variation. Simulations of detectable effect size for the ANOVA analysis of back leg length (Appendix C2: SI. 4) show a mean effect size for back leg length of 1.4mm necessary for detection (>50% replicates) given our sample size (n = 216) and back leg length variation.

Empirical testing for heritable morphological variation

Using the 96 individuals from C3 with GM measurements, we used a LRT to test the hypothesis that the heritability (h^2) was greater than zero (Eq. 6). Testing each principal component (PC1-PC4), improvements in log-likelihood under the alternative hypothesis were negligible in comparison to log-likelihoods under the null hypothesis (λ: PC1: 0.61, PC2: 0, PC3: 0, PC4: 1.67), resulting in four heritability estimates (PC1: $h^2 = 0.26$ [SE = 0.36], PC2: $h^2 = 0$ [SE = 0], PC3: $h^2 = 0$ [SE = 0], PC4: $h^2 = 0.45$ [SE = 0.54],) with insignificant p-values under a $X^2_{0.5}$ distribution (PC1: p = 0.23, PC2: p = 1.0, PC3: p = 1.0, PC4: p = 0.09). CCA permutational significance tests of partial warp scores and paternal genotype were also used to test for significance of heritable morphological variation, which resulted in zero significant canonical correlation coefficients (p = 0.682, 999 permutations).

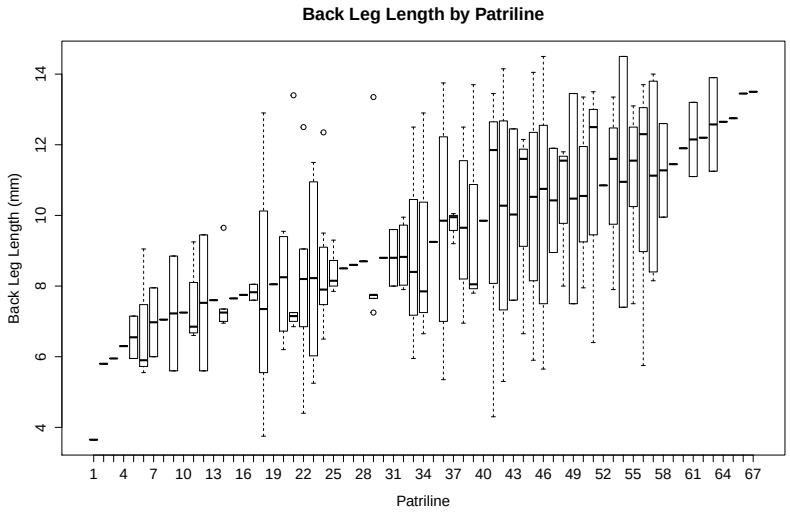

Figure 10: Boxplot of ranges of back leg length for all 73 patrilines from all three colonies. Sample sizes for each patriline range from singletons (indicated by bold dash) to 12 individuals (box and whiskers), and patrilines have been ordered by mean back leg length. Results demonstrated no significant caste bias based on paternal genotype.

Discussion

We do not find any significant heritable morphological variation in *Eciton burchellii* associated with the paternal genotype, despite the demonstrated ability of our novel method to detect heritable variation in several simulations and the empirically-validated salamander hatchlings dataset (Fig. 8, Fig. 9). Our simulations suggest that heritable morphological variation of very modest effect size—such as the minor change (0.01) of landmarks as seen in Fig. 5c–should be detectable ($P > 0.98$) given the sample size and resolution provided by geometric morphometric data (Fig. 8,9, Appendix C2: SI.11). In particular, results from the second data simulation suggest that the standard effect size (HD5 and HD6) should be easily detectable and robust to a variety of mating frequencies and directions (Fig. 9). Therefore, from these simulations and our empirical testing, it is likely that if there is any heritable morphological variation relating to paternal genotype, it is either of negligible effect size or inherited by more complex mechanisms that cannot be captured with narrow-sense heritability (h^2). The absence of this heritable variation in our empirical dataset implies a weak capacity for worker head shape, which is considered a proxy for subcaste and ecological

role, to respond to selection on paternal genotype within this population.

We found higher rates of mating frequency demonstrated in this study compared to previous work on *Eciton burchellii* (Kronauer et al., 2006; Jaffé et al., 2007; Kronauer, Schöning, & Boomsma, 2006; Denny, Franks, Powell, & Edwards, 2004). This is unlikely to reflect genotyping errors because of the robustness of mating frequency to the number of microsatellites used for parentage inference in this study and stringent quality control measures (Appendix C2: SI.1). Factors contributing to intraspecific variation in mating frequency are unknown in Neotropical army ants, but ecological dynamics such as population density could have an important effect on mating frequency. Previous work on mating frequency was conducted in central Panama on a different subspecies, *Eciton burchellii foreli*, so it is also possible that the subspecific taxonomy represents substantial genetic differences between the groups that may be accompanied by different mating dynamics. Although previous work has found significant genetic caste determination in *Eciton burchellii* (Kronauer et al., 2006), this work is debated due to the confounding effects of patriline shifting (Wiernasz & Cole, 2010), an effect to which our work is also susceptible. Since the observed genotypic bias found by Jaffé et al. (2007) was of very small effect size and tested with a larger sample size, it is not surprising that we failed to recover a similar, weak genotypic bias in caste determination among our samples, if their result is in fact valid (Kronauer et al., 2006).

Along with the demonstrated weak capacity for selective response on paternal genotype, the high rates of mating frequency in *Eciton burchellii* have relevant consequences for morphological evolution of the sterile worker phenotypes on generational time scales. Specifically, since any individual male can only mate once and has a very low chance of contributing any genetic material to a successful reproductive (Kronauer, 2009), response to selection on heritable, patrigenic morphological variation among sterile workers is effectively absent. Of course, this study cannot determine the heritable morphological variation via maternal genotype, as the limitation of a single queen per colony prevents our ability to parse environmental and genetic components of morphological variation without exper-

imental manipulation (Falconer, 1960). Nonetheless, given what is known about the role of hormonal signaling and developmental plasticity in social insects, it is more likely that heritable morphological variation in the worker castes passes through the queen rather than the males (Libbrecht et al., 2013; Simola et al., 2013; Zera, 2006). The lack of heritable morphological variation found in our study only strengthens this hypothesis.

Despite the fact that we recovered heritable variation in our positive control using the *Plethodon* dataset, mating system differences between the *Plethodon* salamanders and *Eciton* army ants may make detection of heritable variation in our army ant dataset more difficult than in the salamanders dataset. The most evident difference between the mating systems is that heritability in the *Plethodon* salamanders was calculated by estimating relatedness of hatchlings from the same clutch, rather than direct genotyping (Adams, 2011). While this avoids the potential issue of error in the inference of paternal genotype, it also confounds other environmental factors shared among clutches, which may be interpreted as heritable variation. The relatedness matrix in our study was constructed by whether paternal and maternal genotype was shared by individual workers, rather than using an estimated genetic distance. Although this may have offered lower resolution than using genetic distance, it is still more genetically accurate than the methodology in the *Plethodon* dataset, by the use of direct genotyping. Lastly, the high rates of polyandry may have additional consequences, particularly if the effect sizes of heritable variation between paternal genotypes differ widely. Specifically, if paternal genotypes with large effect sizes are not sampled sufficiently, the power to detect heritable variation will be hindered.

High rates of polyandry can generate intense sexual conflict from divergent genetic interests of males and females (Chapman et al., 2003; Mank et al., 2013). One relevant explanation to resolve the paradox between the observed mating dynamics in eusocial Hymenoptera and the theoretical expectations of sexual conflict with high variance in male reproductive success is parent-of-origin genomic imprinting (Drewell et al., 2012; Haig, 2000; Reik & Walter, 2001; Gregg et al., 2010). Genomic imprinting is a common result of antag-

onism between the parents over growth and provisioning (Mank et al., 2013), and already known to be responsible for sex determination in a haplodiploid system (Verhulst et al., 2010). While the prevalence of imprinting across eusocial species still needs to be tested, epigenetic modification of specific growth-related loci offers a clear mechanism for resolving sexual conflict in mating systems with a multiply-mated single queen (Drewell et al., 2012; Alvarado et al., 2015). Moreover, if in fact maternal silencing of patrigenes is a common response to sexual conflict, this offers a convenient mechanism that could have been co-opted by queens to control their extended phenotype of sterile workers in highly eusocial organisms (Haig, 2000; Reik & Walter, 2001). In this case, we would not expect to detect any heritable morphological variation derived from the fathers, as patrigenic loci would be silenced.

We suggest that our finding of no detectable heritable morphological variation within our sample is the result of stronger environmental determinants and maternally-transmitted genetic variation, which are responsible for the vast majority of morphological variation. While it is possible that morphological variation in this complex quantitative trait has been decoupled from genetic variation, literature suggests that the trait is likely to be controlled maternally (Libbrecht et al., 2013; Zera, 2006; Nijhout, 2003; Nijhout & Wheeler, 1982). Since simulated data did not incorporate structured sources of morphological variation outside of heritable variation and known plastic variation, it is possible that empirical data may deviate from simulation models. However, with no available evidence that unobserved environmental heterogeneity–such as worker diet during development–is responsible for structured morphological variation in Neotropical army ants, we avoided adding complexity to simulations. Lastly, although our data cannot address whether the maternal influence is a result of maternal genotype or environment, future studies may be able to tease these factors apart by comparing age-standardized cohorts from several queens. More directly, a common garden experiment could clarify maternal influence on worker morphology by exchanging developing individuals between colonies and measuring phenotypic difference.

In summary, we present a new approach that leverages the resolution of GM for detecting

heritable variation in non-model organisms. As evidenced by the application of our method to the empirical data in *Eciton burchellii* and *Plethodon cinereus*, our method can recover heritable variation of very modest effect size (Fig. 8c), as well as properly estimate the detectable effect size for a GM dataset. By using dimensionality reduction, our approach offers a roadmap for estimating detectable effect size of concerted heritable variation with GM data, and is a useful advance for the interpretation of morphological variation in non-model organisms. Specifically, although detectable effect size can also be calculated by simulations with some existing methods (Adams, 2011), our method allows for a more precise detection of shared variation through the use of dimensionality reduction, which we may expect in certain systems with demonstrated allometry like ants. Additionally, by parameterizing and estimating the sources of non-heritable variation—such as measurement error and morphological plasticity as accomplished in this study—our method defines what is possible to detect within a given GM dataset. Although we have taken advantage of the highly polyandrous and haplodiploid mating system in *Eciton burchellii* to exhibit the features of our method, we stress that it can be employed in any organism with known relatedness among groups. Given the many advantages of applying GM to non-model organisms, our simulation-based approach for assessing the statistical power for detecting a range of effect sizes is highly valuable to researchers interested in using GM for quantitative genetics.

5 Colony-specific caste allometry in a top Neotropical predator

Abstract

Understanding the nature of developmental plasticity in natural populations is an issue central to evolutionary biology. Social insects present a unique opportunity to investigate this variation in the morphologically and physiologically distinct individuals known as castes, which are primarily produced through specific environmental cues that trigger differential hormonal signaling during development. The Neotropical army ant *Eciton burchellii* has diverse morphological variation among the castes of each colony, facilitating the study of developmental plasticity within and between distinct colonial environments. Yet, the current basis for defining castes in Neotropical army ants is problematic and prone to sampling bias, making comparative work difficult. Using landmark-based geometric morphometrics, we test the current basis for defining the worker subcastes in *Eciton burchellii*, and find that our data are clearly inconsistent with previous definitions. We then establish a more robust morphological basis for worker subcastes, which provides a methodology that can be extended to other Neotropical army ant species for comparative work. Finally, evaluation of intercolonial morphological variation demonstrates colony-specific caste allometry and corroborates our revised caste definition, suggesting that the individuals produced by this developmentally-plastic pathway are less evolutionarily independent than previously suggested.

Introduction

Understanding how a consistent range of phenotypes can be produced in the face of genetic and environmental variation is a central question in evolutionary biology (Nijhout, 2003; West-Eberhard, 2003; Hallgrmsson & Hall, 2005). Developmental plasticity is defined as the potential for a single individual and genotype to produce different phenotypic outcomes in response to environmental conditions during development (Moczek et al., 2011). Some of the

most striking instances of developmental plasticity are found in social insect societies, where morphologically and behaviorally distinct groups of individuals known as castes coexist and cooperate for colony fitness (Wilson, 1971; Holldobler & Wilson, 1990). The process of caste differentiation during metamorphosis is well-documented in social insects, usually initiating towards the end of larval development in response to environmental cues (Watson et al., 1985; Wheeler, 1986; Rachinsky et al., 1990). In the case of ants, many components of the gene network underlying caste polyphenism have been shown to be conserved across great evolutionary distances, with the expression of key metamorphic hormones at specific developmental switch points determining caste fate (Nijhout & Wheeler, 1996; Abouheif & Wray, 2002). In particular, replicated developmental work has demonstrated that juvenile hormone (JH) expression is the central mechanism responsible for generating caste variation within a colony (Nijhout, 1994; Abouheif & Wray, 2002). Yet, while the role of hormonal signaling in developmental plasticity appears consistent across many ant genera, the variation in morphology associated with this pathway is substantial. For example, many ant species show almost no differences between queen and worker castes, while others show extreme morphological and physiological variation among castes. The Neotropical army ant *Eciton burchellii* exhibits of one of the highest levels of morphological diversity within social insects, exemplified by a large range of size polymorphism in addition to several novel subcastes within the worker caste (Franks, 1985; Powell & Franks, 2005; Powell & Franks, 2006). Yet, previous work has found that the vast majority of size variation is robust to the large degree of genetic variation found among the workers of a single *Eciton burchellii* colony (Jaffé et al., 2007; Wiernasz et al., 2010; Winston et al., 2017b).

Despite the unique opportunity castes offer to study developmental plasticity, the distinguishing features that define castes and subcastes vary widely, making comparative work difficult (Oster & Wilson, 1978). More specifically, the basis of worker subcaste identity in many species—including *Eciton burchellii*—has been motivated by ethological work, but is primarily based on worker size (Franks, 1985; Wheeler, 1991; Powell & Franks, 2005; Powell

& Franks, 2006). While informative for examining ecological function, behavioral characteristics and size alone are not sufficient for defining a morphological basis of caste, which is essential to building a better understanding of the relationship between developmental plasticity and evolutionary novelty (Emlen & Nijhout, 2003). Furthermore, it is uncertain whether or not the groupings are truly discrete entities, which necessitates a quantitative framework for morphological delineation. This is important to ascertain, since the degree to which subcastes are truly discrete may fundamentally impact their morphological evolution (Nijhout, 2003; Wagner, 2014).

Evidence suggesting that the worker subcastes of *Eciton burchellii* are in fact discrete and distinct entities has been tied to the distribution of worker body sizes in a colony, known as the size-frequency distribution (Franks, 1985). Although there is previous work supporting the use of the size-frequency distribution for defining castes and subcastes (Oster & Wilson, 1978; Holldobler & Wilson, 1990), in practice using this for caste definition is highly problematic in that biased or sparse sampling of individuals can lead to misleading breaks in size, and thus to faulty inference as to the discreteness of subcastes (Schöning et al., 2005). Furthermore, this problem is exacerbated by the large size of colonies of *Eciton burchellii* (Burchill & Moreau, 2016), where worker subcastes are not distributed evenly throughout the colony, and the sample size used to estimate the size-frequency distribution is often orders of magnitude smaller than the colony size itself (Franks, 1985; Kaspari & Vargo, 1995). Lastly, defining the modality of the sampled distribution is a difficult quantitative problem even without the known sampling biases (McLachlan & Peel, 2004), and previous work utilizing this approach has taken a qualitative approach without clearly defining the criteria for applying this framework (Franks, 1985). Thus, given these issues, defining caste identity from consistent morphology is a more straightforward approach (Schöning et al., 2005).

The strong relationship between size and morphological variation in caste systems presents a useful foundation for exploring developmental plasticity in social insects (Emlen & Nijhout,

2000). Since caste induction is accomplished by maintaining larval growth while arresting developmental stage via hormonal signaling (Libbrecht et al., 2013), size and morphology are inexorably coupled in both queens and workers through an allometric scaling relationship (Emlen & Nijhout, 2000). Discontinuity in scaling relationships can be informative for determining the developmental underpinnings of plastic variation (Nijhout, 2003). Consequently, identifying discontinuity in shape at the boundaries between castes can inform us about underlying developmental mechanisms, and suggest switches in developmental pathways that may have been canalized by evolutionary mechanisms (Nijhout, 2003). Likewise, assessing discontinuity in size between castes is critical to exploring discrete variation, because discrete shape variation generated from discontinuity in size may arise merely from discrete environmental input—such as differential larval nutrition—rather than any fundamental change to the developmental mechanisms (Nijhout, 2003). Thus, discontinuity in scaling relationships is a central part of the morphological basis of caste, and work on the role of hormonal signaling provides a conceptual framework for interpreting morphological variation (Nijhout & Wheeler, 1982; Wheeler, 1991; Libbrecht et al., 2013).

To investigate the morphological basis of the worker caste in *Eciton burchellii* and the intercolonial variation necessary for natural selection, we quantify size and shape variation using geometric morphometrics (GM). This detailed study of variation is then used to test two central questions: First, we ask whether our GM data reveal true polyphenism among the sterile workers—with two or more discrete phenotypes produced by the same genotype, as predicted by previous claims of worker subcastes—or whether the data instead suggest that all observed sterile workers are the product of a single, continuous developmental reaction norm. Second, we ask whether there is detectable morphological variation between colonies, and what type of modification to ontogenetic process is likely responsible for any such intercolonial variation. We interpret our results in light of what is known about developmental plasticity in social insects and generate several testable predictions for future integrative work.

Methods and Results

Landmark data and error analysis for geometric morphometrics

Specimens from two distinct colonies of *Eciton burchellii* were collected in the Area de Conservación Guanacaste of Costa Rica ($N_{Colony1} = 89; N_{Colony2} = 98$). Collections were taken from the colony bivouac and the raiding columns, and specimens for this study were sampled from these collections. All specimens were pin-mounted for imaging on a Leica Z6 APO image stacking system. All images of head capsules were oriented on the anteroposterior axis by placing the clypeus and the occiput in the same focal plane. Lateral orientation was accomplished by placing both eyes in the same focal plane (Fig. 11). Images from different focal points were merged into a tomographic composite using the Leica Application Suite v3.8 for both the head capsules and the bodies (Fig. 11). Images were then imported into ImageJ 1.46 (Rasband, 1997) for digitization of landmark coordinates.

Two-dimensional coordinates of 14 landmarks were digitized across the dorsal surface of the head (Fig. 11; Table 5). Landmark selection was based on morphological features previously used in taxonomic literature and adapted to features and variation specific to the *Eciton* genus (Ward, 1989). The landmarks summarize the shape of head features established to have ecomorphological significance (Powell & Franks, 2006). Error associated with data collection was evaluated by orienting and photographing each of 91 head samples twice. Comparison of landmark data digitized from these replicate images served as a measure of the impact of inconsistency in mounting and in landmark placement on measuring morphological variation. Shape and size variation due to such error was close to two orders of magnitude less than shape and size variation among individuals (Appendix C3: Fig. S1; SI. 1), and error was therefore deemed to be negligible.

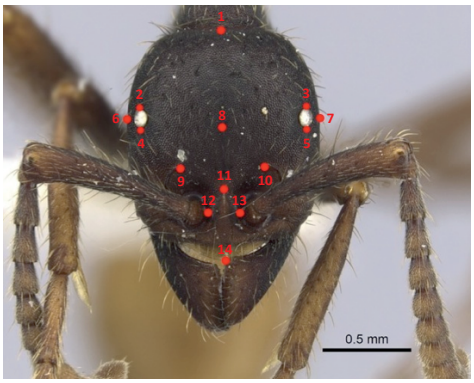

Figure 11: Landmark placement for geometric morphometric analysis. Red dots indicate location of 14 landmarks on head. Description and justification of landmarks on head given in Table 5.

Size as the morphological basis of worker subcaste delimitation

Size data are traditionally used to delimit worker subcastes in ants. In *E. burchellii*, a quadrimodal size-frequency distribution of head width formed the basis of distinguishing minor, media, submajor, and major subcastes (Franks, 1985). We tested for the existence in our GM data of distinct size-clusters representing these four worker subcastes in each colony. First, we calculated the appropriate inter-landmark distance for a linear measurement of head width (HW) to try and reproduce the quadrimodal size-frequency distribution of Franks (1985) with the same variable (Fig. 12). Since the usual measure of size for GM data is centroid size (CS; the square root of the sum of squared distances between each landmark and the centroid of the landmark configuration), we took the head width values most commonly used to distinguish subcastes (Minors: HW $<$ 1.16 mm; Media: 1.27 mm $<$ HW $<$ 1.72 mm; Submajors: 1.84 mm $<$ HW $<$ 2.51 mm; Majors: HW $>$ 2.63 mm; Franks, 1985; Jaffé et al., 2007) and for each calculated the corresponding value of CS (SI. 2). This resulted in expected CS ranges for the putatively discrete subcastes, which were the means of the corresponding CS values (Minors: CS $<$ 2.05; Media: 2.05 $<$ CS $<$ 2.82; Submajors: 2.82 $<$ CS $<$ 3.51; Majors: CS $>$ 3.51).

Our data did not support the existence of four size-distinct worker subcastes in either colony. General density plots of CS (Fig. 12a) and HW (Fig. 12c) reveal no evidence for size discontinuity between the previously recognized subcastes. The possibility that the

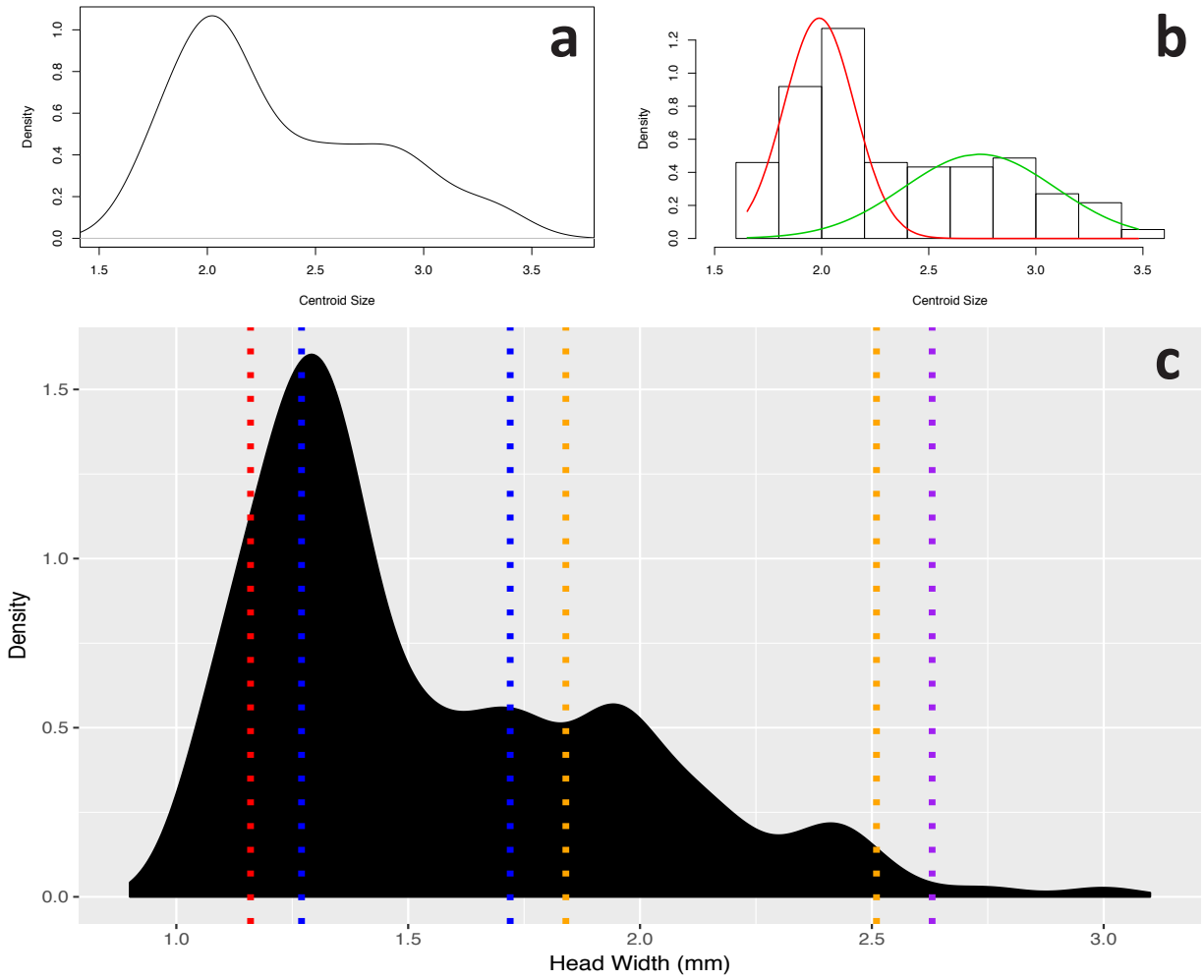

Figure 12: Density distributions of (a) centroid size, (b) maximum likelihood estimate of finite mixture model of centroid size, and (c) head width among worker subcastes for Colony 1. (a) Size frequency spectrum for sampled *E. burchellii* workers. Note the absence of any size discontinuity at the border between minor-media and submajors (indicated by dotted line) in the pure density distribution of centroid size of head data for all specimens. (b) Despite previous studies suggesting a quadrimodal distribution for E. burchellii workers, the MLE of the finite mixture model shows two mixture components (red and green curves) across four putative subcastes, which are not congruent with previous worker subcaste breakpoints. (c) Measurement of head width (HW) taken from inter-landmark distances contained within geometric morphometric measurements for 89 samples from Colony 1. Colored dotted lines show the limits of HW for worker subcastes as previously suggested by Franks (1985): Red = largest HW for minor subcaste (1.16 mm), blue = lower (1.27 mm) and upper (1.72 mm) bounds of HW for the minor-media subcaste, orange = lower (1.84 mm) and upper (2.51 mm) bounds of HW for the submajor subcaste, and purple = smallest head size (2.63 mm) for the major subcaste. Note that the quadrimodal distribution found in Franks (1985) is not recovered here, and that there are several specimens between the bounds of each worker subcaste.

Landmark	Description	Justification
1	Occiput	Part of Head Length measurement
2	Right Eye (Posterior)	Part of Right Eye Length measurement
3	Left Eye (Posterior)	Part of Left Eye Length measurement
4	Right Eye (Anterior)	Part of Right Eye Length measurement
5	Left Eye (Anterior)	Part of Left Eye Length measurement
6	Right Head Margin	Part of Head Width measurement
7	Left Head Margin	Part of Head Width measurement
8	Central Carina (Posterior)	Defines relative area of head musculature
9	Right Carina (Posterior)	Defines action of antennae
10	Left Carina (Posterior)	Defines action of antennae
11	Supraclypeal Area (Centroid)	Defines expansion or contraction of clypeus
12	Right Torulus (Inner margin)	Defines location of antennae
13	Left Torulus (Inner margin)	Defines location of antennae
14	Clypeus (Center of anterior margin)	Part of Head Length measurement

Table 5: Description of head landmarks. Includes justification of landmarks from measurements and terminology commonly used in the ant literature (Bolton, 1994).

distribution was formed from four partially overlapping size-clusters was investigated using a maximum likelihood approach derived from finite mixture coding (Strait et al., 1996; Hunt & Chapman, 2001), implemented in the R package mixtools (Benaglia et al., 2010; R Core Team, 2016). Using a three-step goodness-of-fit approach, the method estimates the most likely mixture of normal density distributions for the continuous dataset. This method has the advantage of both estimating the number of distributions that the data came from, and estimating the density function at the area of the putative gap in size variation. Thus, we would expect a lower density value at the supposed size break between putative subcastes. Again, there is no evidence for size discontinuity between the submajor and media subcastes, nor between the minor and media subcastes (Fig. 12b). Since our sample size for majors was small ($N = 6$), it gave us little power to distinguish that subcaste. Instead, the maximum likelihood estimate (MLE) was a mixture of two normal distributions, and the parameters for the MLE of the finite mixture model suggest heavy density in the size gaps between minors, media, and submajors $[\lambda_1 = 0.60, \lambda_2 = 0.40, \mu_1 = 1.99, \mu_2 = 2.78, \sigma_1 = 0.20, \sigma_2 = 0.33]$. Additionally, as a non-parametric test of gap size, we rank-ordered the gaps (i.e. distances between adjacent measures) within the entire dataset and compared the gaps associated

with the putative discontinuities with the rest of the distribution (Appendix C3: Fig. S2). Neither the gap between the media and submajors (gap = 0.018; p = 0.17) nor the gap between the minors and media (gap = 0.0015; p = 0.83) was unique within the dataset. Results are presented only for Colony 1, but were consistent across both colonies.

The differences between our data and those of Franks (1985) are surprising. Our study has little statistical power to detect any differences between the submajor and major subcastes (see above), and this might account for some of the incongruence between the studies. Some incongruence might result from artifacts associated with sampling a non-uniform distribution of workers across a large colony: Although both studies involved considerable sampling effort ($N_{Colony1} = 89$ and $N_{Colony2} = 98$ in the present study; $N = 573$ in the Franks study), *Eciton burchellii* is known to have colony sizes of several hundred thousand workers (Kronauer, 2009), so sampling in both studies is around three orders of magnitude lower than the true worker population. Nevertheless, our data for both head width and centroid size call into question the generality of the subcaste-defining size gaps between minors, media, and submajors found by previous researchers (Franks, 1985; Schöning et al., 2005).

Shape as the morphological basis of worker subcaste delimitation

To evaluate the possibility of delimiting worker subcastes based on shape alone, we applied principal components analysis (PCA) to our GM data. Since PCA is an exploratory method, the presence of any discrete clusters of data on the primary axes of variation (principal components, PCs) would indicate that those clusters (subcastes) could be delimited based solely on shape. A morphospace of the first three PCs indicated no clear clustering of discrete groups that could be used for worker subcaste delimitation (Fig. 13; the major subcaste was excluded from this shape analysis due to low sample size). While specimens that would traditionally be assigned to the media and submajor worker subcastes demonstrated separation along PC1, this effect of allometry was expected due to the fact that the worker subcastes are traditionally defined by size (see above) and that PC1 correlates strongly with

size. No distinct clusters of specimens are evident along PC2 (Fig. 13a) or PC3 (Fig. 13b). The relationship between PC1 and PC3 does, however, reveal an interesting shift in allometry (Fig. 13b)—switching from a positive to a negative relationship at intermediate scores on PC1—that will be discussed in the following section. There is no clear evidence from PCA that each subcaste is characterized by having a distinct shape.

In order to further assess whether subcastes are discretely different in shape, we performed pairwise comparisons of shape among specimens and compared the difference in shape against the difference in size. Difference in shape between forms is quantified as partial Procrustes distance, the square root of the sum of the summed Euclidean distances between corresponding landmarks of two configurations that have been placed in partial Procrustes superimposition (Bookstein, 1991). If subcastes differed markedly in shape but exhibited similar (or overlapping) size distributions, then at least some of these pairwise comparisons would reveal a combination of large difference in shape and low difference in size. No such combination is evident in our data (Appendix C3: Fig. S3). This demonstrated lack of discrete breaks in size and shape suggests that if there are clear differences between the worker subcastes, then they are likely produced by the interaction of size and shape, in the form of distinct caste allometry.

Allometry as the morphological basis of worker subcaste delimitation

Previous work has suggested that differences in allometry exist between the media and submajor subcastes of *Eciton burchellii* (Franks, 1985; Powell & Franks, 2006). Exploratory analysis of our GM data also revealed a marked difference in allometry of the head capsule between small and large specimens (Fig. 13b). We therefore performed a more detailed series of analyses to determine the nature of the allometric trajectory of the head case, and to test whether any shifts in that allometric trajectory coincided with previously reported size transitions between worker subcastes (Franks, 1985; Powell & Franks, 2006). The nature of the allometric trajectory was determined by calculating the difference in shape and size

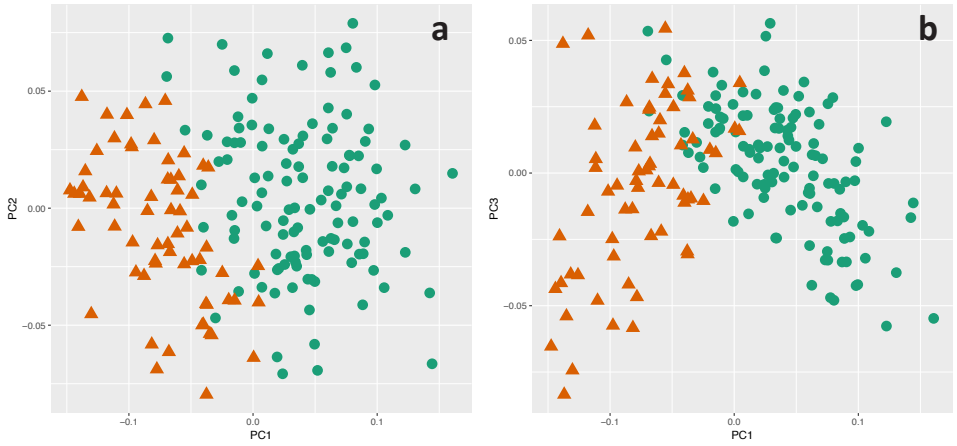

Figure 13: Distribution of submajor and minor-media subcastes among top three principal components for all specimens. (a) Morphospace plot of principal component 1 (PC1) and principal component 2 (PC2). (b) Morphospace plot of principal component 1 (PC1) and principal component 3 (PC3). PC1 explains 57.2% of the variance in the morphological data, PC2 explains 12.4%, and PC3 explains 8.3%. Green circles indicate the minor-media subcaste, orange triangles indicate the submajor subcaste, as defined by head width. Note the lack of discrete, distinct regions in morphospace corresponding to the castes.

between each specimen and a reference form (here defined as the smallest member of the media subcaste within each colony). The difference in shape was described by the uniform and partial warp scores calculated after partial Procrustes superimposition of the landmark configurations (for explanation of these variables see Webster and Sheets (2010) or Zelditch et al. (2012), and references therein; for recent applications of this technique using the head shield of other arthropods see Webster (2007, 2015)). A change in allometric trajectory was identified as a change of slope in the regression of the uniform and partial warp scores (the shape variables) against log-transformed centroid size. Analyses were performed on each colony separately, using the shapes package in R (Dryden & Mardia, 2016).

These analyses revealed three distinct subcastes that were only partially congruent with the standard definitions. In particular, a distinct allometric breakpoint between the media and submajor subcastes was recovered in several independent warp scores (see also Fig. 14), but the size with which this shift in allometry was associated (CS $\sim$ 2.39 or log(CS) = 0.87) was equivalent to a head width of 1.59mm, and thus was not concordant with previously defined breaks (Franks, 1985). This same breakpoint was recovered in both colonies. We stress that this breakpoint does not represent a gap in worker size, but rather a distinct shift

in worker allometry that is conserved across colonies. Furthermore, there were no distinct breakpoints between the minor and media subcastes, suggesting that these subcastes share the same allometry, and are neither distinct nor discrete groupings. Since there is no clear distinction in shape or size-frequency between the media and minor individuals in our data, both subcastes are considered as a broader category of the minor-media subcaste. Although majors were excluded from shape analysis due to small sample size, it is likely from previous work that they may represent a third distinct subcaste (Franks, 1985). These analyses of our morphological data show strong evidence for a continuous size distribution across the minor-media and submajor subcastes, which established the motivation for a morphological basis for defining the worker subcastes (Fig. 14).

Once we had established a common allometric breakpoint for both colonies, we used that breakpoint to define the worker subcastes and test for intracolonial differences in allometry between subcastes (Table 6). First, we compared the allometric trajectories of the minor-media and the submajor subcastes within each colony in order to test whether the breakpoint represented a significant shift in allometric patterning. The allometric trajectory for each subcaste from each colony was quantified as a vector of the regression coefficients calculated from a multivariate regression of the shape variables on geometric size (Webster & Zelditch, 2005). Comparisons of allometric trajectories between subcastes within a colony were performed using VecCompareMac7 (Sheets, 2000). The allometric trajectory of the submajor caste significantly differed from that of the minor-media subcaste within each colony (Table 6).

Taken together, the intracolonial analyses demonstrate that the distinction between minor-media and submajor subcastes is not a distinct size gap—as they fall along a continuous size spectrum—but is instead a significant shift in allometry (Fig. 14). The allometric trajectory as a whole is continuous but distinctly non-linear, with distinct allometric shape deformation which can be visualized by comparing thin plate splines for the minor-media (Fig. 14b) against the submajors (Fig. 14c). Although both shape deformations show

relative increase of head musculature, the increase in submajors is more dramatic, and is accompanied by a broadening—rather than a tightening—of the antennal and clypeal anatomy (Fig. 14b-c). Individuals smaller than 1.60 mm in head width lie along one segment of the kinked trajectory and are herein assigned to the minor-media subcaste, while individuals larger than 1.60 mm in head width lie along the other segment and are herein assigned to the submajor subcaste. This empirically-determined size threshold between the subcastes based on shape data does not correspond precisely to previous empirically-determined size thresholds between subcastes based on size data.

Intercolonial variation in caste allometry

We sought to determine whether and how subcastes could be delimited within a colony using size and shape data for the head case. Conclusions for both colonies were very similar: both exhibited a continuous but non-linear allometric trajectory with the same breakpoint, which can be used to define minor-media and submajor subcastes. The quantitative similarity of caste allometry between the two colonies was further assessed.

We compared the allometric trajectory of the minor-media subcaste within Colony 1 to that within Colony 2 in order to test whether the allometric patterning of that subcaste differed between colonies. This was also done for the submajor subcaste. Methodology followed that for the intracolonial comparison of allometric trajectories except that the two trajectories being compared were of the same subcaste sampled from different colonies. The reference form from which warp scores were calculated was the consensus of the three smallest individuals of that subcaste from Colony 1. Although not presented, results were robust to using the smallest individual from Colony 2. Results demonstrate that, for each subcaste and at 95% confidence, the angle between the allometric trajectories from each colony does not significantly differ from zero (Table 6). The allometric trajectories for a given subcaste from different colonies can therefore be treated as indistinguishable from parallel.

To test whether the trajectories for a given subcaste from different colonies were co-

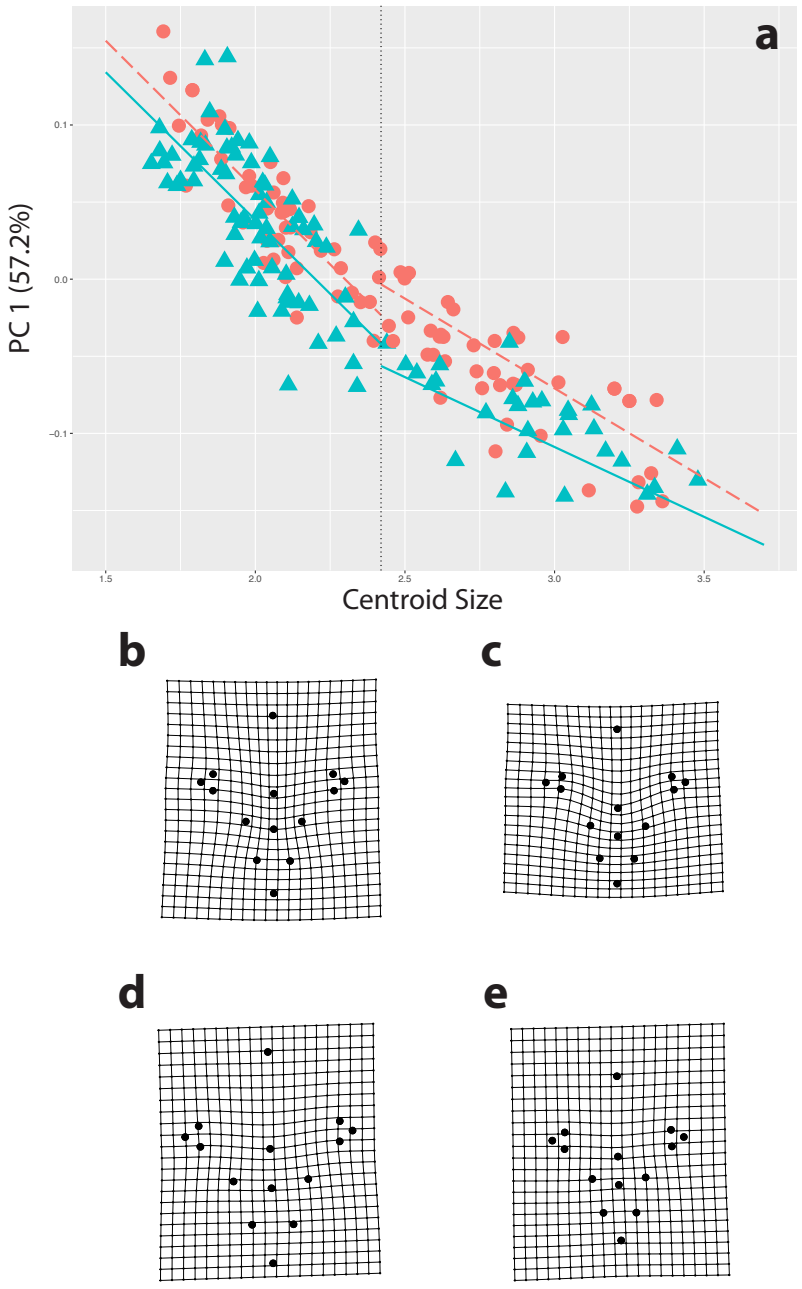

Figure 14: Principal component analysis (PCA) and thin plate splines demonstrating colony-specific caste allometry. (a) PCA was conducted on the partial warp scores of the GM data. The first principal component axis (PC1: 57.2% of the variance) has been plotted against the centroid size of minor-media and submajor individuals, demonstrating clear colony- and caste-specific allometry. Lines are best-fit linear models for each caste and colony. Note when tests use all the variance in the data, slopes are significantly different between castes but not between colonies, and intercepts are significantly different for all comparisons (Table 6). This is reflected here in PC1 as well. Dashed vertical line illustrates empirically-determined size boundary between minor-media and submajor subcastes, red points and dashed line indicate Colony 1, blue points and solid line indicate Colony 2. Thin plate splines represent shape deformation from (b) smallest minor-media to largest minor-media, (c) smallest submajor to largest submajor, (d) mean shape of size-standardized minor-media from Colony 1 to mean shape of size-standardized minor-media from Colony 2, and (e) mean shape of size-standardized submajors from Colony 1 to mean shape of size-standardized submajors from Colony 2. Magnification of thin plate splines is 2 for (b, c), and 3 for (d, e), to aid visualization.

Dynamic Tests

Type	Group	Within Angles (G_1/G_2)	Between Angle	Significant (95%)
Intercolonial	Minor-media	21.7°/23.6°	13.3°	No
Intercolonial	Submajor	27.3°/35.7°	35.0°	No
Intracolonial	Colony 1	23.6°/26.4°	62.0°	Yes
Intracolonial	Colony 2	29.6°/34.7°	83.4°	Yes

Static Tests

Type	Group	Hotelling's T^2	Goodall's F	Bootstrapped F
Intercolonial	Minor-media	F = 2.96, p = 5.29e-5	F = 6.12, p = 0	F = 6.12, p = 0.001
Intercolonial	Submajors	F = 3.32, p = 0	F = 3.94, p = 5.82e-10	F = 3.94, p = 0.001

Table 6: Test results for differences in static and dynamic allometry between worker subcastes and colonies.

incident in addition to being parallel, we performed size-standardization on each sample independently, and then compared the resulting mean forms. To size-standardize, the portion of shape variation within a sample (subcaste) that results from size variation within that sample was analytically removed. This was achieved by performing a multivariate regression of the shape variables (warp scores) on size (log-transformed CS); the residuals of that regression were then added to the predicted form at a given size to produce an estimate of the static (i.e., non-allometric) variation that the entire sample would have exhibited had all specimens been that particular size. Minor-media samples for each colony were size-standardized to a log centroid size (lnCS) of 0.74, and submajor samples for each colony were size-standardized to an lnCS of 1.03: these values are the traditional lower limits of CS for each subcaste. Conclusions were not dependent on the choice of lnCS value for size-standardization. Size-standardization was accomplished using Standard6 (Sheets, 2000); each subcaste was size-standardized separately for each colony. Statistical comparisons of the size-standardized data for all samples were performed in TwoGroup7 (Sheets, 2000). Three statistical tests (Hotellings T^2 test, Goodalls F test, and a bootstrapped F test) all found highly significant differences for both worker subcastes. Results demonstrate that, irrespective of the test employed, the mean shape of the size-standardized minor-media from one colony significantly differed from the mean shape of the size-standardized minor-media from the other colony (Table 6). The same is true for the submajor caste (Table 6). Differences among subcastes in the same colony are much larger compared to the same subcaste across colonies, yet all intercolonial differences were significant (Table 6). Collectively, these

results demonstrate that there is intercolonial variation in caste allometry. This variation can be envisaged as a step-like translation of the non-linear allometric trajectory through morphospace, such that even though the orientation of the trajectory remains unaltered, specimens of a given size significantly differ in shape between the colonies. This is graphically represented in a plot of PC1 against centroid size (Fig. 14a), as well as thin plate splines for both the minor-media (Fig. 14d) and submajor (Fig. 14e) subcastes. Although the intercolonial deformation is more slight than the allometric deformation, it also demonstrates an enlargement of the head musculature and a broadening of the antennal and clypeal anatomy (Fig. 14d-e).

Discussion

Our results for both sampled colonies robustly demonstrate that the minor-media and submajor worker subcastes show significantly different allometric scaling patterns in the same set of GM landmarks placed on the head case (Table 6). Although these worker subcastes were found to follow different allometric trajectories for one of the body regions we measured, they are not discrete in terms of having a distinct size gap between them (Appendix C3: Fig. S2, Fig. S3). Rather, the minor-media and submajor subcastes fall along a continuous but non-linear allometric trajectory. The non-linearity of the trajectory serves as a means by which minor-media and submajor subcastes can be distinguished—a criterion perhaps more robust than subcaste delimitation based purely on size. The continuous nature of the trajectory—lacking distinct jumps in size or shape between subcastes—suggests that the processes controlling subcaste differentiation operate along a continuum. This raises the interesting possibility that subcastes might not be evolutionarily independent: if a particular worker subcaste is subject to selective pressure shaping its morphology, it is conceivable that the response to this selection will affect other worker subcastes due to the high degree of covariation resulting from shared underlying developmental processes (Libbrecht et al., 2013). Such a linkage between the minor-media and submajor subcastes is consistent with

our comparison of caste differentiation among colonies. Analyses of intercolonial variation are interpretable in terms of a step-like translation of an otherwise conserved, continuous, non-linear allometric trajectory (Fig. 14; Table 6): the intercolonial difference is observed in both minor-media and submajor subcastes, and no significant differences in allometric scaling were found across colonies for either subcaste (Table 6).

Extensive work has documented the role of hormonal signaling in the evolution of developmental plasticity among insects (Emlen & Nijhout, 2000). Integrating this body of literature with our results allows us to better understand caste differentiation and evolution in *Eciton burchellii*. Generally, hormonal signaling plays a critical role mediating developmental plasticity, and in social insects it often determines both the pace of development as well as the eventual caste of developing individuals (Nijhout, 2003a; Libbrecht et al., 2013). More specifically, caste induction is accomplished by maintaining larval growth while arresting developmental stage with juvenile hormone (JH) (Nijhout & Wheeler, 1982; Wheeler, 1991; Libbrecht et al., 2013). This JH-driven process fundamentally changes the interior environment of the developing individual through the harboring of nutrients and other hormones—for example, insulin and insulin-like signaling pathways (IIS)—which forms the basis of the relationship between size and morphology in both queens and workers (Libbrecht et al., 2013). Thus, the morphological variation exhibited within many social insect species demonstrates strong allometric scaling precisely due to the mechanisms responsible for the developmental plasticity (Nijhout, 2003b; Turing, 1952).

Despite the large number of individuals in a colony—a minimum of hundreds of thousands—*Eciton burchellii* colonies are restricted to a single queen that produces all sterile workers (Schneirla, 1971). Maternal hormone concentrations in social insect queens have been shown to strongly impact the morphological and physiological outcomes of their progeny (Mousseau & Dingle, 1991; Cahan et al., 2011). Additionally, we know that JH plays an important role in determining caste fate in ants (Abouheif & Wray, 2002), and several studies have shown that shifting the timing of JH signaling can result in substantial changes in form (Stern &

Emlen, 1999; Emlen & Nijhout, 2000). Specifically, differences in the production of JH titer or the sensitivity to JH at the critical developmental time tend to generate a translation of the allometric scaling relationship, rather than a fundamental repatterning of the scaling relationship that is usually produced by rearrangement of pathways downstream of JH (Emlen & Nijhout, 2000). Thus, considering the known role of hormonal maternal effects in social insect development and the type of morphological variation observed in our study, we hypothesize that the most likely explanation for the significant variation between colonies is maternal in nature (Winston et al., 2017b).

Although the genetic or environmental factors behind colony-level morphological variation cannot be determined from this study, future work with careful experimental design could disentangle these mechanisms. One approach for exploring the genetic basis of this variation would be to sample or reconstruct the queen genotype for several colonies and use this to estimate the heritability of the observed variation (Falconer & Mackay, 1996), which has proved successful for other studies demonstrating colony-level trait heritability in social insects (Frohschammer & Heinze, 2009). Given some significant heritable variation, genome-level data could even be leveraged to understand the underlying genetic basis of the putatively heritable, quantitative variation. Although determining environmental factors is more challenging, as the exact environmental factor involved is unknown, given the role of IIS pathways involved in the developmental plasticity of social insects, diet would be a natural factor to explore first. Leveraging quantitative methods for generating dietary ecology data in army ants and the known periodicity of developmental cycles (Schneirla, 1971; Powell & Franks, 2006), analysis could determine whether dietary differences for developing individuals influences quantitative variation between both colonies and worker cohorts.

Regardless of the underlying factors driving colony-level variation in caste morphology, the significant findings from this study demonstrate clear covariation of shape change between the minor-media and submajor subcastes. Combined with strong evidence for a continuous trajectory of worker size between the two castes, and shared breakpoints for distinct allomet-

ric differences, our work suggests that the two subcastes are morphologically coupled, likely constraining independent evolution. Furthermore, our study suggests that defining subcaste identity by the size-frequency distribution alone might have limited general applicability, and that defining subcaste on the basis of allometry offers an alternative and perhaps more robust approach. While our application of this method recovers distinct and significant allometric differences between submajors and minor-media found in previous studies (Franks, 1985), the lack of discrete breaks in size and clear morphological covariation suggests that subcastes should not be treated as independent entities (Nijhout, 2003). Rather, the morphological variation produced by the developmentally plastic pathway should be considered one size-dependent trait for evolution by natural selection.

6 Emergence from subterranean environment shapes Neotropical army ant allometry

Abstract

Eciton army ants are top predators in Neotropical leaf litter communities, composed of large colonies of sterile workers that collectively hunt, kill, and transport their prey. Among the sterile worker caste, *Eciton* species have morphologically and physiologically distinct worker subcastes with specialized roles within the colony. Previous work on dietary ecology has demonstrated a relationship between the morphological diversity in the worker caste and species ecology. In order to investigate the role of ecological and phylogenetic factors on the morphological evolution of the worker caste in *Eciton* species, 709 specimens from eight Neotropical army ant species were imaged and analyzed using geometric morphometrics (GM). In addition, seven ecological characteristics for all species were compiled and synthesized with the recently available phylogenetic context of Neotropical army ants. Results from ancestral state reconstruction unambiguously show that the origin of the novel major worker subcaste coincided with a transition from hypogaeic to epigaiec nesting and foraging. Furthermore, data clearly illustrate a significant morphological shift with the transition out of the subterranean environment, as well as a possible example of convergent allometry associated with a return to subterranean lifestyle. Lastly, to understand the importance of microevolutionary variation in Neotropical army ant evolution, vectors of evolutionary divergence were compared to vectors of species allometry. Results show worker caste morphology preferentially evolves along existing axes of allometric scaling, demonstrating support for developmental plasticity as a means of macroevolutionary change.

Introduction

Novel traits do not arise randomly in time and space, and therefore, identifying the factors that promote innovation is central to evolutionary biology (Wagner, 2014, Jablonski, 2005).

Furthermore, since evolutionary novelty generally occurs on a macroevolutionary scale, the spatiotemporal patterns associated with generation and modification of these novel traits are often significantly different than those at species levels (Jablonski, 2000; Jablonski, 2007). Simultaneously, developmental plasticity has been intimately linked to the origins of evolutionary innovation (Moczek et al., 2011; West-Eberhard, 2005), as many innovations of macroevolutionary significance are also facultatively expressed in closely-related lineages (Abouheif & Wray, 2002; Scoville & Pfrender, 2010; Pfennig et al., 2010; Rajakumar et al., 2010; Powell & Franks, 2006). Some of the most striking examples of both evolutionary novelty and developmental plasticity are found in social insect societies, where division of labor leads to the coexistence of morphologically and behaviorally distinct individuals known as castes (Wilson, 1971; Holldobler & Wilson, 1990). Hormonal signaling plays a universal ontogenetic role mediating developmental plasticity, and in social insects it often determines both the pace of development as well as the eventual caste fate (Libbrecht et al., 2013; Nijhout, 2003). Yet, despite the conservation of the hormonal signaling pathway in social insects (Abouheif & Wray, 2002), the variation in morphology associated with this pathway is substantial, demonstrating diverse evolutionary novelty across ants (Powell, 2008; Powell & Franks, 2005; Wheeler & Nijhout, 1984; Franks, 1985). Neotropical army ants (genus: *Eciton*) exemplify this morphological diversity, with a large range of size polymorphism in addition to two novel subcastes within the worker caste (Franks, 1985; Powell & Franks, 2005; Powell & Franks, 2006).

An *Eciton* colony is composed of hundreds of thousands of sterile workers, all produced by a single queen, mated multiply to several males (Kronauer, 2009; Winston et al., 2017b). Within the sterile worker caste, *Eciton* species contain multiple, morphologically-distinct worker subcastes, which are critical to their efficiency as obligate-cooperative predators (Franks, 2001). Each subcaste plays a different role within the colony during cooperative raids (Schneirla, 1971). For example, the major subcaste—also referred to as soldiers—is found in higher abundance in the nest and near captured prey, in order to defend these

resources from scavengers (Gotwald, 1995). The submajor subcaste on the other hand is specialized for transport of large, bulky prey and only occurs in the *Eciton* species with the broadest diet (Franks, 2001; Powell & Franks, 2005; Powell & Franks, 2006). Lastly, the media and minor subcastes are found throughout the colony, and tend to have the broadest array of behaviors (Schneirla, 1971; Gotwald, 1995). This can include several novel behaviors, such as a collection of individuals building bridges composed of their own bodies for more direct transporting routes (Garnier et al., 2013), or single ants mending rough terrain as pothole plugs (Powell & Franks, 2007). Together, the teams are superefficient, in that they carry prey items heavier than the sum of what the members could carry alone (Franks et al., 1999). The relationship between size and morphology is direct, as each worker subcaste has a defining size range (Franks, 1985; Winston et al., 2017b). Furthermore, the distinct morphologies, physiologies, and behaviors of the different subcastes are produced by a developmentally plastic pathway, with hormonal signaling known to play an important role as the proximal mechanism of caste determination (Abouheif & Wray, 2002).

Size and allometry are central to the developmental plasticity that determines and differentiates castes in ants (Trible & Kronauer, 2017). Caste induction is accomplished by maintaining larval growth while arresting developmental stage with juvenile hormone (JH) (Nijhout & Wheeler, 1982; Libbrecht et al., 2013; Wheeler, 1991). This JH-driven process fundamentally changes the interior environment of the developing individual through the harboring of nutrients and other hormones—for example, insulin and insulin-like signaling pathways (IIS)—which forms the basis of the relationship between size and morphology in both queens and workers (Libbrecht et al., 2013). Thus, the morphological variation exhibited within many social insect species demonstrates strong allometric scaling precisely due to the mechanisms responsible for the developmental plasticity (Nijhout, 2003b). It has been proposed that different components underlying plastic regulatory systems—such as those found in Neotropical army ants—can evolve independently of one another, thereby diversifying the evolutionary trajectories and leading to novel, adaptive phenotypes (Moczek

et al., 2011). Given the established role of size in caste development, it is likely that this process in social insects occurs by modifying the allometric relationships of caste-associated traits, producing mosaic phenotypes that combine traits observed in existing castes (Trible & Kronauer, 2017; Molet, Wheeler, & Peeters, 2012). Moreover, artificial selection experiments and a great number of comparative studies have shown that allometries in holometabolous insects can evolve quite rapidly, perhaps leveraging existing developmental potential to generate novel phenotypes (Emlen & Nijhout, 2000).

The degree to which microevolutionary variation is congruent with macroevolutionary change is a contentious topic that has attracted a plethora of interdisciplinary work (Jablonski, 2000; Schluter, 1996; Hunt, 2007; Renaud et al., 2006; Badyaev & Foresman, 2000; Eroukhmanoff & Svennson, 2008; Marriog & Cheverud, 2001). More specifically, it is unclear whether abundant within-population variation actually facilitates long-term evolutionary divergence (Hunt, 2007; Eroukhmanoff & Svensson, 2008; Merila & Bjorklund, 1999). Yet, despite the uncertainty on the continuity of evolutionary processes across scales, several studies have documented a link between these disparate spatiotemporal scales. Schluter (1996) provided an early link between micro- and macroevolution in demonstrating the repeated tendency for morphological differentiation between species to be biased in the multivariate direction of greatest additive genetic variance. This effect was shown to decay over evolutionary time, but persisted despite the presence of natural selection for millions of years. Similarly, Hunt (2007) used a paleontological approach to demonstrate that the ostracode genus *Poseidonamicus* preferentially moved in directions of high phenotypic variation through deep time, also noting that the influence weakened with increasing phylogenetic distance. Renaud et al. (2006) revealed within rodent lineages that the direction of high phenotypic variation was important, but could be overwhelmed by a strong selection regime, making the case that the persistence of genetic constraints may depend greatly on ecological context. Thus collectively, while the relationship between intra- and interspecific phenotypic variation depends on the context, research has demonstrated the influence of both ecology

and phylogeny.

The ecological factors that influence the roles of Neotropical army ants as cooperative predators are numerous (Perez-Espona et al., 2012; Bulova et al., 2016; von Beeren et al., 2016; Rettenmeyer et al., 2011; ODonnell & Kumar, 2006; Wrege et al., 2005). For over 60 million years the ancestors of Neotropical army ants lived and hunted in the subterranean environment, before the epigaiec predation associated with the Neotropical army ant genus *Eciton* arose (Bulova et al., 2016; Brady, 2003; Brady et al., 2014; Winston et al., 2017a). The hypogaeic lifestyle posed different challenges and ecological pressures than those above ground, the results of which can be observed in concerted morphological and physiological evolutionary transitions (Bulova et al., 2016; Franks et al., 2001; Powell & Franks, 2005). More specifically, the transition to hunting above ground from subterranean predation involved new parasites and competition for food (Rettenmeyer et al., 2011; Wrege et al., 2005), direct exposure to environmental fluctuations (Baudier et al., 2015; Meisel, 2006; ODonnell & Kumar, 2006), increased light exposure (Bulova et al., 2016), as well as diet expansion in some epigaeic species (Powell & Franks, 2006). Considering the many concerted morphological changes found in a similar transition out of the subterranean environment in Old World army ants—such as increased head width, antennal length, leg length, and mandible length—we might expect similar convergent changes in Neotropical army ants (Schöning et al., 2005). Furthermore, it has been posited that once the evolution of adaptive specializations allowing for diet expansion have become entrenched, that they cannot be undone (Brady, 2003). Specifically, it has been suggested that the specialist Neotropical army ant *E. rapax* is the ancestral species in the group, probably resembling the smaller colonies of the ancestral *Eciton* (Burton & Franks, 1985), although recent phylogenetic work has shown this to not be true (Winston et al., 2016). Given the various ecological roles found within *Eciton* and established ecomorphological relationships within the worker caste (Powell, 2005; Powell & Franks, 2006), the genus represents a unique opportunity to explore the macroevolutionary impact of a major environmental transition on developmental plasticity.

For the first time, a thorough species-level phylogeny of *Eciton* army ants has been inferred, allowing for rigorous comparative work (Winston et al., 2017a). We collected, imaged, and performed geometric morphometric analysis on the head cases of 709 individuals from eight Neotropical army ant species, producing a large morphological dataset for comparing within-species variation produced by a known developmental pathway. We also compiled relevant ecological metadata for all Neotropical army ant species in the study and apply these data to the newly available phylogenetic reconstruction. In order to explore the role of ecological and phylogenetic factors on worker caste allometry, we ask the following four questions to understand the evolution of morphological variation within *Eciton*. First, given known ecomorphological relationships (Powell & Franks, 2006) we ask whether worker caste allometry among Neotropical army ant species is significantly different between species. Next, we ask whether there is significant morphological change associated with the transition between subterranean to epigaeic environments. Third, we ask whether there is evidence of constrained evolution of worker caste allometry in Neotropical army ants. Lastly, we ask whether evolutionary divergence in *Eciton* tends to preferentially evolve along the axes of allometric variation. Together, our study provides a comprehensive understanding of the evolution of morphological and developmental plasticity in top predators.

Methods

Data Collection

Samples for the study were collected from several locations across the Neotropics between December 2010—January 2015 (Appendix C4: Fig. S1). Collections were sampled from the colony bivouac and the raiding columns, and all specimens for this study were subsampled from these collections. In total, we collected and prepared 709 individual sterile workers for downstream analyses, sampled from 19 colonies of 9 distinct lineages from 8 established *Eciton* species and one closely related genus (Appendix C4: Table S1). All specimens were pin-mounted for imaging on a Leica Z6 APO image stacking system. All images of specimen

head capsules were oriented as according to Winston et al. (2017b). Briefly, this included orientation on the anteroposterior axis by placing the clypeus and the occiput in the same focal plane, and lateral orientation by placing both eyes in the same focal plane.

Following the landmark configuration of Winston et al. (2017b), two-dimensional coordinates of 14 landmarks were digitized across the dorsal surface of the head. Landmark selection was based on morphological features previously used in the taxonomic literature and adapted to features and variation specific to the *Eciton* genus (Ward, 1989). The landmarks summarize the shape of head features previously established to have ecomorphological significance (Powell & Franks, 2006). Two-dimensional coordinates of a further nine landmarks were digitized across the lateral surface of the body, also known as the mesosoma. Error in imaging and landmarking has been previously established to be negligible (Winston et al., 2017b).

Ecological Metadata

In order to understand the influence of ecological factors on morphological evolution in Neotropical army ants, we compiled seven ecological and three additional morphological characteristics for each species in our study (Table 7) from the relevant literature (Appendix C4: Table S3). The three morphological characteristics compiled were whether each species contained the presence of the minor-media, submajors, and major worker subcastes as defined in the literature. Ecological metadata included nesting environment, foraging environment, time of day of foraging, colony size, dietary ecology, range size, and raiding type. Environmental metadata consisted of a subset of the first two variables in the ecological metadata—nesting and foraging environments. Definitions of ecological variables can be found in Appendix C4: Table S3.

Ecological

Variable	Data Type	Definition
Nesting Environment	Binary	Indicates if species is known to nest above-ground
Foraging Environment	Binary	Indicates if species primarily hunts above-ground
Foraging Time	Binary	Indicates if species hunts primarily diurnally
Colony Size	Numeric	Estimated number of workers in a colony
Dietary Ecology	Discrete Ordinal	Higher number equates to greater breadth of diet
Raiding Type	Binary	Indicates if raids are swarm or column
Range Size	Numeric	Estimate of Log Area (km^2)
Morphological		
Variable	**Data Type**	**Definition**
Minor-media Subcaste	Binary	Indicates presence of minor-media subcaste
Submajor Subcaste	Binary	Indicates presence of submajor subcaste
Major Subcaste	Binary	Indicates presence of major subcaste

Table 7: Ecological and morphological variables collected for this study.

Phylogenetic Inference and Ancestral State Reconstruction

We leveraged the phylogeny from Winston et al. (2017a) for delineating lineages and species relationships in our study. For use in our study, we dropped tips in the highly-supported phylogeny to a single sample for each distinct lineage defined by Winston et al. (2017a).

We estimated ancestral character states for discretely valued traits using a continuous-time Markov chain model, commonly known as the Mk model using the *ape* package (Paradis et al., 2004) in R (R Core Development Team, 2017). For robust inference of the ancestral states, we performed reconstruction with three models of different complexity: (1) an equal rate model (ER), (2) a symmetric rates model (SYM), and (3) an all-rates-different model (ARD). For continuous traits, maximum likelihood estimation was performed (Pagel, 1994).

We also implemented stochastic character mapping—a Markov chain Monte Carlo (MCMC) approach to sample character histories from their posterior distributions (Huelsenbeck et al., 2003; Bollback, 2006). Stochastic character mapping was implemented in the *phytools* R package (Revell, 2012). For all unknown character states, flat priors were assigned to these tips, as suggested by Revell (2012). For each trait we ran 1,000 simulations, and the percentage of simulations for each trait state were inferred at each node was then plotted as a pie chart on our maximum clade credibility tree. We also assessed the evolutionary lability

of each trait using this approach, which returns the inferred number and type of changes occurring across the phylogeny for each trait.

Breakpoint Analysis

We examined plots of shape variables versus log-transformed centroid size to determine whether the known worker subcastes demonstrated changes in allometric slope (Winston et al., 2017c). The shape variables used in the analysis were the uniform and partial warp scores, calculated from a Procrustes analysis of landmark data for each colony. The smallest member of the minor-media subcaste was used as the reference form for analyses for each colony. To evaluate putative differences in allometric slope, locally-weighted scatterplot smoothing (LOWESS) was implemented with the R 'stats' package (R Core Team, 2016; Winston et al., 2017b). LOWESS curves for all 28 uniform and partial warp scores were inspected for linear allometry, and subsequently, any consistent shifts in demonstrated allometry at a particular centroid size (Loy et al., 2001).

Testing Worker Caste Allometry

After defining caste with our breakpoint analysis as per Winston et al. (2017c), it was necessary to establish whether worker caste allometry differed significantly between Neotropical army ant species. Differences in allometry between Neotropical army ant species were tested using a Procrustes regression and ANOVA with permutation procedures, including a homogeneity of slopes test (Adams & Collyer, 2009). These tests were performed using the *'procD.allometry'* function in the *geomorph* package (Collyer & Adams, 2013). In order to assess the similarity of worker caste allometry between species, tests were performed together as a group, as well as with pairwise comparisons.

We performed Procrustes regression to test for significant allometry of all the worker subcastes together, as well as individual worker subcastes in the dataset. Likewise, the putative differences in allometry between species were tested both using the entire worker

caste allometry and the individual worker subcastes. By testing the individual worker subcastes, we were able to understand the degree to which caste differences between species were constrained to one another.

Allometric Trajectory Analysis

Standard multivariate analyses alone are not sufficient for understanding how shape changes, and how these changes compare among relevant groupings, such as different species or worker subcastes (Collyer & Adams, 2013). In order to explore the relevance of ecological and phylogenetic factors on shape change within Neotropical army ants, we employed phenotypic trajectory analysis (PTA) on the allometric variation of the worker subcaste (Collyer & Adams, 2013). Broadly, this method characterizes each allometric trajectory by a multivariate regression of shape (partial warp scores) on size, yielding a vector of shape change (β) for a given change of size. As a vector, β can be geometrically described by its length ($d = |\beta|$) and direction, and compared to the allometric trajectories of other species. Specifically, for our study we employed PTA by comparing vector lengths ($\Delta d = |d_1 - d_2|$), and the angle (θ_β) between each pair of species (Collyer & Adams, 2013; Collyer et al., 2015; Adams & Collyer, 2009; Adams & Collyer, 2007). The angle (θ_β) between two allometric trajectories was calculated as the arc-cosine of the inner product of the two vectors after both were scaled to length (Hunt, 2007; Collyer & Adams, 2013). This application of PTA yielded a useful tool for quantitatively defining allometric change between species, as theoretical expectations for the summary statistics d and have been described in previous publications (Adams & Collyer, 2007; Adams & Collyer 2009).

Evolutionary Divergence

Understanding the path of evolution is a difficult task due to a lack of proper methods for ancestral reconstruction of allometric trajectories (Collyer & Adams, 2013). Thus, ancestral forms were assumed to be intermediate in the most common recent ancestor. To properly

quantify evolutionary divergence between groups, three vectors of evolutionary divergence (z) were calculated (Hunt, 2007): First, the mean evolutionary divergence (z_{mean}); next the evolutionary divergence of the minimum size (z_{min}), which uses the minimum predicted shape for each trajectory; and lastly the evolutionary divergence of the maximum size (z_{max}). Through this approach, evolutionary divergence of the entire trajectory is incorporated, rather than simply the mean shape that would disregard important allometric information. Once vectors of evolutionary divergence (z) were calculated, the direction of these vectors were compared with the vectors of allometric shape change for each of the species (β_1, β_2) used for calculating the three vectors of evolutionary divergence ($z_{min}, z_{mean}, z_{max}$). This was accomplished by calculating the angle (θ_z), defined as the arc-cosine of the inner product of the evolutionary divergence vector (z) and the vector of allometric shape change (β) after both were scaled to length.

Calculation of three vectors ($z_{min}, z_{mean}, z_{max}$) was accomplished using *'pred.val'* and *'shape.predictor'* with *'procD.allometry'* in the *geomorph* R package (Adams & Otarola-Castillo, 2013). Specifically, z_{min} was calculated as the vector of shape change between the predicted shapes based on the species allometry for the minimum size observed in both groups. Likewise, z_{max} was calculated as the vector of shape change between the predicted shapes based on the species allometry for the maximum size observed in both groups. Lastly, z_{mean} was calculated as the vector of shape change between the predicted shape for the mean size between groups. Due to the known strength of allometry in Neotropical army ants (Winston et al., 2017b), we calculated three vectors to ensure that the patterns were robust to the size chosen for evolutionary divergence.

Hypothesis Testing

In order to assess the contribution of phylogenetic and ecological factors to putative differences in morphology, phylogenetic and ecological distance matrices were constructed from the Winston et al. (2017a) ultrametric phylogeny and the ecological metadata (Table 7),

respectively. These distance matrices were used in conjunction with the morphological distance matrix generated from PTA, to quantitatively assess putative influence on shifts in worker caste allometry. Specifically, to test for significance of these factors, mantel tests were applied to the distance matrices, measuring matrix correlation between the factors and morphological change (Legendre & Legendre, 1998; Marriog & Cheverud, 2001). Due to limited sample size and weak allometry, individuals from the major subcaste were not tested as their own group, but were included in tests including all subcastes. All mantel tests were implemented in R, using the *'mantel'* function from the *vegan* R package (Oksanen et al., 2017).

The phylogenetic distance matrix was created using the *'cophenetic'* function in the R package *ape* for each pair of taxa, totaling 15 distances for the submajor subcaste and 28 distances for minor-media subcaste (Paradis et al., 2004). Two ecological distance matrices were created for the analysis: First, an ecological distance matrix constructed from all seven ecological variables ("Ecology"), and second, an environmental distance matrix constructed from the two environmental variables ("Environment"). This environmental distance matrix was motivated by several studies that have demonstrated significant shifts in morphology with the shift from hypogaeic to epigaeic environments (Bulova et al., 2016; Powell & Franks, 2006; Franks et al., 2001).

Phylogenetic signal was also tested by using generalized K statistic (K_{mult}) for high-dimensional multivariate data (Adams, 2014). For each worker subcaste, the predicted shape for three separate sizes—minimum size, mean size, and maximum size—was estimated with shape.predictor from the geomorph R package for all species (Adams & Otarola-Castillo, 2013). This approach ensured that each representative sample was of the same comparable size, removing the known effects of allometry. Once each predicted triplet was produced for each worker subcaste for all species, physignal from geomorph (Adams & Otarola-Castillo, 2013) was employed to test for significance with the phylogeny from Winston et al. (2017a).

To test whether the vectors of evolutionary divergence ($z_{min}, z_{mean}, z_{max}$) between two

		Size		*Species*		*Size-Species*	
Worker Subcaste	N	R^2	p	R^2	p	R^2	p
All	709	0.32	0.001	0.29	0.001	0.05	0.001
Minor-media	434	0.21	0.001	0.40	0.001	0.05	0.001
Submajor	202	0.17	0.001	0.43	0.001	0.02	0.003
Major	53	0.04	0.09	0.51	0.001	-	-

Table 8: Results from group comparisons of worker caste allometry. Statistics shown for all workers, minor-media subcaste, submajor subcaste, and major subcaste.

species were overlapped significantly in the direction of maximum variation—the allometric axis—the angle (θ_z) between each vector of evolutionary divergence (z) and each allometric trajectory (β) was calculated as the arc-cosine of the inner product of the two vectors after both were scaled to length (Hunt, 2007). To test for significance, the distribution of angles (θ_z) was compared against a null distribution (θ_{null}) generated by computing the angle of 10,000 pairs of random vectors using the algorithm of Knuth (1969) for drawing vectors equally from all possible directions (Hunt, 2007). To test the difference in these distributions, three tests were employed to identify differences in sample variance: Bartletts test of homogeneity (Bartlett, 1937), the non-parametric Fligner-Killeen test of homogeneity of variances (Conover et al., 1981), and the non-parametric F test to compare two variances (R Core Team, 2016). Additionally, to investigate the possibility of a relationship between magnitude of shape change (d) and coincidence of the vectors of evolutionary divergence (z) and allometric trajectory (β), we tested for significant correlations between the magnitude of shape change (Δd) and the angle (θ_β).

Lastly, to test the hypothesis that worker subcastes may constrain one another (Winston et al., 2017b), we compared summary statistics of the pairwise comparisons from minor-media and submajors—majors were excluded due to insufficient sample size and weak allometry. After constructing a matrix of the pairwise comparisons, the significance of these correlations were measured using Mantel tests. Furthermore, an additional mantel test was performed using a distance matrix based on the presence of the submajor and major caste as indicators of potential constraints on morphological change in the minor-media caste ("Caste").

Results

Breakpoint Analysis

All the species investigated in the study except for two—*Eciton rapax* and *Nomamyrmex esenbeckii*—were found to have consistent breakpoints across several of the partial warp scores (Appendix C4: Table S2), as reflected by changes in linear allometry in the LOWESS curves (Appendix C4: Fig. S2). Interestingly, all discovered breakpoints fell in close range to one another ($2.4 < \text{CS} < 2.62$), and the two species that did not demonstrate evidence for breakpoints are known not to have the major worker subcaste. All recovered breakpoints fell between media and submajor worker subcastes. Since no breakpoints were recovered between minor and media subcastes, these samples were treated as a single minor-media subcaste for all analyses.

Ancestral State Reconstruction

Ancestral state reconstructions revealed a concerted evolutionary shift at the base of *Eciton* army ants, demonstrating the appearance of facultative epigaeic nesting and primarily epigaiec foraging (Fig. 15) at the same time as the generation of the novel major worker subcaste (Fig. 15a). Across the phylogeny, we see only a single origin of the major worker subcaste (Fig. 15a), and potentially as many as three origins of the submajor worker subcaste (Fig. 15b). Reconstruction of foraging and nesting environments demonstrated unequivocal support for single origins of both epigaiec nesting and foraging primarily above ground (Fig. 15). Lability was greater in the other ecological traits (Appendix C4: Fig. S3), as traits like colony size, raiding type, time of raiding, and geographic range varied across the tree.

Allometric Tests

Group comparisons for the entire worker caste ($N = 709$) were highly significant for size ($R^2 = 0.32; p = 0.001$), species ($R^2 = 0.29; p = 0.001$), and the interaction between size

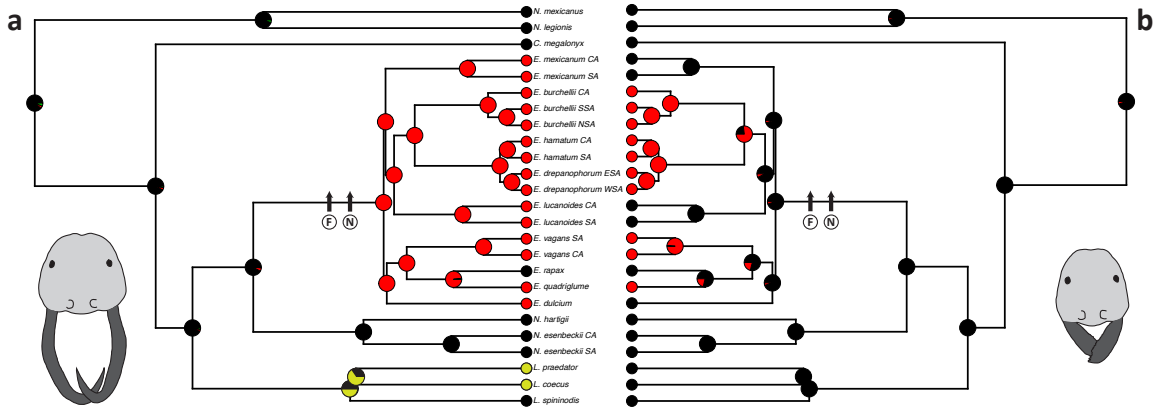

Figure 15: Stochastic character mapping of the presence of (a) major and (b) submajor subcastes for Neotropical army ant species with evolutionary origin of epigaeic nesting and epigaeic foraging. Circles at nodes indicate proportion of 1,000 simulations recovered as each state. Origin of facultative epigaiec nesting demarcated on trees with circled **N** symbol, and origin of primarily epigaiec foraging demarcated on trees with circled **F** symbol. Note that no species has the submajor subcaste without the presence of the major subcaste. In stochastic map indicating the presence of the major caste, the major subcaste in *Labidus* is colored in yellow to indicate the lack of homology with the major subcaste in *Eciton*. Drawing of major and submajor subcastes traced from images of *Eciton hamatum*.

and species ($R^2 = 0.05; p = 0.001$) (Table 8). Likewise, group comparisons for the minor-media worker caste ($N = 434$) were highly significant for size ($R^2 = 0.21; p = 0.001$), species ($R^2 = 0.40; p = 0.001$), and the interaction between size and species ($R^2 = 0.05; p = 0.001$). Group comparisons for the submajor worker caste ($N = 202$) were highly significant for size ($R^2 = 0.17; p = 0.001$), species ($R^2 = 0.43; p = 0.001$), and the interaction between size and species ($R^2 = 0.02; 0.003$). Group comparisons for the major caste ($N = 53$) were highly significant for species ($R^2 = 0.51; p = 0.001$), but insignificant for size ($R^2 = 0.04; p = 0.09$). Logically, the heterogeneity-of-slopes test demonstrated significant differences in slopes for the entire worker caste ($p = 0.01$), the minor-media subcaste ($p = 0.01$), and the submajor subcaste ($p = 0.01$), but not the major subcaste ($p = 0.11$).

All pairwise comparisons between the minor-media subcaste were significant for size and species, and most demonstrated significantly different slopes by the heterogeneity-of-slopes test (Fig. 16; Appendix C4: Table S4). Likewise, all pairwise comparisons between the submajor subcastes were significant for size and species, yet most species pairs did not exhibit significantly different slopes by the same test (Fig. 16; Appendix C4: Table S4).

All species showed significance for pairwise comparisons of species, yet only one species—*E. drepanophorum*—demonstrated significant allometry in the major caste. However, due to low sample sizes for all major castes for all species we caution interpretation with respect to the major subcaste (Table 10). Results of all pairwise comparisons for the minor-media, submajor, and major worker subcastes (Fig. 16) can be found in Appendix C4: Table S4.

Allometric Trajectory Analysis

PTA was performed on (*i*) the entire worker caste allometry, (*ii*) the minor-media worker subcaste, and (*iii*) the submajor worker subcaste, yielding vectors of shape change (b) for all species that had specimens in the respective analyses (Appendix C4: Table S5). Due to the lack of allometry found in the major subcaste (Appendix C4: Table S4), PTA was not performed on these samples alone. Common allometric component was applied for visualization of the worker caste allometry (Fig. 17), illustrating the major patterns of allometry in a two-dimensional space (Adams & Collyer, 2009). Once the major vectors of shape change were obtained, the Δd and θ_β statistics from pairwise comparisons were calculated (Fig. 18; Appendix C4: Table S6).

Evolutionary Divergence

Calculating the vectors of evolutionary divergence ($z_{min}, z_{mean}, z_{max}$) between all pairs of species (Appendix C4: Table S6) yielded 28 triplets for the minor-media subcaste [$N_z = 86$] and 15 triplets for the submajor subcaste [$N_z = 45$]. Comparisons of the vectors within each triplet demonstrated high correlation, suggesting that the direction of evolutionary divergence between species in shape space was similar for all sized specimens. We then calculated theta (θ_z)—where each vector of evolutionary divergence was then compared against the allometric vector (β) from each of the species from which is was derived—resulting in 56 triplets for the minor-media subcaste [$N_{\theta z} = 172$], and 30 triplets for the submajor subcaste [$N_{\theta z} = 90$] (Appendix C4: Table S7).

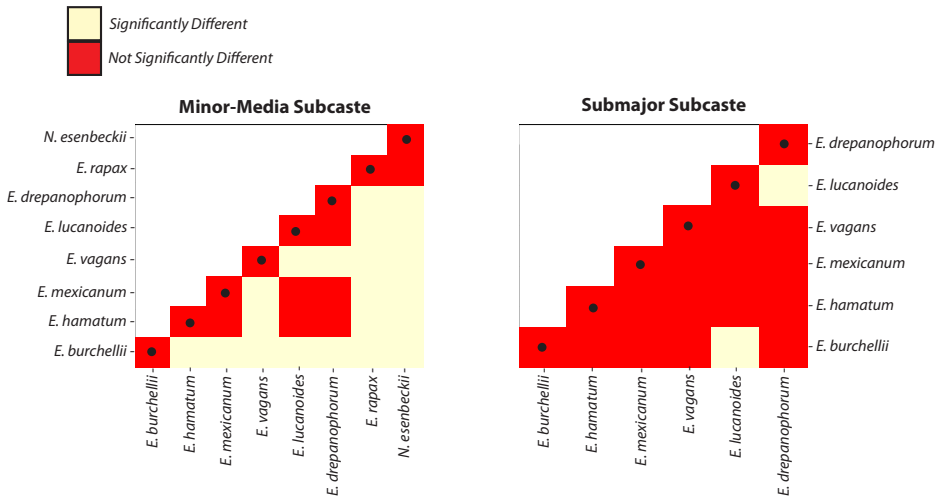

Figure 16: Visualization of significant interspecific differences in theta (θ_β) between (a) minor-media and (b) submajor allometry. Ivory colored squares represent significantly different slope of allometric vectors ($\beta_1 \neq \beta_2$), whereas red squares represent allometric vectors which were not found to have significantly different slopes. Additional details on statistics of pairwise allometric tests are provided in Table S4.

Hypothesis Testing

Tests between phylogenetic and theta (θ_β) matrices demonstrated significant relationships for both the minor-media $[r = 0.491; p = 0.035]$ and submajor $[r = 0.526; p = 0.042]$ subcastes, although not for all specimens as a group $[r = 0.253; p = 0.202]$. Similarly, results from testing whether the multivariate data had significant phylogenetic signal using method from Adams (2014) also showed positive results for both the minor-media [*min*: $K = 0.9091, p = 0.067$; *mean*: $K = 1.257, p = 0.006$; *max*: $K = 1.28, p = 0.001$] and submajor [*min*: $K = 1.070, p = 0.01$; *mean*: $K = 1.133, p = 0.005$; *max*: $K = 0.798, p = 0.262$] subcastes. Although the majority of tests between both ecological matrices and theta (θ_β) matrices were not significant (Table 9), the environmental matrix demonstrated a significant relationship with all specimens $[r = 0.580; p = 0.005]$, and a strong correlation statistic with the submajor subcaste $[r = 0.777; p = 0.067]$. Lastly, the minor-media showed a significantly different shape change in the presence of the major subcaste $[r = 0.648; p = 0.023]$, although this same pattern was not recovered in the submajor subcaste $[r = 0.052; p = 0.330]$.

Tests between the phylogenetic and difference in magnitude (Δd) matrices showed no

significant relationships or strong correlations (Table 9). Tests between the two ecological matrices and difference in magnitude (Δd) matrices revealed a single significant relationship between the species ecology and the submajor subcaste [$r = 0.904; p = 0.011$], whereas all other relationships were insignificant. Although the presence of the major subcaste had no effect on the difference in magnitude of change between species in submajors, it did show a relationship with the minor-media subcaste [$r = 0.465; p = 0.039$].

Testing distribution of theta (θ_z) from vectors of evolutionary divergence ($z_{min}, z_{mean}, z_{max}$) compared to vectors of allometric shape change (β_1, β_2) against Knuth's null (θ_{null}) yielded significant results (Fig. 19) for all three tests on both the minor-media subcaste [*Bartlett*: $K^2 = 804.2; p < 2.2e-16$; *Fligner-Killeen*: $\chi^2 = 541.81; p < 2.2e-16$; *F-test*: $F = 8.36; p < 2.2e-16$] and the submajor subcaste [*Bartlett*: $K^2 = 610.98; p < 2.2e-16$; *Fligner-Killeen*: $\chi^2 = 453.95; df = 1; p < 2.2e-16$; *F-test*: $F = 10.64; p < 2.2e-16$]. Vectors for each pairwise comparison were all highly correlated (Appendix C4: Table S6, Table S7), and comparison against Knuth's null was still significant when removing this redundancy.

Testing for worker constraints by comparing the theta matrix (θ_β) for minor-media (Fig. 18b) and submajor (Fig. 18c) subcastes showed a high degree of correlation, but was insignificant [$r = 0.668; p = 0.082$]. The same test for the difference in the magnitude of shape change (Δd) showed little correlation and was insignificant [$r = -0.046; p = 0.557$].

Discussion

Stochastic mapping results unequivocally demonstrate that the emergence of *Eciton* army ants from the subterranean environment coincided with the evolutionary innovation of a novel morphological form—the major subcaste (Fig. 15). Specifically, simulations show that the most recent common ancestor in *Eciton* army ants hunted primarily and nested facultatively above ground with the morphologically distinct major subcaste (Fig. 15). Although the presence of the submajor subcaste among *Eciton* species depended on definition (Franks, 1985; Winston et al., 2017b), it is clear that it only occurs in the presence of the major

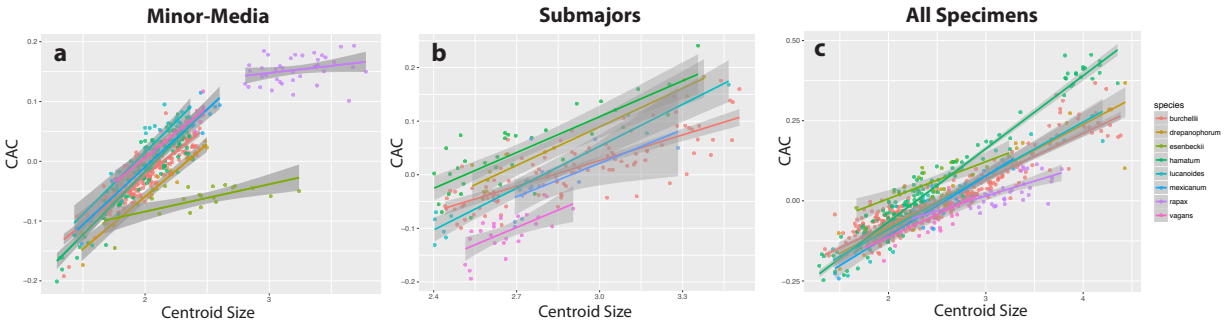

Figure 17: Common allometric component (CAC) plotted against centroid size with linear models for (a) minor-media worker subcaste, (b) submajor worker subcaste, and (c) all specimens. Linear model plotted for each species, including 95% confidence intervals. All species are indicated by the color of the points. Note that the two species without the major subcaste—*N. esenbeckii* and *E. rapax*—have very different relationships for the minor-media subcaste.

subcaste (Fig. 15). Reconstruction of other ecological traits—such as preferred time of foraging, raiding type, dietary ecology, and colony size (Table 7)—were uncertain in the most recent common ancestor of *Eciton* due to the lability and variation across *Eciton* species.

Morphological variation in the worker caste revealed a strong shift in allometry associated with the transition from hypogaiec to epigaiec environments (Fig. 16; Fig. 17; Fig. 18). This shift is exemplified by the subterranean predator *Nomamyrmex esenbeckii*, which showed radically different allometry than the epigaiec *Eciton* species for all applicable compared groups, with the exception of *E. rapax* (Fig. 16; Fig. 17; Fig. 18). Although the shape differences between the two species were highly significant (Fig. 17; Table 8; Appendix C4: Table S4), the slopes of the allometric trajectories were not significantly different (Fig. 16; Fig. 17; Fig. 18), suggesting possible convergence in allometric patterning. Despite the fact that *E. rapax* has been known to occasionally nest aboveground (Kazan, 1972), it is widely considered the most subterranean of all the *Eciton* species, frequently nesting underground or even cohabiting with leafcutter ant species (Schneirla, 1971; Kazan, 1972). Furthermore, it is the only *Eciton* species without the major subcaste, suggesting that the convergent allometry between *N. esenbeckii* and *E. rapax* could be a result of different worker

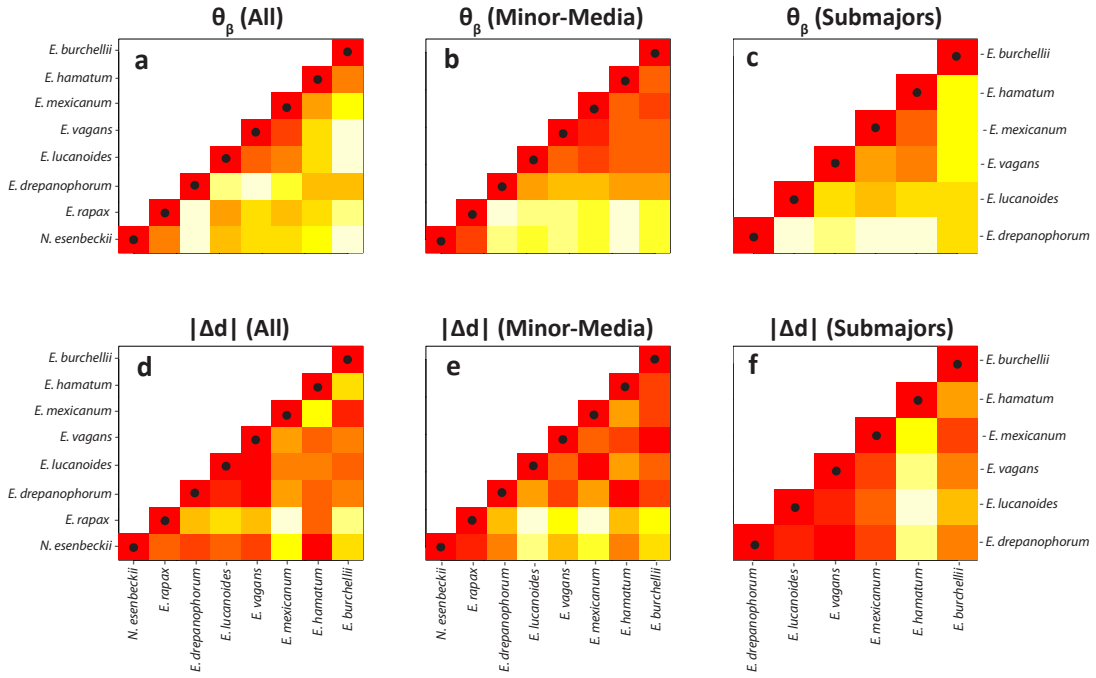

Figure 18: Visualization of theta (θ_β) and delta-d ($|\Delta d|$) matrices for (a) entire worker caste, (b) minor-media subcaste, (c) submajor subcaste. The color of the square indicates difference in metric, with red indicating no difference, and white indicating maximal difference. Comparisons to same species are demarcated with a back dot, and the upper left of each plot is empty to avoid duplicating comparisons.

subcaste composition. Mantel tests between worker subcaste composition and difference in allometric scaling (θ_β) corroborate this hypothesis, demonstrating a significant relationship ($r = 0.6483; p = 0.023$).

The numerous significant differences in caste allometry between Neotropical army species revealed by our study (Fig. 16; Fig. 17; Table 8; Appendix C4: Table S4) reinforce the central role of size in caste development (Trible & Kronauer, 2017; Molet, Wheeler, & Peeters, 2012). Furthermore, although intraspecific variation found previously in Neotropical army suggests that evolution on short time scales may be constrained to similar allometric scaling patterns (Winston et al., 2017b), these results suggest that this is not true for larger time scales since many species exhibit different allometric scaling patterns between subcastes (Fig. 16; Fig. 17; Table 8; Appendix C4: Table S4). While the submajor subcaste showed fewer significant differences in allometric scaling between species than the minor-media subcaste (Fig. 16), it

Matrix 1	Matrix 2	Group	Mantel Statistic (r)	p-value
θ	Environment	All	0.5797	0.005**
θ	Phylogeny	All	0.2529	0.202
θ	Ecology	All	0.0619	0.356
θ	Caste	All	0.1506	0.235
θ	Environment	Minor-Media	0.2414	0.127
θ	Phylogeny	Minor-Media	0.4830	0.055
θ	Ecology	Minor-Media	0.1957	0.187
θ	Caste	Minor-Media	0.6483	0.023*
θ	Environment	Submajor	0.7767	0.067
θ	Phylogeny	Submajor	0.5259	0.042*
θ	Ecology	Submajor	-0.2912	0.905
θ	Caste	Submajor	0.0521	0.330
Δd	Environment	All	-0.2009	0.840
Δd	Phylogeny	All	-0.1418	0.589
Δd	Ecology	All	-0.0911	0.554
Δd	Caste	All	0.0722	0.390
Δd	Environment	Minor-Media	0.0189	0.402
Δd	Phylogeny	Minor-Media	0.2470	0.165
Δd	Ecology	Minor-Media	0.0571	0.343
Δd	Caste	Minor-Media	0.4650	0.039*
Δd	Environment	Submajor	-0.2735	1
Δd	Phylogeny	Submajor	0.0467	0.511
Δd	Ecology	Submajor	0.9043	0.011*
Δd	Caste	Submajor	-0.1735	0.730

Table 9: Mantel test results for phylogenetic and ecological factors on theta and d. For all tests the correlation method used was Pearsons product-moment, which is given along with the p-value, with significant relationships denoted by * ($p < 0.05$) and ** ($p < 0.01$). All tests used 999 permutations.

is difficult to discern whether this pattern is the result of sampling, ecology, or neither.

Application of PTA to the entire worker caste (Fig. 18a, d), minor-media subcaste (Fig. 18b, e), and submajor subcaste (Fig. 18c, f) yielded informative statistics ($\theta_\beta, |\Delta d|$) for understanding the differences in caste allometry. Mantel tests for correlation between the environmental distance matrix and the differences in allometric scaling (θ_β) indicate that this transition significantly impacted the allometric scaling relationships across the entire worker subcaste in Neotropical army ants (Table 9). Additionally, mantel tests yielded significant relationship between phylogenetic distance and allometric scaling patterns (θ_β), showing evidence for phylogenetic signal in caste allometry (Adams, 2014; Blomberg et al., 2003; Munkemuller et al., 2012).

Given the diverse morphology associated with allometry in Neotropical army ants (Trible & Kronauer, 2017), one of the central questions of the study was whether Neotropical army ants tend to use this variation within species for evolution between species—thus bridging microevolutionary and macroevolutionary frameworks (Hunt, 2007; Schluter, 1996). By calculating the angles (θ_z) between allometric trajectories (β) and evolutionary divergence ($z_{min}, z_{mean}, z_{max}$), our results show that the distribution of these angles are more often parallel in multivariate shape space (Fig. 19) then would be expected under Knuth's null (1969). This held true for the minor-media subcaste (Fig. 19b), the submajor subcaste (Fig. 19c), as well as the entire worker caste together (Fig. 19d). These findings are particularly interesting given that allometric variation tends to be developmentally-plastic in social insects (Nijhout, 2003; Wheeler, 1991; Trible & Kronauer, 2017), and has been shown to have little to no heritability in Neotropical army ants (Jaffé et al., 2007; Wiernasz et al., 2010; Winston et al., 2017b).

Considering the known mechanisms behind allometric variation in Neotropical army ants (Abouheif & Wray, 2002; Libbrecht et al., 2013), our data suggest that developmental plasticity plays a significant role in the creation of morphological differences between species as predicted by West-Eberhard (2005). Although the mechanisms behind such macroevolutionary change are unclear, mutations in the JH pathway affecting the heritability of allometric variation would imply genetic accommodation, since existing variation has shown to have little to no heritable variation (Suzuki & Nijhout, 2006; West-Eberhard, 2005). This type of change has also been seen in artificial selection experiments and many comparative studies, where rapid evolution among insects may leverage existing developmental potential to generate novel phenotypes (Emlen & Nijhout, 2002). Work by Rajakumar et al. (2012) substantiates these claims, by inducing a novel worker subcaste in closely-related *Pheidole* species by treating larvae with JH, thereby leveraging ancestral developmental potential to create a new form. Thus, the major worker subcaste found in *Eciton* army ants may simultaneously constrain alternative allometries—such as those seen in *E. rapax* and *N. es-*

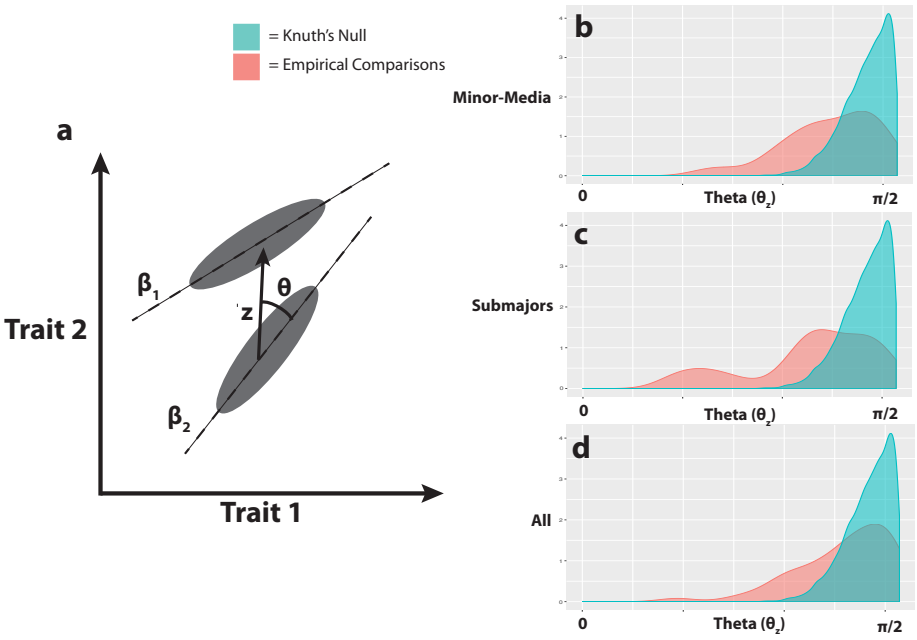

Figure 19: Empirical evidence showing preferential evolutionary divergence in the direction of allometric trajectories. (a) Schematic of estimation of vector of evolutionary divergence (z) between two species, and the angle (θ_z). Empirical comparisons from the (b) minor-media subcaste, (c) minor-media subcaste, and (d) all worker subcastes show distributions of angle of evolutionary divergence (θ_z; orange color) significantly more parallel than Knuths null (θ_{null}; blue color).

enbeckii—as well as provide useful developmental potential for macroevolutionary change (Orr & Betancourt, 2001).

Despite the fact that the ecological mechanisms driving morphological change in the worker caste are unknown, it is likely that increased predatory and competitive pressures above ground played a role, which have been hypothesized factors in other studies documenting changes associated with this transition in army ants (Bulova et al., 2016; Franks et al., 2001; Powell & Franks, 2006; Schöning et al., 2005). For example, linear morphometrics in Old World army ants found an increase in multiple measurements made on workers—such as head width, antennal length, mandible length, and leg lengths—associated with a transition to epigaiec lifestyles (Schnoning et al., 2005). As suggested by physiological work in Neotropical army ants, these morphological characteristics correlate with changes in the brain size and function associated with increased visual processing (Bulova et al., 2016), and increased efficiency of transporting prey (Franks et al., 2001; Powell & Franks, 2005; Powell & Franks,

		N			
Genus	**Species**	**All**	**Minor-Media**	**Submajor**	**Major**
Nomamyrmex	*esenbeckii*	20	20	0	0
Eciton	*rapax*	40	40	0	0
Eciton	*drepanophorum*	29	14	10	5
Eciton	*lucanoides*	39	26	10	3
Eciton	*vagans*	43	18	25	0
Eciton	*mexicanum*	27	14	13	0
Eciton	*hamatum*	166	113	34	19
Eciton	*burchellii*	345	206	112	27
Total		**709**	**451**	**204**	**54**

Table 10: Sample sizes for GM analysis on Neotropical army ants. Number of specimens for each of the eight species, broken down by recognized worker subcastes.

2006). Interestingly, analysis of allometric trajectories in Old World army ants show that the increase in these traits was most profound in the largest individuals, suggesting that the trajectory was altered as a response for increased need for colony defense (Schöning et al., 2005).

In sum, our study reveals an important macroevolutionary trend where Neotropical army ant species preferentially evolve along existing axes of allometric scaling (Fig. 19). Furthermore, by synthesizing recent phylogenetic work, compiled ecological characteristics, and geometric morphometrics (GM) analysis of worker morphology, we have shown a concerted ecological and morphological shift in *Eciton*, coinciding with the generation of a novel worker type—the major subcaste. Combining the results of our GM analysis and ancestral state reconstruction, our work suggests that the worker subcastes do not evolve completely independently, and that the presence of the major subcaste may even constrain the allometry of the worker caste generally. Future work should focus on more quantitative research on the dietary and foraging ecology in different Neotropical army ant species to help reveal the ecological factors shaping the significant morphological differences uncovered by our study.

7 Conclusions

The ultimate value of this work lies in investigating the unique biology of Neotropical army ants while leveraging our understanding of these non-model organisms to reveal interactions of evolutionary processes across broad spatial and temporal scales. Although each chapter accomplishes part of this goal, the dissertation in its entirety provides a more complete portrait of macroevolution in these top Neotropical predators, including how the variation within each species contributes to this greater whole. As evidenced above, the basis for inference in my work is genomic and morphological variation, which I attempt to put into a rich developmental context by using the extensive literature on hormonal signaling and gene regulation in social insects. Here, I discuss what I believe can be concluded from my collection of studies in Neotropical army ants.

The first chapter of my dissertation exploits new advances in *de novo* genomic assembly and the unique life history traits of army ants to understand how the rise of the isthmus of Panama impacted Neotropical biodiversity. Although it is well known that the rise of the isthmus radically changed global climate and incited the Great American Biotic Interchange by providing a corridor for organisms to migrate between North and South America, the timing and exact role of the event remain contentious. I found several cases of parallel speciation within the Neotropical army ants associated with the colonization of Central America, dating far before the full closure. Given that army ants cannot disperse across water—even by improbable "sweepstakes events"—my work corroborates recent geological evidence for land connections preceding the full closure of the isthmus. More importantly, it provides concrete geological mechanisms to explain the increased diversification in the region. In addition to suggesting an outsized role of the rise of the isthmus in generating Neotropical diversity, my work indicates that the use of these early land connections were likely widespread for organisms migrating at this time, and that the spatiotemporal complexity of the geological record needs to be considered more heavily when interpreting biogeographic patterns.

The remaining chapters of my dissertation aim to elucidate evolutionary processes in

the evolution of the worker caste in Neotropical army ants through the use of morphological variation. The phylogenomic work accomplished in the first chapter allows for proper macroevolutionary context and analysis, while additional genotyping of individuals within species—both in terms of microsatellite and reduced-representation genomic sequencing—provides genetic variation at the microevolutionary scale. It is these large morphological and genomic datasets that facilitated my examination of the evolution of the developmental plasticity responsible for producing the distinct morphologies, physiologies, and behaviors of the different worker subcastes.

When considering the developmental plasticity found in Neotropical army ants, it is clear that the variational properties of the phenotype are fundamental to its evolution by natural selection (Wagner & Altenberg, 1996). The modular nature of castes—where the same developmental programs are deployed within different internal environments as controlled by JH and IIS—facilitates the capacity to evolve (Libbrecht et al., 2013; Molet et al., 2012). Specifically, sensitivity to the signaling involved in patterning these environments can change both the size of the developing organism, as well as tissue-specific responses that can generate new forms through allometric repatterning (Nijhout, 2003; Wheeler, 1991; Trible & Kronauer, 2017). My work suggests that the evolution along allometric axes of variation in Neotropical army ants is similar to other adaptive developmental programs, such as *Anolis* lizards (Losos et al., 1997; Losos et al., 2003), or Darwins finches (Abzhanov et al., 2004; Abzhanov et al., 2006). In the case of *Eciton* army ants, my results show that the innovation of the major worker subcaste brought the capacity for the submajor worker subcaste, which has shown conditional expression depending on the niche of the organism (Powell & Franks, 2006; Pigliucci, 2008).

Of course, although my quantitative genetic work has demonstrated a lack of heritable morphological variation associated with the paternal genotype, the limits of additive genetic variation are well-established (Bégin & Roff, 2004; Houle 1992). Moreover, as shown by work in evolutionary quantitative genetics, key elements of hormonal signaling can rapidly

evolve and exhibit high levels of genetic variability (Zera, 2008). Aside from the potential of genetic accommodation in the paternal genotype, my work also suggests that queen genotype could offer additive genetic variance: The colony-specific allometry demonstrated in my third chapter could easily be produced by heritable sensitivities to key hormones involved in the developmentally-plastic pathway. More quantitative research and increased sampling would be required to detect this potential genetic source of morphological variation.

Regardless of whether current populations show heritable variation within the worker caste, results from my fourth chapter and existing evolutionary quantitative genetics suggest an important connection between phenotypic variation within species and evolutionary divergence between species: The finding that Neotropical army ant species preferentially evolve along the axes of allometric scaling suggests an additional way in which the adaptive developmental program of the worker caste facilitates evolutionary divergence (Schluter, 1996; West-Eberhard, 2005). Not only can forms be produced by conditional expression (Powell & Franks, 2006; Rajakumar et al., 2012), but the existing axis of variation—in the form of allometry—can be co-opted in the creation of new forms (Molet et al., 2012; Trible & Kronauer, 2017; West-Eberhard, 2005). Thus, the innovation of the major worker subcaste—and subsequently the submajor worker subcaste—represents an extension of an existing evolutionary channel previously exploited by Neotropical army ants (Pigliucci, 2008; Wagner & Altenberg, 1996).

In sum, the body of work I have presented in this document falls along two central themes. The first is that the biological quirks that can make work in non-model organisms difficult may provide unique perspective if applied to the right question. For example, although the impossibility of replicating the colonial environment in Neotropical army ants made direct evolutionary developmental work unfeasible for my dissertation, their unique combination of nomadism and dependent colony foundation was the exact lens necessary to uncover broader patterns of the Great American Biotic Interchange. The second theme is much more obvious, especially for those scientists lucky enough to work in non-model organisms

where little is known and there is much to discover. Collaboration and community are critical elements to successful science: The most interesting results from my dissertation were those that addressed questions across broad spatial and temporal scales, which would not have been possible without the plethora of contributions from other scientists in the field. Yet, perhaps more importantly is the basic fact that productive interdisciplinary synthesis relies upon willing members of existing communities to think and engage beyond their discipline. Having the luxury of the thriving Darwinian community during my dissertation work, my experience has suggested that it is only through the redeployment of scientific methods into different disciplinary environments that we can properly align existing paradigms towards consilience (Kuhn, 1962; Wilson, 1998).

8 Future Work

As with any scientific endeavor, this work has generated many answers, but also a variety of questions worthy of future study. I have outlined a few research directions that I believe to be particularly fruitful below.

Given the striking pattern of parallel speciation along the Isthmus of Panama found in at least three *Eciton* species, perhaps the strongest direction for future work would be an explicit population genomic study of this parallel speciation. Although I have sampled throughout species ranges and the secondary contact zones, more concentrated sampling in the secondary contact zones could more directly address questions of hybridization and gene flow for these species pairs. It would also be prudent to add at least two *de novo* genome assemblies for *E. mexicanum* and *E. vagans*—I have already done so for *E. burchellii*—which would aid analysis of structural and functional variation.

Along these lines, concurrent investigation of the ecology of the species pairs in these secondary contact zones would be extremely valuable for understanding parallel cases of evolutionary divergence. For example, if there is no evidence of hybridization, what sort of

pre-zygotic or post-zygotic barriers are responsible for this genetic separation (Coyne & Orr, 2002; Kronforst et al., 2006)? Does further exploration of species ecology actually confirm similarities between species pairs or is this a relic of cryptic speciation? Has competition between species pairs produced evolutionarily stable range limits (Price & Kirkpatrick, 2009)? Is there evidence that Dobzhansky-Muller incompatibilities have accumulated in the distinct lineages (Orr & Turelli, 2001)? Are the hundreds of army ant associated organisms that live in colonies being passed in between these species pairs (Rettenmeyer et al., 2011)? Is there demonstrable coevolution of obligate symbionts as high host-specificity may suggest (von Beeren et al., 2016)? The questions here are seemingly endless when considering the unique and interesting biology of Neotropical army ants.

Alternative directions for future work generated by this dissertation are more methodological in nature. The application of genomic sequencing across evolutionary scales brings with it a variety of inference problems. Specific to this work is potential biases of reduced-representation sequencing on population genomic and phylogenomic inferences. Although there has been extensive work on these biases and suggested solutions (Rubin et al., 2012; Eaton, 2014; Eaton et al., 2015; Huang & Knowles, 2014), there has not been a simulation study directly demonstrating the impact of locus sparsity and taxon-sampling on branch length and parameter estimation for phylogenomic inference. As reduced-representation methods continue to be used more frequently, understanding these fundamental biases becomes increasingly critical to avoid the positive reinforcement of evolutionary patterns based on faulty inference.

Lastly, despite the fact that I have shown an interesting and convergent transition in morphology resulting from exiting the subterranean environment, our data is restricted to geometric morphometric analysis of the head case of the worker caste. Future work would benefit from scrutinizing this transition more broadly, both morphologically and ecologically. First, a more focused and rigorous ecological understanding of the foraging, nesting, and dietary ecology of *Eciton* species would avoid issues of data fidelity associated with meta-

analyses used in this study. Second, if new ecological data could better define niche and environmental determinants associated with *Eciton* behavior and success, we could better grasp the important ecological factors at play. Given the existing literature, the most logical place to start would be extending the quantitative work on dietary ecology of Powell & Franks (2006). Next, more morphological data would be useful to form a better understanding of the transition out of the subterranean environment. Specifically, data from other body parts such as the legs, antennae, mandibles, and mesosoma would better connect the morphological data to the ecological determinants. Finally, questions of integration across worker subcastes could be asked (Webster & Zelditch, 2011), which would be particularly interesting given the constraints that seem apparent from the data Ive presented in the third and fourth chapters. Data not presented in this dissertation is also suggestive of the potential of this system in understanding the link between saltation and modular evolution, as a singular hybrid colony of *E. burchellii* and *E. hamatum* discovered in Peru [MEW#214] demonstrates completely unique morphology that departs from patterns of allometric scaling seen within the clade. Thus, if synthesized in concert with recently published brain and physiology data (Bulova et al., 2016), *Eciton* army ants would be an ideal study system for the study of developmental constraints and modular evolution.

9 Acknowledgements

This project was a highly collaborative effort, and would not have been possible without the generous researchers who sent specimens from across the Neotropics: Leanne Alonso, Fabricio Baccaro, Kaitlin Baudier, Christoph von Beeren, Séan Brady, Michael Branstetter, Alain DeJean, Fernando Fernández, Brian Fisher, Dan Janzen, Ana Jesovnik, John LaPolla, Jack Longino, Piotr Lukasik, Sean McCann, Sean O'Donnell, Scott Powell, Ben Rubin, Jeffrey Sosa-Calvo, Ted Schultz, Andrew Suarez, Phil Ward and Steve Yanoviak. Research was conducted in the Pritzker Laboratory for Molecular Systematics and Evolution and the

Collaborative Invertebrate Laboratory at the Field Museum of Natural History, Chicago, Illinois, USA. For assistance in the Pritzker Laboratory, I thank Andrea Thompson, Dr. Ben Rubin, Brian Wray, Dr. Kevin Feldheim, & Dr. Erica Zahnle. For assistance in the field I thank Elizabeth Pringle, Arista Tischner and Alexandra Westrich. For assistance in the Collective Invertebrate Laboratory I thank Gracen Brilmyer, Alexandra Westrich, and Andrea Thompson. I also thank the generous support of the CEB program and graduate student community.

Field research was made possible through the help of Dr. Corrie Moreau, Dr. Daniel Janzen, Winnie Hallwachs, members of the Área de Conservación Guanacaste, the Costa Rican government, Ant Course 2014 organizers, and the Peruvian government.

This work was financially supported by many institutions and individuals, including: The National Science Foundation (DEB1442316 and IOS1354193 to Dr. Moreau and NSF DDIG1501672 to Dr. Moreau and myself), the Negaunee Foundation, the Society for Systematic Biology, the Hinds Fund, the Steiner Travel Award, the Brown Family Fellowship, the GAANN fellowship, and an anonymous donor.

I would like to thank my committee for all their help—Dr. Corrie Moreau, Dr. Marcus Kronforst, Dr. Trevor Price, and Dr. Mark Webster. I'd also like to thank a number of professors and curators that were instrumental in my education. This includes but is not limited to Dr. Mark Alvey, Dr. Jack Gilbert, Dr. John Novembre, Dr. Matthew Stephens, Dr. John Bates, Dr. Shannon Hackett, Dr. Bruce Patterson, Dr. Larry Heaney, Dr. Bill Wimsatt, Dr. Scott Lidgard, Dr. Richard Ree, Dr. Stefano Allesina, Dr. Michael Coates, Dr. David Jablonski, Dr. Sue Kidwell, Dr. Michael Foote, Dr. Cathy Pfister, Dr. Urs Schmidt-Ott, Dr. Scott Powell. Lastly, I would like to especially thank Dr. Carolyn Johnson for all of her advice and support throughout my time in the CEB program.

Likewise, there were a number of classmates that were critical in developing my dissertation: Dr. Tom Stewart, Dr. Ben Rubin, Dr. Rob Arthur, Dr. Joyce Pieretti, Dr. Jon Mitchell, Dr. Deren Eaton, Dr. Sean Gibbons, Dr. Nicole Bitler, Tim Sosa, Giselle Garcia,

Dan Hooper, Shane Dubay, Victoria Flores, Joel Smith, Nicholas Knoblauch, Evan Koch, Simon Lax, Dallas Krentzel, Katherine Silliman, Peter Smits, Daniela Palmer, Haley Stinnett, Darcy Ross, my entire Darwinian cohort, and the Philosophy of Biology reading group.

Lastly, I need to thank my advisor Dr. Corrie Moreau. Interdisciplinary work can be nearly impossible to accomplish in a Ph.D. without an advisor who provides freedom and independence. Not only did I benefit from her understanding of this fact, but I absolutely would not have been able to complete my doctorate without her unwavering enthusiasm and support.

10 Data Accessibility

Early and dynamic colonization of Central America drives speciation in Neotropical army ants

- *Publication*: (Winston et al., 2017a)
- *DNA Sequences*: GenBank Accession no SRP072129.
- *Concatenated Data Matrix*: Dryad Accession doi:10.5061/dryad.3075h.
- *Reproducible Assembly Code*: Github repository (https://github.com/mewinsto).
- *Geographic and Sample Data*: Supporting Information.

Novel approach to heritability detection suggests robustness to paternal genotype in a complex morphological trait

- *Publication*: (Winston et al., 2017b)
- *Simulation Code*: Github repository (https://github.com/mewinsto).

Colony-specific caste allometry in a top Neotropical predator

- *GM Data*: Dryad

Emergence from the subterranean environment shapes Neotropical army ant allometry

- *GM Data*: Dryad

11 References

[1] **Abbott R, Albach D, Ansell S, Arntzen JW, Baird SJE, et al. (2013).** Hybridization and speciation. J Evol Bio. 26(2), 229246.

[2] **Aberer AJ, Kobert K, & Stamatakis A (2014).** ExaBayes: massively parallel bayesian tree inference for the whole-genome era. Mol Biol Evol. 31, 25532556.

[3] **Abouheif E & Wray GA (2002).** Evolution of the gene network underlying wing polyphenism in ants. Science. 297(5579), 24952.

[4] **Abzhanov A, Protas M, Grant BR, Grant PR, & Tabin, CJ (2004).** Bmp4 and morphological variation of beaks in Darwins finches. Science. 305(5689), 14621465.

[5] **Abzhanov A, Kuo WP, Hartmann C, Grant BR, Grant PR, & Tabin CJ (2006).** The calmodulin pathway and evolution of elongated beak morphology in Darwins finches. Nature. 442(7102), 5637.

[6] **Adams DC (2011).** Quantitative genetics and evolution of head shape in Plethodon salamanders. Evol Biol. 38(3), 278286.

[7] **Adams DC & Otarola-Castillo E (2013).** geomorph: an R package for the collection and analysis of geometric morphometric shape data. Methods Ecol Evol. 4, 393-399.

[8] **Adams DC (2014).** A Generalized K Statistic for Estimating Phylogenetic Signal from Shape and Other High-Dimensional Multivariate Data. Syst Biol. 0(0), 113.

[9] **Adams DC & Collyer ML (2009).** A general framework for the analysis of phenotypic trajectories in evolutionary studies. Evolution. 63: 1143-1154.

[10] **Alvarado S, Rajakumar R, Abouheif E, & Szyf M (2015).** Epigenetic variation in the Egfr gene generates quantitative variation in a complex trait in ants. Nat Comm. 6, 6513.

[11] **Aubin-Horth N & Renn SCP (2009).** Genomic reaction norms: using integrative biology to understand molecular mechanisms of phenotypic plasticity. Mol Ecol. 18(18), 376380.

[12] **Bacon CD, Silvestro D, Jaramillo C, Smith BT, Chakrabarty P, & Antonelli A (2015).** Biological evidence supports an early and complex emergence of the Isthmus of Panama. P Natl Acad Sci USA. 112, 61106115.

[13] **Badyaev AV & Foresman KR (2000).** Extreme environmental change and evolution: stress-induced morphological variation is strongly concordant with patterns of evolutionary divergence in shrew mandibles. Proc Roy Soc B Biol Sci. 267(1441), 3717.

[14] **Bagley JC & Johnson JB (2014).** Phylogeography and biogeography of the lower Central American Neotropics: diversification between two continents and between two seas. Biol Rev. 89, 767790.

[15] **Barth MB, Moritz RFA, & Kraus FB (2015).** Genetic differentiation at species level in the Neotropical army ant *Labidus predator*. Insectes Soc. 62, 299306.

[16] **Bartlett MS (1937).** Properties of sufficiency and statistical tests. Proc Roy Soc A. 160, 268282.

[17] **Bartoli G, Sarnthein M, Weinelt M, Erlenkeuser H, Garbe-Schoonberg D, & Lea DW (2005).** Final closure of Panama and the onset of northern hemisphere glaciation. Earth Planet Sci Lett. 237, 3344.

[18] **Baudier KM, Mudd AE, Erickson SC, & ODonnell S (2015).** Microhabitat and body size effects on heat tolerance: implications for responses to climate change (army ants: Formicidae, Ecitoninae). J Anim Ecol. 84(5), 132230.

[19] **von Beeren C, Maruyama M, & Kronauer DJC (2016).** Cryptic diversity, high host specificity and reproductive synchronization in army ant-associated *Vatesus* beetles. Mol Ecol.

[20] **Bégin M & Roff DA (2004).** From micro- to macroevolution through quantitative genetic variation: positive evidence from field crickets. Evolution. 58(10), 22872304.

[21] **Benaglia T, Hunter DR, & Young, DS (2010).** mixtools: An R Package for Analyzing Finite Mixture Models.

[22] **Berghoff SM, Kronauer DJC, Edwards KJ, & Franks NR (2008).** Dispersal and population structure of a New World predator, the army ant *Eciton burchellii*. J Evol Biol. 21, 11251132.

[23] **Berghoff SM (2003).** Army ants: an evolutionary bestseller? Curr Biol. 13(17), R676R677.

[24] **Blomberg SP, Garland T, & Ives AR (2003).** Testing for phylogenetic signal in comparative data: behavioral traits are more labile. Evolution. 57:717745.

[25] **Bollback JP (2006).** SIMMAP: stochastic character mapping of discrete traits on phylogenies. BMC Bioinformatics, 7, 88.

[26] **Bolker B (2016).** bbmle: Tools for general maximum likelihood estimation. CRAN.

[27] **Bolton B (1994).** Identification guide to the ant genera of the world. Cambridge, Mass.: Harvard University Press, 222 pp.

[28] **Bookstein FL (1991).** Morphometric Tools for Landmark Data: Geometry and Biology. Cambridge University Press, New York.

[29] **Boswell GP, Britton NF, & Franks NR (1998).** Habitat fragmentation, percolation theory and the conservation of a keystone species. Proc Roy Soc B: Biol Sci. 265, 19211927.

[30] **Brady SG (2003).** Evolution of the army ant syndrome: the origin and long-term evolutionary stasis of a complex of behavioral and reproductive adaptations. Proc Natl Acad Sci USA. 100, 6575 6579.

[31] **Brady SG, Fisher BL, Schultz TR, & Ward PS (2014).** The rise of army ants and their relatives: diversification of specialized predatory doryline ants. BMC Evol Biol. 14, 114.

[32] **Brakefield PM (2006).** Evo-devo and constraints on selection. Trends Ecol Evol. 21(7), 362368.

[33] **Bulova S, Purce K, Khodak P, Sulgar E, & ODonnell S (2016).** Into the black, and back: The ecology of brain investment in Neotropical army ants (Formicidae: Dorylinae). Naturwissenschaften.

[34] **Burchill AT & Moreau CS (2016).**Colony size evolution in ants: macroevolutionary trends. Insectes Soc. 63:2, 291-298.

[35] **Burton JL & Franks NR (1985).** The foraging ecology of the army ant *Eciton rapax*: an ergonomic enigma? Ecol Entomol. 10, 131141.

[36] **Butler IA, Siletti K, Oxley PR, & Kronauer, DJC (2014).** Conserved microsatellites in ants enable population genetic and colony pedigree studies across a wide range of species. PLoS ONE. 9(9), e107334.

[37] **Cahan SH, Graves CJ, & Brent CS (2011).** Intergenerational effect of juvenile hormone on offspring in Pogonomyrmex harvester ants. J Comp Physiol B Biochem Syst Environ Physiol. 181:8, 9919.

[38] **Carson EA (2006).** Maximum likelihood estimation of human craniometric heritabilities. Am J Phys Anthro. 180, 169180.

[39] **Chapman T, Arnqvist G, Bangham J, & Rowe, L (2003).** Sexual conflict. Trends Ecol Evol. 18(1), 41-47.

[40] **Chen G, Yuan A, Shriner D et al. (2015).** An improved F_{st} estimator. PLoS ONE. 10, e0135368.

[41] **Coates AG, Jackson JBC, Collins LS, et al. (1992).** Closure of the Isthmus of Panama: the near-shore marine record of Costa Rica and western Panama. Geol Soc Am Bull. 104, 814828.

[42] **Coates AG, Collins LS, Aubry MP, & Berggren WA (2004).** The Geology of the Darien, Panama, and the late Miocene-Pliocene collision of the Panama arc with northwestern South America. Geol Soc Am Bull. 116, 1327.

[43] **Collyer ML & Adams DC (2013).** Phenotypic trajectory analysis: comparison of shape change patterns in evolution and ecology. Hystrix. 24: 75-83.

[44] **Conover WJ, Johnson ME, & Johnson MM (1981).** A comparative study of tests for homogeneity of variances, with applications to the outer continental shelf bidding data. Technometrics. 23, 351361.

[45] **Cowie RH & Holland BS (2006).** Dispersal is fundamental to biogeography and the evolution of biodiversity on oceanic islands. J Biogeogr. 33, 193198.

[46] **Coyne J & Orr HA (2004).** Speciation. Sinauer, Sunderland, Massachusetts.

[47] **Cruaud A, Gautier M, Galan M, Foucaud J, Saun L, et al. (2014).** Empirical assessment of RAD sequencing for interspecific phylogeny. Mol Biol Evol. 31(5), 12721274.

[48] **Denny AJ, Franks NR, & Edwards KJ (2004).** Eight highly polymorphic microsatellite markers for the army ant *Eciton burchellii*. Mol Ecol Notes. 3, 1-3.

[49] **Denny AJ, Franks NR, Powell S, Edwards KJ (2004).** Exceptionally high levels of multiple mating in an army ant. Naturwissenschaften. 91, 396399.

[50] **Drewell RA, Lo N, Oxley PR, & Oldroyd BP (2012).** Kin conflict in insect societies: a new epigenetic perspective. Trends Ecol Evol. 27(7), 36773.

[51] **Dryden I & Mardia KV (1998).** Statistical Shape Analysis. John Wiley & Sons, Chichester.

[52] **Dryden I & Mardia KV (2016).** Statistical Shape Analysis: with Applications in R. John Wiley & Sons.

[53] **Eaton DAR (2014).** PyRAD: assembly of *de novo* RADseq loci for phylogenetic analyses. Bioinformatics. 30, 18441849.

[54] **Eaton DAR, Ree RH (2013).** Inferring phylogeny and introgression using RADseq data: an example from flowering plants (Pedicularis: Orobanchaceae). Syst Biol. 62, 689706.

[55] **Eaton DAR, Spriggs EL, Park B, & Donoghue MJ (2015).** Misconceptions on missing data in RAD-seq phylogenetics with a deep scale example from flowering plants. BioArxiv.

[56] **Eizirik E (2012).** A molecular view on the evolutionary history and biogeography of Neotropical carnivores. Bones, Clones, and Biomes: The History and Geography of Recent Neotropical Mammals, Vol. 3, pp. 123143. University of Chicago Press, Chicago, Illinois.

[57] **Elshire RJ, Glaubitz JC, Sun Q et al. (2011).** A robust, simple genotyping-by-sequencing (GBS) approach for high diversity species. PLoS ONE. 6, 19371939.

[58] **Emlen DJ, & Nijhout HF (2000).** The Development and Evolution of Exaggerated Morphologies in Insects. Annu Rev Entomol. 661708.

[59] **Eroukhmanoff F, & Svensson EI (2008).** Phenotypic integration and conserved covariance structure in calopterygid damselflies. J Evol Biol. 21(2), 514526.

[60] **Erwin DH (2000).** Macroevolution is more than repeated rounds of microevolution. Evol Dev. 2(2), 7884.

[61] **Falconer DS (1960).** Introduction to quantitative genetics, Oliver & Boyd, Edinburgh/London.

[62] **Falconer DS, & Mackay TFC (1996).** Introduction to quantitative genetics, Edition 4. Longmans Green, Harlow, Essex, UK.

[63] **Flatt T, Tu MP, & Tatar M (2005).** Hormonal pleiotropy and the juvenile hormone regulation of Drosophila development and life history. Bioessays. 27:10, 9991010.

[64] **Franks NR, & Fletcher CR (1983).** Spatial Patterns in Army Ant Foraging and Migration: *Eciton burchelli* on Barro Colorado Island, Panama. Behav Ecol Sociobiol. 12(4), 261270.

[65] **Franks N, Sendova-Franks AB, & Anderson CA (2001).** Division of labour within teams of New World and Old World army ants. Anim Behav. 62(4), 635642.

[66] **Franks NR (1985).** Reproduction, foraging efficiency and worker polymorphism in army ants. In: B. Hlldobler & M. Lindauer, Experimental behavioral ecology and sociobiology. G. Fischer Verlag, Stuttgart, Germany. Pp. 9-107.

[67] **Franks NR (1986).** Teams in social insects: group retrieval of prey by army ants (Eciton burchelli, Hymenoptera: Formicidae). Behav Ecol Sociobiol. 18(6), 425429.

[68] **Frohschammer S, & Heinze J (2009).** A heritable component in sex ratio and caste determination in a Cardiocondyla ant. Front Zool. 6, 27.

[69] **Garnier S, Murphy T, Lutz M, Hurme E, Leblanc S, & Couzin ID (2013).** Stability and responsiveness in a self-organized living architecture. PLoS Comp Biol. 9(3), e1002984.

[70] **Gosti DA, Sanders NJ, Fitzpatrick MC, Laurent E, Lessard JP, et al. (2007).** Global ant (Hymenoptera: Formicidae) biodiversity and biogeography—a new database and its possibilities. Myrmecological News. 7783.

[71] **Gotwald WH (1995).** Army ants: The biology of social predation. Cornell University Press. Pp. 94-161.

[72] **Gould SJ (1966).** Allometry and size in ontogeny and phylogeny. Biol Rev Camb Philos Soc. 41, 587640.

[73] **Gould SJ (2002).** The structure of evolutionary theory. Harvard University Press.

[74] **Grant PR, & Grant R (2011).** How and why species multiply: the radiation of Darwin's finches. New Jersey: Princeton University Press.

[75] **Gregg C, Zhang J, Butler JE, & Haig D (2010).** Sex-specific parent-of-origin allelic expression in the mouse brain. Science. 329(5992), 682685.

[76] **Gutiérrez-García TA, Vázquez-Domínguez E (2013).** Consensus between genes and stones in the biogeographic and evolutionary history of Central America. Quat Res. 79, 311324.

[77] **Haig D (2000).** The kinship theory of genomic imprinting. Ann Rev Ecol Evol Syst. 31, 932.

[78] **Hallgrímsson B & Hall B (2005).** Variation: A Central Concept in Biology. Burlington, MA: Elsevier Publishing. Pp. 303-322.

[79] **Haug GH & Tiedemann R (1998).** Effect of the formation of the Isthmus of Panama on Atlantic Ocean thermohaline circulation. Nature. 393, 16991701.

[80] **Haug GH, Tiedemann R, Zahn R, & Ravelo AC (2001).** Role of Panama uplift on oceanic freshwater balance. Geology. 29, 207210.

[81] **Haug GH, Ganopolski A, Signman DM et al. (2005).** North Pacific seasonality and the glaciation of North America 2.7 million years ago. Nature. 433, 821825.

[82] **Hohenlohe PA, Amish SJ, Catchen JM, Allendorf FW, & Luikart G (2011).** Next-generation RAD sequencing identifies thousands of SNPs for assessing hybridization between rainbow and westslope cutthroat trout. Mol Ecol Res. 11 Suppl 1, 11722.

[83] **Hölldobler B & Wilson EO (1990).** The Ants. Cambridge: Harvard University Press. Pp. 746.

[84] **Hoorn C, Wesselingh FP, Steege H, Bermudez MA, Mora A, et al. (2010).** Amazonia through time: Andean uplift, climate change, landscape evolution, and biodiversity. Science. 330, 927931.

[85] **Houle D (1992).** Comparing evolvability and variability of quantitative traits. Genetics. 130(1), 195204.

[86] **Huang H & Knowles LL (2014).** Unforeseen Consequences of Excluding Missing Data from Next-Generation Sequences: Simulation Study of RAD Sequences. Syst Biol. 0(0), 19.

[87] **Huelsenbeck JP, Nielsen R, & Bollback JP (2003).** Stochastic Mapping of Morphological Characters. Syst Biol. 52(2), 131158.

[88] **Hughes WOH & Boomsma JJ (2006).** Does genetic diversity hinder parasite evolution in social insect colonies? J Evol Biol. 19(1), 13243.

[89] **Hughes WOH, Sumner S, Van Borm S, & Boomsma JJ (2003).** Worker caste polymorphism has a genetic basis in Acromyrmex leaf-cutting ants. Proc Natl Acad Sci USA. 100(16), 93947.

[90] **Hunt G (2007).** Evolutionary divergence in directions of high phenotypic variance in the ostracode genus *Poseidonamicus*. Evolution. 61(7), 156076.

[91] **Hunt G & Chapman RE (2001).** Evaluating hypotheses of instar-grouping in arthropods: a maximum likelihood approach. Paleobiology. 27:3, 466484.

[92] **Jablonski D, Roy K, & Valentine J (2006).** Out of the tropics: evolutionary dynamics of the latitudinal diversity gradient. Science. 314, 102106.

[93] **Jablonski D (2007).** Scale and hierarchy in macroevolution. Palaeontology. 50(September 2006), 87109.

[94] **Jablonski D (2000).** Micro- and macroevolution: Scale and hierarchy in evolutionary biology. Paleobiology. 26(4), 1552.

[95] **Jablonski D (2003).** Evolutionary innovations in the fossil record: Patterns in time and space. Integr Comp Biol. 43(6), 969.

[96] **Jaffé R, Moritz RFA, & Kraus FB (2009).** Gene flow is maintained by polyandry and male dispersal in the army ant *Eciton burchellii*. Pop Ecol. 51(2), 227236.

[97] **Jaffé R, Kronauer DJC, Kraus FB, Boomsma JJ, & Moritz RFA (2007).** Worker caste determination in the army ant *Eciton burchellii*. Biol Lett. 3(5), 5136.

[98] **Johannsdottir B, Thorarinsson F, Thordarson A, & Magnusson TE (2005).** Heritability of craniofacial characteristics between parents and offspring estimated from lateral cephalograms. Am J Ortho Dent Orthoped. 127(2), 200207.

[99] **Jones OR & Wang J (2010).** COLONY: a program for parentage and sibship inference from multilocus genotype data. Mol Ecol Res. 10(3), 5515.

[100] **Kaspari M & ODonnell S (2003).** High rates of army ant raids in the Neotropics and implications for ant colony and community structure. Evol Ecol. 5, 933939.

[101] **Kaspari M & Vargo EL (1995).** Colony size as a buffer against seasonality: Bergmanns rule in social insects. Am Nat. 145, 610632.

[102] **Kazan PL (1972).** The biology and behavior of an army ant, *Eciton rapax*. Masters thesis, Kansas State University.

[103] **Kearse M, Moir R, Wilson A, Stones-Havas S, Cheung M, et al. (2012).** Geneious Basic: an integrated and extendable desktop software platform for the organization and analysis of sequence data. Bioinformatics. 28(12), 1647-1649.

[104] **Keller L, Sundström L, & Chapuisat M (1997).** Male reproductive success: Paternity contributions to queens and workers in *Formica* ants. Behav Ecol Sociobiol. 41, 11-15.

[105] **Klingenberg CP, Leamy L, & Cheverud J (2004).** Integration and modularity of quantitative trait locus effects on geometric shape in the mouse mandible. Genetics. 166, 1909-1921.

[106] **Klingenberg CP (1998).** Heterochrony and allometry: the analysis of evolutionary change in ontogeny. Biol Rev Camb Philos Soc. 73:1, 79123.

[107] **Klingenberg CP (2008).** Morphological integration and developmental modularity. Annu Rev Ecol Syst. 39:1, 115132.

[108] **Knuth DE (1969).** The art of computer programming. Addison Wesley, Reading, MA.

[109] **Kronauer DJC (2009).** Recent advances in army ant biology (Hymenoptera: Formicidae). Myrmecological News. 9, 5165.

[110] **Kronauer DJC, Johnson, R.A., & Boomsma, J.J. (2007).** The evolution of multiple mating in army ants. Evolution. 61(2), 41322.

[111] **Kronauer DJC, Schöning C, & Boomsma JJ (2006).** Male parentage in army ants. Mol Ecol. 15(4), 114751.

[112] **Kronauer DJC, Berghoff SM, Powell S, Denny AJ, Edwards KJ, et al. (2006).** A reassessment of the mating system characteristics of the army ant *Eciton burchellii*. Naturwissenschaften. 93(8), 4026.

[113] **Kronforst MR, Young LG, Blume LM, & Gilbert LE (2006).** Multilocus analyses of admixture and introgression among hybridizing *Heliconius* butterflies. Evolution. 60(6), 125468.

[114] **Kuhn TS (1962).** The structure of scientific revolutions. The University of Chicago Press. Pp. 92-94.

[115] **Lande R (1979).** Quantitative genetic analysis of multivariate evolution, applied to brain: Body size allometry. Evolution. 33(1), 402416.

[116] **Legendre P & Legendre L (1998).** Numerical Ecology. 2nd English Edition. Elsevier Publishing.

[117] **Libbrecht R, Corona M, Wende F, Azevedo DO, Serrão JE, & Keller L (2013).** Interplay between insulin signaling, juvenile hormone, and vitellogenin regulates maternal effects on polyphenism in ants. Proc Natl Acad Sci USA. 110(27), 110505.

[118] **Losos JB, Warheit KI, & Schoener TW (1997).** Adaptive differentiation following experimental island colonization in Anolis lizards. Lett Nat.

[119] **Losos JB & Mahler DL (2010).** Adaptive radiation: the interaction of ecological opporunity, adaptation, and speciation. In: Evolution since Darwin: the first 150 years. Sinauer Associates. 381-420.

[120] **Losos JB, Leal M, Glor RE, De Queiroz K, Hertz PE, et al. (2003).** Niche lability in the evolution of a Caribbean lizard community. Nature. 424(6948), 5425.

[121] **Mank JE, Wedell N, Hosken DJ, & Mank JE (2013).** Polyandry and sex-specific gene expression. Philos T Roy Soc B. 368.

[122] **Marroig G & Cheverud JM (2001).** A comparison of phenotypic variation and covariation patterns and the role of phylogeny, ecology, and ontogeny during cranial evolution of new world monkeys. Evolution. 55(12), 2576600.

[123] **Marshall LG, Webb SD, Sepkoski JJ, & Raup DM (1982).** Mammalian evolution and the Great American Interchange. Science. 215, 12.

[124] **McGee MD, Schluter D, & Wainwright PC (2013).** Functional basis of ecological divergence in sympatric stickleback. BMC Evol Biol. 13, 277.

[125] **McGuigan N, Nishimura N, Currey M, Hurwit D, & Cresko WA (2010).** Quantitative genetic variation in static allomtery in the threespine stickleback. Integr Comp Biol. 50, 1067-1080.

[126] **McLachlan GJ & Peel D (2004).** Finite Mixture Models. John Wiley & Sons. Pp. 1 37.

[127] **Meisel JE (2006).** Thermal ecology of the Neotropical army ant *Eciton burchellii*. Ecol Appl. 16(3), 913922.

[128] **Merilä J & Björklund M (1999).** Population divergence and morphometric integration in the greenfinch (*Carduelis chloris*)—Evolution against the trajectory of least resistance? J Evol Biol. 12(1), 103112.

[129] **Mitteroecker P, Gunz P, Bernhard M, Schaefer K, Bookstein FL (2004).** Comparison of cranial ontogenetic trajectories among great apes and humans. J Hum Evol. 46(6), 67997.

[130] **Mitteroecker P & Gunz P (2009).** Advances in geometric morphometrics. Evol Biol. 36(2), 235-237.

[131] **Moczek AP, Sultan S, Foster S, Ledón-Rettig C, Dworkin I, et al. (2011).** The role of developmental plasticity in evolutionary innovation. Proc R Soc Lond B Biol Sci. 278:1719, 270513.

[132] **Molet M, Wheeler DE, & Peeters C (2012).** Evolution of novel mosaic castes in ants: modularity, phenotypic plasticity, and colonial buffering. Ame Nat. 180(3), 32841.

[133] **Montes C, Cardona A, Jaramillo C et al. (2015).** Middle Miocene closure of the Central American Seaway. Science. 348, 226 228.

[134] **Moreau CS (2014).** A practical guide to DNA extraction, PCR, and gene-based DNA sequencing in insects. Halteres. 5,32 42.

[135] **Moreau CS & Bell CD (2013).** Testing the museum versus cradle tropical biological diversity hypothesis: phylogeny, diversification, and ancestral biogeographic range evolution of the ants. Evolution. 67, 22402257.

[136] **Morrone JJ (2006).** Biogeographic areas and transition zones of Latin America and the Caribbean islands based on panbiogeographic and cladistic analyses of the entomofauna. Annu Rev Entomol. 51, 467494.

[137] **Mousseau TA & Dingle H (1991).** Maternal effects in insect life histories. Annu Rev Entomol. 36, 511534.

[138] **Munkemuller T, Lavergne S, Bzeznik B, Dray S, Jombart T, et al. (2012).** How to measure and test phylogenetic signal. Methods Ecol Evol. 3:743756.

[139] **Nijhout HF & German RZ (2012).** Developmental causes of allometry: New models and implications for phenotypic plasticity and evolution. Integr Comp Biol. 52(1), 4352.

[140] **Nijhout HF & Wheeler DE (1996).** Growth models of complex allometries in holometabolous insects. Am Nat. 148(1), 40-56.

[141] **Nijhout HF (2003).** Development and evolution of adaptive polyphenisms. Evol Dev. 18, 918.

[142] **Nijhout HF & Wheeler DE (1982).** Juvenile hormone and the physiological basis of insect polymorphisms. Q Rev Biol. 57(2), 109133.

[143] **Nijhout HF (2003).** The control of body size in insects. Dev Biol. 261:1, 19.

[144] **Novembre J, Johnson T, Bryc K, Kutalik Z, Adam R, et al. (2008).** Genes mirror geography within Europe. Nature. 456(7218), 98101.

[145] **O' Donnell S & Kumar A (2006).** Microclimatic factors associated with elevational changes in army ant density in tropical montane forest. Ecol Entomol. 31(5), 491498.

[146] **Oksanen J, Blanchet FG, Friendly M, Kindt R, Legendre P, et al. (2017).** vegan: Community Ecology Package. R Package, version 2.4.2.

[147] **Oldroyd BP & Fewell JH (2007).** Genetic diversity promotes homeostasis in insect colonies. Trends Ecol Evol. 22(8), 40813.

[148] **Orr HA & Betancourt AJ (2001).** Haldanes sieve and adaptation from the standing genetic variation. Genetics. 157: 875-884.

[149] **Orr HA & Turelli M (2001).** The Evolution of Postzygotic Isolation: Accumulating Dobzhansky-Muller Incompatibilities. Evolution. 55(6), 10851094.

[150] **Oster G & Wilson EO (1978).** Caste and Ecology in the Social Insects. Princeton University Press.

[151] **Pagel M (1994).** Detecting Correlated Evolution on Phylogenies: A General Method for the Comparative Analysis of Discrete Characters. Proc Roy Soc B: Biol Sci. 255(1342), 3745.

[152] **Paradis E (2013).** Molecular dating of phylogenies by likelihood methods: a comparison of models and a new information criterion. Mol Phylo Evol. 67, 436444.

[153] **Paradis E, Claude J, & Strimmer K (2004).** APE: analyses of phylogenetics and evolution in R language. Bioinformatics. 20, 289 290.

[154] **Pease JB & Hahn MW (2013).** More accurate phylogenies inferred from low-recombination regions in the presence of incomplete lineage sorting. Evolution. 67(8), 237684.

[155] **Pérez-Espona S, McLeod JE, & Franks NR (2012).** Landscape genetics of a top neotropical predator. Mol Ecol. 21, 59695985.

[156] **Pfennig DW, Wund MA, Snell-Rood EC, Cruickshank T, Schlichting CD, & Moczek AP (2010).** Phenotypic plasticity's impacts on diversification and speciation. Trends Ecol Evol. 25, 459467.

[157] **Pigliucci M (2008).** Is evolvability evolvable? Nature Reviews. Genetics. 9(1), 7582.

[158] **Pinhero JC & Bates DM (2000).** Mixed-effects models in S and S-Plus. Statistics and computing Series. Ed. Springer-Verlag, New York, NY.

[159] **Postma E (2014).** Four decades of estimating heritabilities in wild vertebrate populations: improved methods, more data, better estimates? In: Charmentier A, Garant D, & Kruuk LEB. Quantitative genetics in the wild. Pp. 16-33

[160] **Powell S & Franks NR (2005).** Caste evolution and ecology: a special worker for novel prey. Proc Roy Soc B: Biol Sci. 272(1577), 217380.

[161] **Powell S & Franks NR (2006).** Ecology and the evolution of worker morphological diversity: a comparative analysis with *Eciton* army ants. Funct Ecol. 20(6), 11051114.

[162] **Powell S (2008).** Ecological specialization and the evolution of a specialized caste in *Cephalotes* ants. Funct Ecol. 22(5), 902911.

[163] **Price TD, Kirkpatrick M (2009).** Evolutionarily stable range limits set by interspecific competition. Proc Roy Soc B: Biol Sci. 276, 14291434.

[164] **R Core Team (2016).** R: A language and environment for statistical computing. R Foundation for Statistical Computing, Vienna, Austria. URL https://www.R-project.org/.

[165] **Rachinsky A, Strambi C, Strambi A, & Hartfelder K (1990).** Caste and metamorphosis hemolymph titers of juvenile hormone and ecdysteroids in last instar honeybee larvae. Gen Comp Endocr. 79, 31-38.

[166] **Rajakumar R, San Mauro D, Dijkstra MB, Huang MH, Wheeler DE, et al. (2012).** Ancestral developmental potential facilitates parallel evolution in ants. Science. 335(6064), 7982.

[167] **Rasband WS (1997).** ImageJ. National Institutes of Health. Maryland, USA: Bethesda.

[168] **Ree RH & Sanmartín I (2009).** Prospects and challenges for parametric models in historical biogeographical inference. J Biogeogr. 36, 12111220.

[169] **Reik W & Walter J (2001).** Genomic imprinting: Parental influence on the genome. Nat Rev Gen. 2(January), 21-32.

[170] **Renaud S, Auffray JC, & Michaux J (2006).** Conserved phenotypic variation patterns, evolution along lines of least resistance, and departure due to selection in fossil rodents. Evolution. 60(8), 17011717.

[171] **Rettenmeyer CW & Watkins JF (1978).** Polygyny and monogyny in army ants. J Kansas Entomol Soc. 51(4), 581591.

[172] **Rettenmeyer CW, Rettenmeyer ME, Joseph J, & Berghoff SM (2011).** The largest animal association centered on one species: the army ant *Eciton burchellii* and its more than 300 associates. Insectes Soc. 58(3), 281292.

[173] **Revell LJ (2012).** phytools: An R package for phylogenetic comparative biology (and other things). Methods Ecol Evol. 3(2), 217223.

[174] **Reznick DN & Ricklefs RE (2009).** Darwins bridge between microevolution and macroevolution. Nature. 457, 837842.

[175] **Roff DA (1986).** The genetic basis of wing dimorphism in the sand cricket, *Gryllus firmus* and its relevance to the evolution of wing dimorphism in insects. Heredity. 57, 221-231.

[176] **Roff DA & Mousseau TA (1987).** Quantitative genetics and fitness: Lessons from *Drosophila*. Heredity. 58, 103-118.

[177] **Rubin BER, Ree RH, & Moreau CS (2012).** Inferring phylogenies from RAD sequence data. PloS ONE. 7(4), e33394.

[178] **Rull V (2011).** Neotropical biodiversity: timing and potential drivers. Trends Ecol Evol. 26, 508513.

[179] **Rundle H & Nosil P (2005).** Ecological speciation. Ecol Lett. 8(3): 336-352.

[180] **Sanderson MJ (2002).** Estimating absolute rates of molecular evolution and divergence times: a penalized likelihood approach. Mol Biol Evol. 19, 101109.

[181] **Schluter D (1996).** Adaptive radiation along genetic lines of least resistance. Evolution. 50(5), 17661774.

[182] **Schluter D & McPhail JD (1992).** Ecological character displacement and speciation in sticklebacks. Am Nat. 140: 85 - 108.

[183] **Schneider CA, Rasband WS, & Eliceiri KW (2012).** NIH Image to ImageJ: 25 years of image analysis. Nat Methods. 9(7), 671675. doi:10.1038/nmeth.2089.

[184] **Schneirla TC (1971).** Chapter 4: Raiding. In: Army Ants: A Study in Social Organization (ed. Topoff HR), pp. 69100. Freeman, San Francisco, California.

[185] **Schneirla TC (1971).** Army ants: a study in social organization. San Francisco, CA: WH Freeman and Company.

[186] **Schöning C, Kinuthia W, & Franks NR (2005).** Evolution of allometries in the worker caste of *Dorylus* army ants. Oikos. 2.

[187] **Schwander T, Rosset H, & Chapuisat M. (2005).** Division of labour and worker size polymorphism in ant colonies: the impact of social and genetic factors. Behav Ecol Sociobiol. 59(2), 215221.

[188] **Scotese CR (2014).** Atlas of Earth History, Vol. 1. Paleogeography. PALEOMAP project, Arlington, Texas. 52 pp.

[189] **Scoville A & Pfrender M (2010).** Phenotypic plasticity facilitates recurrent rapid adaptation to introduced predators. Proc Natl Acad Sci USA. 107, 42604263.

[190] **Seehausen O (2006).** African cichlid fish: a model system in adaptive radiation research. Proc R Soc Lond B. 27:19871998.

[191] **Seehausen O (2004).** Hybridization and adaptive radiation. Trends Ecol Evol. 19(4), 198207.

[192] **Self SG & Liang KY (1987).** Asymptotic properties of maximum likelihood estimators and likelihood ratio tests under nonstandard conditions. J Am Stat Assoc.

[193] **Selz OM, Lucek K, Young KA, & Seehausen O (2013).** Relaxed trait covariance in interspecific cichlid hybrids predicts morphological diversity in adaptive radiations. J Evol Biol. 114.

[194] **Sheets HD (2000).** IMP Package. Department of Physics, Canisius College, Buffalo, New York.

[195] **Simola DF, Ye C, Mutti NS, Dolezal K, Bonasio R, et al. (2013).** A chromatin link to caste identity in the carpenter ant *Camponotus floridanus*. Genome Res. 23(3), 8696.

[196] **Simons AM (2002).** The continuity of microevolution and macroevolution. J Evol Biol. 15(5), 688701.

[197] **Simpson GG (1980).** Splendid Isolation: The Curious History of South American Mammals. Yale University Press, New Haven, Connecticut.

[198] **Smith BT, McCormack JE, Cuervo AM, Hickerson MJ, Aleixo A, et al. (2014).** The drivers of tropical speciation. Nature. 515, 406409.

[199] **Soare TW, Kumar A, Naish KA, & ODonnell S (2014).** Genetic evidence for landscape effects on dispersal in the army ant *Eciton burchellii*. Mol Ecol. 23,96109.

[200] **Speed D, Hemani G, Johnson MR, & Balding DJ (2012).** Improved heritability estimation from genome-wide SNPs. Am J Hum Genet. 91, 1011-1021.

[201] **Stamatakis A (2006).** RAxML-VI-HPC: maximum likelihood- based phylogenetic analyses with thousands of taxa and mixed models. Bioinformatics. 22, 26882690.

[202] **Stehli FG & Webb SD (1985).** The Great American Biotic Interchange, pp. 357386. Plenum Press, New York, NY.

[203] **Stern DLS & Emlen DJ (1999).** The developmental basis for allometry in insects. Development. 126, 1091-101.

[204] **Stone R (2013).** Battle for the Americas. Science. 341, 230233.

[205] **Strait DS, Moniz MA, & Strait PT (1996).** Finite mixture coding: a new approach to coding continuous characters. Syst Biol. 45:l, 6778.

[206] **Suzuki Y & Nijhout HF (2006).** Evolution of a polyphenism by genetic accommodation. Science. 311: 650-652.

[207] **Trible W & Kronauer DJC (2017).** Caste development and evolution in ants: its all about size. Journal of Experimental Biology, 5362.

[208] **Turing AM (1952).** The chemical basis of morphogenesis. Proc R Soc Lond B Biol Sci. 237:641, 3772.

[209] **Van Baalen M & Beekman M (2006).** The costs and benefits of genetics heterogeneity in resistance against parasites in social insects. Am Nat. 167(4), 568577.

[210] **Verhulst EC, Beukeboom LW, & van de Zande L (2010).** Maternal control of haplodiploid sex determination in the wasp *Nasonia*. Science. 328(5978), 6203.

[211] **Visscher PM, Hill WG, & Wray NR (2008).** Heritability in the genomics era—concepts and misconceptions. Nat Rev Genet. 9(4), 25566.

[212] **Wagner GP (2014).** Homology, Genes, and Evolutionary Innovation. p. 495.

[213] **Wagner GP & Altenberg L (1996).** Complex adaptations and the evolution of evolvability. Evolution. 50(3), 967976.

[214] **Ward PS (1989).** Systematic studies on pseudomyrmecine ants: revision of the *Pseudomyrmex oculatus* and *P. subtilissimus* species groups, with taxonomic comments on other species. Quaest Entomol. 25, 393-468.

[215] **Ward PS & Downie DA (2005).** The ant subfamily Pseudomyrmecinae (Hymenoptera: Formicidae): Phylogeny and evolution of big-eyed arboreal ants. Syst Entomol. 30(2), 310335.

[216] **Watkins JF (1976).** The Identification and Distribution of New World Army Ants, pp. 1109. Baylor University Press, Waco, Texas.

[217] **Watson JAL, Okot-Kotber BM, & Noirot C (1985).** Caste differentiation in social insects. Vol 3. Pergamon Press.

[218] **Webster M & Sheets D (2010).** A practical introduction to landmark-based geometric morphometrics. In: Quantative Methods in Paleobiology, pp. 163190.

[219] **Webster M (2007).** A Cambrian peak in morphological variation within trilobite species. Science. 317:5837, 499502.

[220] **Webster M (2015).** Ontogeny and intraspecific variation of the early Cambrian trilobite *Olenellus gilberti*, with implications for olenelline phylogeny and macroevolutionary trends in phenotypic canalization. J Syst Palaeontol. 13:1, 1-74.

[221] **Webster M & Zelditch ML (2005).** Evolutionary modifications of ontogeny: heterochrony and beyond. Paleobiology. 31:3, 354372.

[222] **Webster M & Zelditch ML (2011).** Modularity of a Cambrian ptychoparioid trilobite cranidium. Evol Dev. 13(1), 96109.

[223] **West-Eberhard MJ (2003).** Developmental plasticity and evolution. Oxford University Press, New York.

[224] **West-Eberhard MJ (2005).** Developmental plasticity and the origin of species differences. Proc Natl Acad Sci USA.

[225] **Westwood JO (1842).** Monograph of the hymenopterous group, Dorylides. Arcana Entomologica; or illustrations of new, rare, and interesting insects, Volume 1, No. 5. London Pp. 73-80.

[226] **Wheeler DE (1986).** Developmental and physiological determinants of caste in social hymenoptera: evolutionary implications. Am Nat. 128, 13-34.

[227] **Wheeler DE (1991).** The Developmental Basis of Worker Caste Polymorphism in Ants. Am Nat. 138:5, 12181238.

[228] **Wheeler DE & Nijhout HF (1984).** Soldier determination in *Pheidole bicarinata*. J Insect Physiol. 30(2), 127135.

[229] **Wiernasz DC & Cole BJ (2010).** Patriline shifting leads to apparent genetic caste determination in harvester ants. Proc Natl Acad Sci USA. 107(29), 1295862.

[230] **Willson SK, Sharp R, Ramler IP, & Sen A (2011).** Spatial movement optimization in Amazonian *Eciton burchellii* army ants. Insectes Soc. 58, 325334.

[231] **Wilson EO (1985).** Ants of the Dominican amber (Hymenoptera: Formicidae). 2. The first fossil army ants. Psyche, 92,1116.

[232] **Wilson EO (1971).** The Insect Societies. Cambridge: Harvard University Press. Pp. 562.

[233] **Wilson EO (1953).** The origin and evolution of polymorphism in ants. Q Rev Biol. 28(2), 136157.

[234] **Wilson EO & Hölldobler B (2005).** Eusociality: origin and consequences. Proc Natl Acad Sci USA. 102(38), 1336771.

[235] **Winston ME, Kronauer DJC, & Moreau CS (2017a).** Early and dynamic colonization of Central America drives speciation in Neotropical army ants. Mol Ecol.

[236] **Winston ME, Thompson A, Trujillo G, Burchill AT, & Moreau CS (2017b).** Novel approach to heritability detection suggests robustness to paternal genotype in a complex morphological trait. Ecol Evol.

[237] **Woodburne MO (2010).** The Great American biotic interchange: dispersals, tectonics, climate, sea level and holding pens. J Mamm Evol. 17, 245264.

[238] **Wrege P, Wikelski M, Mandel J, Rassweiler T, & Couzin ID (2005).** Antbirds parasitize foraging army ants. Ecology. 86(3), 555559.

[239] **Wund MA, Baker JA, Clancy B, Golub JL, & Foster SA (2008).** A test of the flexible stem model of evolution: ancestral plasticity, genetic accommodation, and morphological divergence in the threespine stickleback radiation. The American Naturalist, 172(4), 44962.

[240] **Zelditch ML, Swiderski DL, & Sheets HD (2012).** Geometric morphometrics for biologists: A primer, Academic Press (Elsevier).

[241] **Zelditch ML, Swiderski DL, Sheets HD, & Fink WL (2004).** Geometric Morphometrics for Biologists: A Primer.

[242] **Zera AJ (2006).** Evolutionary genetics of juvenile hormone and ecdysteroid regulation in *Gryllus*: a case study in the microevolution of endocrine regulation. Comp Biochem Physiol A: Mol Integr Physiol. 144(3), 36579.

Appendix A

[243] Swift MJ, Izac MN, van Noordwijk M (2004) Biodiversity and ecosystem services in agricultural landscapesare we asking the right questions? Agricult Ecosys Environ 104: 113134.

[244] Mendes R, Kruijt M, de Bruijn I, Dekkers E, van der Voort M, et al. (2011) Deciphering the rhizosphere microbiome for disease-suppressive bacteria. Science 332: 1097100.

[245] Doornbos RF, Loon LCV, Bakker PAHM (2011) Impact of induced systemic resistance on the bacterial microbiome of Arabidopsis thaliana. Multitrophic Interactions in Soil 71: 169172.

[246] Berendsen RL, Pieterse CMJ, Bakker PHM (2012) The rhizosphere microbiome and plant health. Trends Plant Sci 19.

[247] Whipps JM (2001) Microbial interactions and biocontrol in the rhizosphere. J Exp Bot 52: 487511.

[248] Bonfante P, Anca IA (2009) Plants, mycorrhizal fungi, and bacteria: a network of interactions. Annu Rev Microbiol 63: 36383.

[249] Citterio S, Prato N, Fumagalli P, Aina R, Massa N, et al. (2005) The arbuscular mycorrhizal fungus Glomus mosseae induces growth and metal accumulation changes in Cannabis sativa L. Chemosphere 59: 219.

[250] Marschner P, Yang CH, Lieberei R, Crowley DE (2001) Soil and plant specific effects on bacterial community structure in the rhizosphere. Soil Biol Biochem 33: 14371445.

[251] Marschner P, Crowley D, Yang CH. 2004. Development of specific rhizosphere bacterial communities in relation to plant species, nutrition and soil type. Plant and Soil 261: 199208.

[252] Smalla K, Wieland G, Buchner A, Zock A, Parzy J, et al. (2001) Bulk and Rhizosphere Soil Bacterial Communities Studied by Denaturing Gradient Gel Electrophoresis: Plant-Dependent Enrichment and Seasonal Shifts Revealed. Appl Environ Microbiol 67(10): 47424751 doi:10.1128/AEM.67.10.4742.

[253] da Rocha UN, van Overbeek L, van Elsas JD (2009) Exploration of hitherto-uncultured bacteria from the rhizosphere. FEMS Microbiol Ecol 69: 31328.

[254] Turpault MP, Gobran GR, Bonnaud P (2007) Temporal variations of rhizosphere and bulk soil chemistry in a Douglas fir stand. Geoderma 137: 490496.

[255] Krivtsov V, Garside A, Brendler A, Liddell K, Griffiths BS, et al. (2007) A study of population numbers and ecological interactions of soil and forest floor microfauna. Anim Biol 57: 467484.

[256] Nelson DR, Mele PM (2006) The impact of crop residue amendments and lime on microbial community structure and nitrogen-fixing bacteria in the wheat rhizosphere. Aust J Soil Res 44: 319329.

[257] Jossi M, Fromin N, Tarnawski S, Kohler F, Gillet F, et al. (2006) How elevated pCO2 modifies total and metabolically active bacterial communities in the rhizosphere of two perennial grasses grown under field conditions. FEMS Microbiol Ecol 55: 339350.

[258] Chiarini L, Bevivino A, Dalmastri C, Nacamulli C, Tabacchioni S, et al. (1998) Influence of plant development, cultivar and soil type on microbial colonization of maize roots. Appl Soil Ecol 8: 1118.

[259] Milling A, Smalla K, Maidl FX, Schloter M, Munch C (2004) Effects of transgenic potatoes with an altered starch composition on the diversity of soil and rhizosphere bacteria and fungi. Plant and Soil 266: 2339.

[260] Andreote FD, de Arajo WL, de Azevedo JL, van Elsas JD, da Rocha UN, et al. (2009) Endophytic colonization of potato (Solanum tuberosum L.) by a novel competent bacterial endophyte, Pseudomonas putida strain P9, and its effect on associated bacterial communities. Appl Environ Microbiol 75: 3396406.

[261] Lekberg Y, Gibbons SM, Rosendahl S, Ramsey PW (2013) Severe plant invasions can increase mycorrhizal fungal abundance and diversity. ISME J 7(7): 142433.

[262] van Overbeek L, van Elsas JD (2008) Effects of plant genotype and growth stage on the structure of bacterial communities associated with potato (Solanum tuberosum L.). FEMS Microbiol Ecol 64: 28396.

[263] Jesus C, Susilawati E, Smith SL, Wang Q, Chai B, et al. (2010) Bacterial Communities in the Rhizosphere of Biofuel Crops Grown on Marginal Lands as Evaluated by 16S rRNA Gene Pyrosequences. BioEnergy Research 3(1): 2027 doi:10.1007/s12155-009-9073-7.

[264] Mahaffee W, Kloepper JW (1997) Temporal Changes in the Bacterial Communities of Soil, Rhizosphere, and Endorhiza Associated with Field-Grown Cucumber (Cucumis sativus L.). Microb Ecol 34(3): 210223.

[265] Lambert B, Joos H (1989) Fundamental aspects of rhizobacterial plant growth promotion research. Trends Biotechnol 7: 215219.

[266] Frommel MI, Nowak J, Lazarovits G (1991) Growth enhancement and developmental modifications of in vitro grown potato (Solanum tuberosum spp. Tuberosum) as affected by a nonfluorescent Pseudomonas sp. Plant Physiol 96: 92836.

[267] Glick BR, Penrose DM, Li J (1998) A model for lowering plant ethylene concentrations by plant growth promoting bacteria. J Theor Biol 190: 6368.

[268] Barac T, Taghavi S, Borremans B, Provoost A, Oeyen L, et al. (2004) Engineered endophytic bacteria improve phytoremediation of water-soluble, volatile, organic pollutants. Nat Biotechnol 22: 583588.

[269] Taghavi S, Barac T, Greenberg B, Borremans B, Vangronsveld J, et al. (2005) Horizontal gene transfer to endogenous endophytic bacteria from poplar improves phytoremediation of toluene. Appl Environ Microbiol 71: 85008505.

[270] Diaz CL (1989) Root lectin as a determinant of host-plat specificity in the Rhizobium-legume symbiosis. Nature 4: 338.

[271] Gilbert J, van der Lelie D, Zarraonaindia I (2014) Microbial terroir for wine grapes. PNAS doi: 10.1073/pnas.1320471110.

[272] Bokulich NA, Thorngate JH, Richardson PM, Mills DA (2013) Microbial biogeography of wine grapes is conditioned by cultivar, vintage, and climate. PNAS doi: 10.1073/pnas.1317377110.

[273] Verginer M, Leitner E, Berg G (2010) Production of volatile metabolites by grape-associated microorganisms. J Agricult Food Chem 58(14): 834450 doi:10.1021/jf100393w.

[274] Bulgarelli D, Schlaeppi K, Spaepen S, Ver Loren van Themaat E, Schulze-Lefert P (2013) Structure and Functions of the Bacterial Microbiota of Plants. Annu Rev Plant Biol doi:10.1146/annurev-arplant-050312-120106.

[275] Garbeva P, van Veen JA, van Elsas JD (2004) Microbial diversity in soil: selection microbial populations by plant and soil type and implications for disease suppressiveness. Ann Rev Phytopathol 42(29): 24370 doi:10.1146/annurev.phyto.42.012604.135455.

[276] Berg G, Smalla K (2009) Plant species and soil type cooperatively shape the structure and function of microbial communities in the rhizosphere. FEMS Microbiol Ecol 68(1): 113 doi:10.1111/j.1574-6941.2009.00654.x.

[277] Caporaso JG, Lauber CL, Walters WA, Berg-Lyons D, Huntley J, et al. (2012) Ultra-high-throughput microbial community analysis on the Illumina HiSeq and MiSeq platforms. ISME J 6(8): 16211624.

[278] Winston M (2014) Cannabis Microbiome Raw Sequence Data. Figshare

[279] Caporaso JG, Kuczynski J, Stombaugh J, Bittinger K, Bushman FD, et al. (2010) QIIME allows analysis of high-throughput community sequencing data. Nature Methods 7(5): 335336.

[280] McDonald D, Price MN, Goodrich J, Nawrocki EP, Desantis TZ, et al. (2012) An improved Greengenes taxonomy with explicit ranks for ecological and evolutionary analyses of bacteria and archaea. ISME J 6: 6108.

[281] Price MN, Dehal PS, Arkin AP (2009) FastTree: Computing Large Minimum Evolution Trees with Profiles instead of a Distance Matrix. Mol Biol Evol 26(7): 16411650.

[282] Wang Q, Garrity GM, Tiedje JM, Cole JR (2007) Nave Bayesian Classifier for Rapid Assignment of rRNA Sequences into the New Bacterial Taxonomy. Appl Environ Microbiol 73: 52615267.

[283] Lozupone C, Knight R (2005) UniFrac: a New Phylogenetic Method for Comparing Microbial Communities. Appl Environ Microbiol 71(12): 8228 DOI: 10.1128/AEM.71.17.82288235.2005.

[284] Oksanen J, Guillaume BF, Kindt R, Legendre P, Minchin PR, et al. (2013). vegan: Community Ecology Package. R package version 2.010. http://CRAN.R-project.org/package=vegan

[285] Berg B, Hofsten B, Petterson G (1972) Growth and Cellulase Formation by Cellvibrio fulvus. J Appl Bacteriol 35: 201214.

[286] Beattie GA (2006) Survey Molecular Phylogeny, Genomics and Recent Advances. In: Plant-Associated Bacteria, pp. 156.

[287] van der Lelie D, Taghavi S, Monchy S, Schwender J, Miller L, et al. (2009) Poplar and its Bacterial Endophytes: Coexistence and Harmony. Crit Rev Plant Sci 28: 346358.

[288] Gottel NR, Castro HF, Kerley M, Yang Z, Pelletier D, et al. (2011) Distinct microbial communities within the endosphere and rhizosphere of Populus deltoides roots across contrasting soil types. Appl Environ Microbiol 77: 593444.

[289] Bulgarelli D, Rott M, Schlaeppi K, van Themaat EVL, Ahmadinejad N, et al. (2012) Revealing structure and assembly cues for Arabidopsis root-inhabiting bacterial microbiota. Nature 488(7409): 9195 doi:10.1038/nature11336.

[290] Duineveld MD, Rosado AS, Van Elsas JD, Van Veen JA (1998) Analysis of the dynamics of bacterial communities in the rhizosphere of chrysanthemum via denaturing gradient gel electrophoresis and substrate utilization patterns. Appl Environ Microbiol 64: 49504957.

[291] Bezemer TM, Lawson CS, Hedlund K, Edwards AR, Brook AJ, et al. (2006) Plant species and functional group effects on abiotic and microbial soil properties and plant-soil feedback responses in two grasslands. J Ecol 94: 893904.

[292] Bonanomi G, Rietkerk M, Dekker SC, Mazzoleni S (2005) Negative plant-soil feedback and positive species interaction in a herbaceous plant community.Plant Ecology. 181: 269278.

Appendix B

[293] Berish CW. 1986. Leaf-cutting ants (Atta cephalotes) select nitrogen-rich forage. Am Midl Nat. 115:268276.

[294] Burd M, Howard JJ. 2005. Central-place foraging continues beyond the nest entrance: the underground performance of leaf- cutting ants. Anim Behav. 70:737744.

[295] Chazdon RL. 2003. Tropical forest recovery: legacies of human impact and natural disturbances. Perspect Plant Ecol Evol Syst. 6:5171.

[296] Cherrett JM. 1986. History of the leaf-cutting ant problem. Leaf- cutting ants: biology and management. Boulder: Westview Press; p. 1017.

[297] Covich A. 1976. Analyzing shapes of foraging areas: some ecologi- cal and economic theories. Annu Rev Ecol Syst. 7:235257.

[298] Dohm C, Leal IR, Tabarelli M, Meyer ST, Wirth R. 2011. Leaf- cutting ants proliferate in the Amazon: an expected response to forest edge? J Trop Ecol. 27:645649.

[299] Farji-Brener AG. 2001. Why are leaf-cutting ants more common in early secondary forests than in old-growth tropical forests? An evaluation of the palatable forage hypothesis. Oikos. 92:169177.

[300] Farji-Brener AG, Chinchilla F, Umaa MN, Ocasio-Torres ME, Chauta-Mellizo A, Acosta-Rojas D, Marinaro S, Curth MT, Amador-Vargas S. 2014. Branching angles reflect a tradeoff between reducing trail maintenance costs or travel distances in leaf-cutting ants. Ecology.

[301] Farji-Brener AG, Rica C, Laverde O. 2007. Fallen branches as part of leaf-cutting ant trails: their role in resource discovery and leaf transport rates in Atta cephalotes. Biotropica. 39:211215.

[302] Farji-Brener AG, Silva J. 1996. Leaf-Cutter Ants aid to the estab- lishment success of Tapirira velutinifolia Seedlings in a Parkland Savanna.

[303] Folgarait P. 1998. Ant biodiversity and its relationship to ecosystem functioning: a review. Biodivers Conserv. 7:12211244.

[304] Fonte SJ, Schowalter TD. 2005. The influence of a neotropical herbivore on nutrient cycling and soil processes. Oecologia. 146:423431.

[305] Herz H, Beyschlag W, Hlldobler B. 2007a. Herbivory rate of leaf- cutting ants in a tropical moist forest in panama at the popula- tion and ecosystem scales. Biotropica. 39:482488.

[306] Herz H, Beyschlag W, Hlldobler B. 2007b. Assessing herbivory rates of Leaf-Cutting Ant (Atta colombica) colonies through short-term refuse deposition counts. Biotropica. 39:476481.

[307] Howard JJ. 1988. Leafcutting ant diet selection: relative influence of leaf chemistry and physical features. Ecology. 69:250260.

[308] Howard JJ. 2001. Costs of trail construction and maintenance in the leaf-cutting ant Atta columbica. Behav Ecol Sociobiol. 49:348356.

[309] Hudson TM, Turner BL, Herz H, Robinson JS. 2009. Temporal patterns of nutrient availability around nests of leaf-cutting ants (Atta colombica) in secondary moist tropical forest. Soil Biol Biochem. 41:10881093.

[310] Kost C, De Oliveira EG, Knoch TA, Wirth R. 2005. Spatio-tem- poral permanence and plasticity of foraging trails in young and mature leaf-cutting ant colonies (Atta spp.). J Trop Ecol. 21:677.

[311] Laurance WF, Goosem M, Laurance SGW. 2009. Impacts of roads and linear clearings on tropical forests. Trends Ecol Evol. 24:659 669.

[312] Leal IR, Wirth R, Tabarelli M. 2014. The multiple impacts of leaf- cutting ants and their novel ecological role in human-modified Neotropical forests. Biotropica. 46:516528.

[313] Lewis OT, Martin M, Czaczkes TJ. 2008. Effects of trail gradient on leaf tissue transport and load size selection in leaf-cutter ants. Behav Ecol. 19:805809.

[314] Lugo AE, Farnworth EG, Pool D, Jerez P, Kaufman G. 1973. The impact of the leaf-cutter ant atta colombica on the energy flow of a tropical west forest. Ariel. 54:12921301.

[315] Rockwood L. 1976. Plant selection and foraging patterns in two species of leaf-cutting ants (Atta). Ecology. 57:4861.

[316] Rockwood L, Hubbell SP. 1987. Host-plant selection, diet diversity, and optimal foraging in a tropical leafcutting ant. Oecologia. 74:5561.

[317] Shepherd JD. 1985. Adjusting foraging effort to resources in adja- cent colonies of the leaf-cutter ant, Atta colombica. Biotropica. 17:245252.

[318] Silva PSD, Bieber AGD, Knoch TA, Tabarelli M, Leal IR, Wirth R. 2013. Foraging in highly dynamic environments: leaf-cutting ants adjust foraging trail networks to pioneer plant availability. Entomol Exp Appl. 147:110.

[319] Silva PSD, Bieber AGD, Leal IR, Wirth R, Tabarelli M. 2009. Decreasing abundance of leaf-cutting ants across a chronose- quence of advancing Atlantic forest regeneration. J Trop Ecol. 25:223227.

[320] Sternberg LSL, Pinzon MC, Moreira MZ, Moutinho P, Rojas EI, Herre EA. 2007. Plants use macronutrients accumulatedin leaf-cutting ant nests. Proc R Soc B: Biol Sci. 274: 315321.

[321] Traniello JFA. 1989. Foraging strategies of ants. Ann Rev Entomol. 34:191210.

[322] Urbas P, Araujo MVJ, Leal IR, Wirth R. 2007. Cutting more from cut forests: edge effects on foraging and herbivory of Leaf- Cutting Ants in Brazil. Analyzer. 39:489495.

[323] Vasconcelos HL. 1990. Habitat selection by the queens of the leaf-cutting ant Atta sexdens L. in Brazil. J Trop Ecol. 6:249252.

[324] Vasconcelos HL, Ehm V-N, Mundim FM, Bruna EM. 2006. Roads alter the colonization dynamics of a keystone herbivore in neo- tropical savannas. Biotropica. 38:661665.

[325] Venables WN, Ripley BD 2002. Modern Applied Statistics with S. New York (NY): Springer-Verlag.

[326] Wirth R, Herz H, Ryel RJ, Beyschlag W, Hlldobler B. 2003. Herbivory of leaf-cutting ants: a case study on Atta colombica in the tropical forest of Panama. Berlin, Heidelberg, New York. Germany/New York: Springer.

[327] Wirth R,Meyer ST, AlmeidaWR, Arajo VJ, Barbosa VS, Leal IR. 2007. Increasing densities of leaf-cutting ants (Atta spp.) with proximity to the edge in a Brazilian Atlantic forest. J Trop Ecol. 23:501.

[328] Wirth R, Meyer ST, Leal IR, Tabarelli M. 2008. Plant Herbivore Interactions at the Forest Edge. Prog Bot. 69:423448.

12 Appendix A: Understanding cultivar-specificity and soil determinants of the *Cannabis* microbiome.

Abstract

Understanding microbial partnerships with the medicinally and economically important crop *Cannabis* has the potential to affect agricultural practice by improving plant fitness and production yield. Furthermore, *Cannabis* presents an interesting model to explore plant-microbiome interactions as it produces numerous secondary metabolic compounds. Here we present the first description of the endorhiza-, rhizosphere-, and bulk soil-associated microbiome of five distinct *Cannabis* cultivars. Bacterial communities of the endorhiza showed significant cultivar-specificity. When controlling cultivar and soil type the microbial community structure was significantly different between plant cultivars, soil types, and between the endorhiza, rhizosphere and soil. The influence of soil type, plant cultivar and sample type differentiation on the microbial community structure provides support for a previously published two-tier selection model, whereby community composition across sample types is determined mainly by soil type, while community structure within endorhiza samples is determined mainly by host cultivar.

Introduction

Soil microbes play a major role in plant ecology by providing a variety of benefits such as nitrogen fixation, production of growth stimulants, improved water retention, and suppression of root diseases (Swift et al., 2004; Mendes et al., 2011; Doornbos et al., 2011; Berendsen et al., 2012). These vital microbial processes occur predominantly within the rhizosphere and rhizoplane, and are heavily influenced by fungal saprotrophs and plant-mutualists such as endomycorrhizal and ectomycorrhizal fungi (Whipps, 2001; Bonfante, 2009). Despite the economic and medicinal importance of *Cannabis* spp., little is known about its soil-based microbial associations (Citterio et al., 2005; Liste & Prutz, 2006).

Microbial composition in soil depends on complex interactions between the soil type, root zone location, and plant species (Marschner et al., 2001; Marschner et al., 2004; Smalla et al., 2001). Rhizosphere microbiota are highly dynamic [12], and the composition of bacterial communities can fluctuate in response to seasonal and diel temperature changes (Turpault et al., 2007), water content (Krivstov et al., 2007), pH (Nelson & Mele, 2006), CO_2 concentration, and O_2 levels (Jossi et al., 2006). Although evidence has been found for significant effects of plant cultivar on rhizosphere communities (Chiarini et al., 1998; Milling et al., 2004; Andreote et al., 2009) and endomycorrhizal fungal communities (Lekberg et al., 2013), some work suggests that these effects are minimal compared to edaphic factors (particularly pH) or plant growth stage (von Overbeek & van Elsas, 2008; Jesus et al., 2010).

Rhizosphere bacteria not only colonize the rhizosphere and/or the rhizoplane soil, but can also colonize plant tissues. Bacteria that have colonized root tissue—more specifically known as the endorhiza (Mahafee & Kloepper, 1997)—have been reported to support plant growth and suppress plant diseases by providing phytohormones, low molecular weight compounds or enzymes involved in regulating growth and metabolism (Lambert & Joos, 1989; Frommel et al., 1991; Glick et al., 1998). In addition, endorhiza bacteria assist their host plants in tolerating the phytotoxic effects of environmental toxicants (Barac et al., 2004; Taghavi et al., 2005). Endorhiza communities tend to be more plant-specific, and are often shaped by the compounds or proteins produced by their host (Diaz, 1989). Both endophytes and epiphytes may also play a role in localized flavor or terroir for crop plants, as has been shown recently for wines (Gilbert et al., 2014; Bokulich et al., 2013; Verginer et al., 2010).

A growing body of work has united the colonization of both the rhizosphere and plant tissues under the two-tier selection model, where soil type defines the composition of rhizosphere and root-inhabiting bacterial communities (Bulgarelli et al., 2013; Garbeva et al., 2004; Berg & Smalla, 2009). Under this model, edaphic factors determine the structure of the local soil microbiota, which become the source for the first bacterial community shift into the nutrient rich environment of the rhizosphere. Following this first shift, migration from

the rhizosphere into the plant tissues is based on plant genotype-dependent selection of the endorhiza environment (Bulgarelli et al., 2013). Along with the prediction that rhizosphere and endorhiza microbiota should be soil-derived, the two-tier selection model predicts several broad changes in phylum-level taxon abundance associated with the shifting microbiota, such as dramatic reduction in Acidobacteria within the endosphere.

This study aims to characterize bacterial diversity in the root and soil systems of five strains of *Cannabis* in order to explore how soil microbiota and plant strain affect the endorhiza microbial community of this commercially important crop. We hypothesize that different cultivars maintain significantly different microbial communities, and that these differences diminish from endorhiza to rhizosphere to bulk soil.

Materials and Methods

Experiments

The data for this paper were collected in two experiments: First, an experiment to identify variation in the microbial communities, and second, an experiment designed to understand the nature and strength of cultivar-specificity. The first experiment was composed of bulk soil, rhizosphere, and endorhiza samples taken from nine plants of the three different *Cannabis* spp. tested strains—Burmese, BooKoo Kush, and Sour Diesel. Soil physicochemical data was taken for all bulk soil samples in the first experiment, however there was minimal edaphic variation. The second experiment sought to understand the effect of strain with more significant edaphic variation, and was accomplished using two different strains—White Widow and Maui Wowie—and two different soil types. Four plants of the two strains were grown in the same soil, and then two plants of White Widow were grown in a completely distinct soil type. Triplicate samples were taken from each plant for both the rhizosphere and endorhiza, as well as for each of the two soil types.

Cultivars

Different cultivars were used for each one of the experiments. For the first experiment, we used Sour Diesel, Bookoo Kush, and Burmese cultivars. Sour Diesel is a cultivar of Cannabis sativa, associated with a high tetrahydrocannabinol (THC) to cannabidiol (CBD) ratio. Bookoo Kush is a sativa-dominant hybrid cultivar of *Cannabis sativa* and *Cannabis indica*, associated with a moderately high THC to CBD ratio. Burmese is a balanced hybrid cultivar of both *Cannabis sativa* and *Cannabis indica*, associated with a moderate THC to CBD ratio. For the second experiment, we used Maui Wowie and White Widow cultivars. Maui Wowie is a cultivar of *Cannabis sativa*, associated with a high THC to CBD ratio. White Widow is a balanced hybrid cultivar of both *Cannabis sativa* and *Cannabis indica*, known to have a more moderate THC to CBD ratio.

Sample collection

Endorhiza, rhizosphere soil, and bulk soil samples for the first experiment were taken from 9 organically-grown Cannabis plants of three different strains (Burmese, Bookoo Kush, Sour Diesel) in Vista, California, in November, 2011, for a total of 27 samples. Therefore, the triplicate DNA extracts were acquired for endorhiza, rhizosphere and bulk-soil for each of the 3 Cannabis spp. strains, resulting in a single endorhiza, rhizosphere, and bulk soil sample for each plant. The plants were grown in locally composted soil. Eight weeks following the harvesting of the Cannabis flowering bud and foliage from each plant, a 50 g bulk soil sample was taken 10 cm from the stem of each of the nine plants at a depth of 20 cm, as well as a larger sample of soil for testing edaphic factors (Table 1). The bulk soil sample was immediately capped and transported to a 4C refrigerator. In addition, endorhiza samples were taken from the root ball of each of the six plants. The soil that remained adhered to the roots after removal from the ground was used to produce the rhizosphere soil samples. The rhizosphere soil was removed from the roots by shaking the root into a whirlpak bag. All samples were immediately transferred to storage at 4C for shipping back

Soil ID	Physical Composition	pH	Salinity	Total N	Total Organic C	Water Content
MB.1.B	64.6 sand, 17.6 silt, 17.8 clay	6.94	7.15	1.41	5.00	0.164
MB.1.SD	66.0 sand, 16.3 silt, 17.7 clay	6.80	7.10	1.51	4.32	0.178
MB.1.BK	63.1 sand, 17.7 silt, 19.2 clay	6.82	7.44	1.30	3.31	0.101
MB.2	62.0 sand, 17.3 silt, 20.7 clay	6.63	5.12	0.26	3.02	0.113
OC.2	64.0 sand, 16.0 silt, 20.0 clay	6.77	1.73	0.53	20.0	0.371

Physical composition and tested edaphic factors for five soil types from both experiments. Abbreviations for Soil ID are: MB indicates Mo-Bio soil, OC indicates Orange County soil, number indicates experiment (1 = first experiment, 2 = second experiment), and final letter abbreviations detail the associated cultivar with the bulk soil. B = Burmese, SD = Sour Diesel, BK = Bookoo Kush.
doi:10.1371/journal.pone.0099641.t001

to the laboratory for processing (approximately 4 hours). All root samples were rinsed with alcohol and sterile water before the extraction. DNA was isolated from 0.25 g of soil or root per extraction using standard protocol for PowerSoil DNA Isolation Kit (MO BIO, USA), with the modification of heating the extraction at 65C for 10 minutes prior to the initial vortex step. The soil physicochemical data was generated by Fruit Growers Laboratory (Santa Paula, CA), including total carbon and nitrogen concentrations, pH, salinity, and water content for all samples.

Endorhiza, rhizosphere, and bulk soil samples for the second experiment were taken from 6 organically-grown Cannabis plants of two different strains (White Widow and Maui Wowie) from two locations in August, 2012: Vista and Orange County, California. Triplicate samples were taken from each of the six plants (18 samples) and surrounding rhizosphere (18 samples), as well as from each of the two bulk soils used in the different locations (6 samples), totaling 42 samples. In contrast to the first experiment, all samples were taken two weeks prior to harvest. Additionally, triplicate samples from the second experiment were taken from different roots on the same plant (pseudoreplicates). Cannabinoid data was taken from the buds of three White Widow plants and one Mauie Wowie plant (Table S1). All cannabinoid data was processed at Delta-9-Technologies, LLC (Santa Ana, California). Otherwise, sampling procedure matched the first experiment.

Illumina sequencing of the V4 region of the 16S rRNA gene

We utilized Illumina 16S rRNA sequencing to analyze samples of the endorhiza, the rhizosphere, and the bulk soil of three different strains of Cannabis in the first study (27 samples), and two different strains of Cannabis in the second study (42 samples), for a total of 69 samples. The V4 region of the 16S rRNA gene was amplified and sequenced using the primers specified in Caporaso et al. (2012) following the Earth Microbiome Project's standard pipeline. The 291 bp length V4 region amplification was performed using the 515F primer and the 806R Golaybarcoded reverse primers. Each 25 L PCR reaction contained 12 L of MO BIO PCR Water (Certified DNA-Free), 10 L of 5 Prime HotMasterMix (1x), 1 L of Forward Primer (5 M concentration, 200 pM final), 1 L Golay Barcode Tagged Reverse Primer (5 M concentration, 200 pM final), and 1 L of template DNA. The conditions for PCR are as follows: 94C for 3 minutes to denature the DNA, with 35 cycles at 94C for 45 s, 50C for 60 s, and 72C for 90 s, with a final extension of 10 min at 72C to ensure complete amplification. PCR was completed in triplicate and products were pooled. Each pool was then quantified using Invitrogen's PicoGreen and a plate reader. Once quantified, different volumes of each of the products were pooled into a single tube so an equal amount (ng) of DNA was in the pool, and cleaned using the UltraClean PCR Clean-Up Kit (MO BIO). After quantification, the molarity of the pool is determined and diluted down to 2 nM, denatured, and then diluted to a final concentration of 6.1 pM with a 30% PhiX spike for sequencing on the Illumina MiSeq. A 151 bp x 12 bp x 151 bp MiSeq run was performed using the custom sequencing primers and procedures described in the supplementary methods in Caporaso et al. (2012). All raw sequence data is available publicly.

Bioinformatic analysis of the 16S rRNA V4 sequence data

All sequence analysis was done using QIIME 1.7.0 (Caporaso et al., 2010). QIIME defaults were used for quality filtering of raw Illumina data. In the second study, both closed and open reference OTU-picking methods were employed. In the first study, OTUs were picked

against the Greengenes (McDonald et al., 2012) database pre-clustered at 97% identity, and sequences that did not hit the reference collection were clustered *de novo* (i.e. open reference). Representative sequences were aligned to the Greengenes core set with PyNAST (Caporaso et al., 2010). All sequences that failed to align were discarded. A phylogenetic tree was built from the alignment using FastTree (Price et al., 2009), and taxonomy was assigned to each sequence using the RDP classifier (Wang et al., 2007) retrained on Greengenes. Samples for the first experiment were rarified to an even depth of 3,000 sequences. Four samples were discarded due to insufficient sequence coverage. For the second experiment, samples were rarified to an even depth of 45,000 sequences. One sample was discarded due to insufficient coverage. Alpha, and beta-diversity metrics were produced using QIIME (Caporaso et al., 2010). Relationships between samples were visualized and evaluated using redundancy analysis (RDA) and principal coordinate analyses (PCoA) calculated from pairwise sample distances (weighted and unweighted UniFrac metrics) (Lozupone & Knight, 2005). Significance tests (ANOSIM, ADONIS, ANOVA, RDA, and Mantel) were run using scripts in QIIME (Caporaso et al., 2010). To evaluate the most important abiotic factors in structuring the communities, a Best Subset of Environmental Variables with Maximum (Rank) Correlation with Community Dissimilarities (BEST) analysis was run in QIIME (see *vegan::bioenv*) (Oksanen et al., 2013).

Results

Work for this study was accomplished in two experiments. First, we performed an experiment to identify variation in the microbial communities between roots and soil in three different *Cannabis* strains (Burmese, BooKoo Kush, and Sour Diesel), and second, an experiment designed to understand the nature and strength of plant cultivar-specificity between two different strains (White Widow and Maui Wowie) in two different soil types (with significant differences in edaphic variables). Triplicate samples were taken from each plant for both the rhizosphere and endorhiza, as well as for each of the two soil types.

Both endorhiza and bulk soil microbiomes were significantly distinct from other sample types, and strain level differences were only observed in the endorhiza. In the first experiment, using unweighted UniFrac, beta-diversity comparisons of each individual sample type against all other sample types (Fig. 1a) yielded significant clustering of endorhiza (ADONIS: $R^2 = 0.26, p = 0.001$) and bulk soil (ADONIS: $R^2 = 0.14, p = 0.001$) samples from the other categories, but rhizosphere samples were not significantly different (ADONIS: $R^2 = 0.07, p = 0.07$). Weighted UniFrac distances yielded similar results with endorhiza (ADONIS: $R^2 = 0.59, p = 0.001$) and bulk soil (ADONIS: $R^2 = 0.29, p = 0.004$) samples demonstrating significant differences from other sample types, but no significant differences for rhizosphere (ADONIS: $R^2 = 0.09, p = 0.10$) samples. Division of all communities via strain (Fig. 1b) was not significant for weighted (ADONIS: $R^2 = 0.11, p = 0.25$) or unweighted (ADONIS: $R^2 = 0.11, p = 0.15$) analyses, however, division of endorhiza communities via strain was significant for both weighted (ADONIS: $R^2 = 0.59, p = 0.004$) and unweighted (ADONIS: $R^2 = 0.39, p = 0.003$) analyses. The abundance of *Methylophilus* explained a significant portion of this difference (FDR: $p = 0.012$), comprising 13% of the microbial community in the endorhiza of Bookoo Kush, 0.13% in Burmese and was absent in Diesel. Despite these significant differences, all endorhiza samples maintained a core community of *Pseudomonas*, *Cellvibrio*, *Oxalobacteraceae*, *Xanthomonadaceae*, *Actinomycetales*, and *Sphingobacteriales*. With the exception of the aerobic cellulytic bacterium *Cellvibrio*, all prevalent members of the core endorhiza community were well known endophytic bacteria (Berg et al., 1972; Beattie, 2006) primarily within the orders *Gammaproteobacteria* and *Alphaproteobacteria*, which supports observations from other plant systems (van der Lelie et al., 2009; Gottel et al., 2011).

Community composition across all samples was determined predominantly by soil properties, but differences in community structure (abundance) within endorhiza were driven by *Cannabis* cultivar. In the second experiment, using unweighted UniFrac, community beta diversity was significantly different between soil types (Fig. 2a) (ADONIS: $R^2 = 0.32, p =$

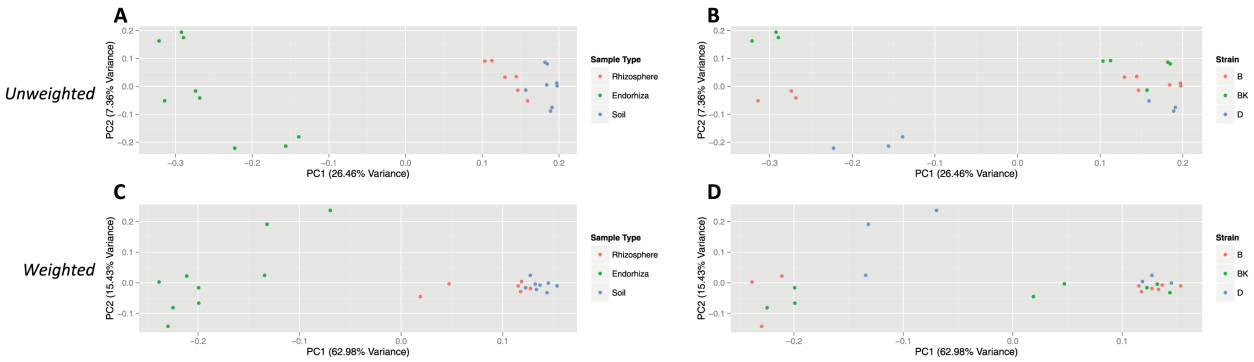

Figure 20: PCoA plots of microbial community similarity in first experiment for unweighted analysis (AB) and weighted analysis (CD). Plots for unweighted analysis are based on unweighted UniFrac distance, and demonstrate relationship between sample type (A), strain (B), and the major PC axes (PC 1=26.46% variance, PC 2=7.36% variance). Plots for weighted analysis are based on weighted UniFrac distances, and demonstrate relationship between sample type (C), strain (D), and the major PC axes (PC 1=62.98% variance, PC 2=15.43% variance). Abbreviations for strains are denoted by B (Burmese), BK (BooKoo Kush), and D (Sour Diesel).

0.001), among sample types (Fig. 2b) (ADONIS: $R^2 = 0.12, p = 0.005$), and strains (Fig. 2c) (ADONIS: $R^2 = 0.10, p = 0.008$). Cluster comparisons of each individual sample type against all other sample types (Fig. 2b) yielded significant differences for endorhiza (ADONIS: $R^2 = 0.10, p = 0.001$) and rhizosphere (ADONIS: $R^2 = 0.05, p = 0.04$) samples, but no significant differences for bulk soil (ADONIS: $R^2 = 0.04, p = 0.12$) samples. Using weighted UniFrac, community beta diversity varied significantly by soil type (Fig. 2d) (ADONIS: $R^2 = 0.21, p = 0.001$), sample type (Fig. 2e) (ADONIS: $R^2 = 0.27, p = 0.001$), and strain (Fig. 2f) (ADONIS: $R^2 = 0.27, p = 0.001$). Cluster comparisons of each individual sample type against all other sample types (Fig. 2e) yielded significant differences for endorhiza (ADONIS: $R^2 = 0.26, p = 0.001$) and rhizosphere (ADONIS: $R^2 = 0.13, p = 0.001$) samples, with mixed results for bulk soil samples (ADONIS: $R^2 = 0.06, p = 0.054$; ANOSIM: $R = 0.012, p = 0.459$; RDA: $F = 2.41, p = 0.045$).

Pooling the first and second experiments together, division of all communities via soil type (Fig. 3a) (ADONIS: $R^2 = 0.196, p = 0.001$), sample type (Fig. 3b) (ADONIS: $R^2 = 0.086, p = 0.001$), and strain (Fig. 3c) (ADONIS: $R^2 = 0.178, p = 0.001$) were highly significant for all tests using unweighted UniFrac. Cluster comparisons of each individual sample type against all other sample types yielded significant results for endorhiza samples

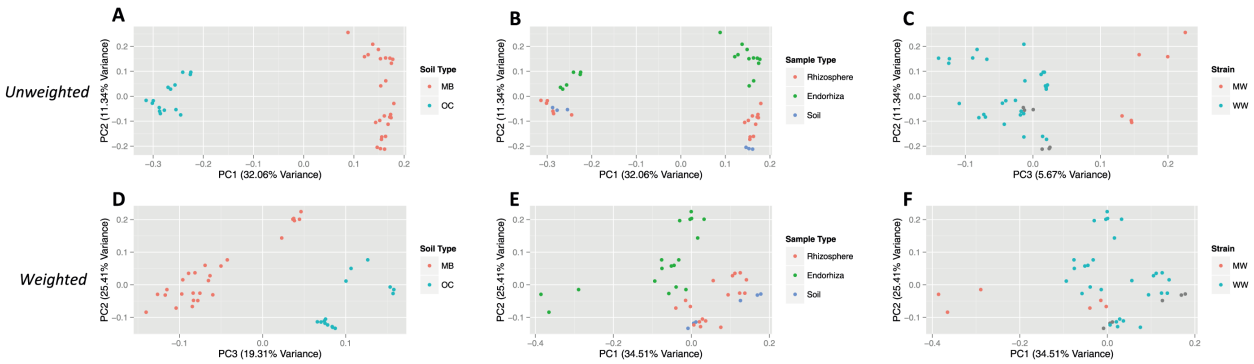

Figure 21: PCoA plots of microbial community similarity in second experiment for unweighted analysis (AC) and weighted analysis (DF). Plots for unweighted analysis are based on unweighted UniFrac distances, and demonstrate relationship between soil type (A), sample type (B), strain (C), and the major PC axes (PC 1=32.06% variance, PC 2=11.34% variance, PC 3=5.67% variance). Plots for weighted analysis are based on weighted UniFrac distances, and demonstrate relationship between soil type (D), sample type (E), strain (F), and the major PC axes (PC 1=34.51% variance, PC 2=25.41% variance, PC 3=19.31% variance). Note that PC 1 in the unweighted analysis is dominated by variation in soil type (A), but PC 1 in weighted analysis is dominated by strain (F). Grey points (Fig. 2c, 2f) represent bulk soil samples that aren't associated with either strain. Abbreviations for strains are denoted by MW (Mauie Wowie) and WW (White Widow), and abbreviations for soil type are denoted by MB (Mo-Bio soil) and OC (Orange County soil).

(ADONIS: $R^2 = 0.069, p = 0.001$), and mixed results for rhizosphere (ADONIS: $R^2 = 0.034, p = 0.004$; ANOSIM: $R = 0.005, p = 0.365$; RDA: $F = 2.17, p = 0.001$) and bulk soil samples (ADONIS: $R^2 = 0.031, p = 0.005$; ANOSIM: $R = 0.032, p = 0.628$; RDA: $F = 2.00, p = 0.003$). Likewise, using weighted UniFrac, the division of all communities via soil type (Fig. 3d) (ADONIS: $R^2 = 0.323, p = 0.001$), sample type (Fig. 3e) (ADONIS: $R^2 = 0.229, p = 0.001$), and strain (Fig. 3f) (ADONIS: $R^2 = 0.301, p = 0.001$) was highly significant for all tests. Cluster comparisons of each individual sample type against all other sample types yielded significant results for endorhiza samples (ADONIS: $R^2 = 0.215, p = 0.001$), and mixed results for rhizosphere (ADONIS: $R^2 = 0.093, p = 0.002$; ANOSIM: $R = 0.045, p = 0.129$; RDA: $F = 6.36, p = 0.002$) and bulk soil samples (ADONIS: $R^2 = 0.057, p = 0.008$; ANOSIM: $R = 0.041, p = 0.691$; RDA: $F = 3.76, p = 0.006$).

Soil followed by strain had the largest affect on OTU abundances, but strain showed no impact on OTU presence/absence. For individual OTUs, both unweighted (g-test) and weighted (ANOVA) analyses showed that soil type had the strongest influence over significant OTU differences (Table 2). While strain showed a larger effect than sample type for weighted

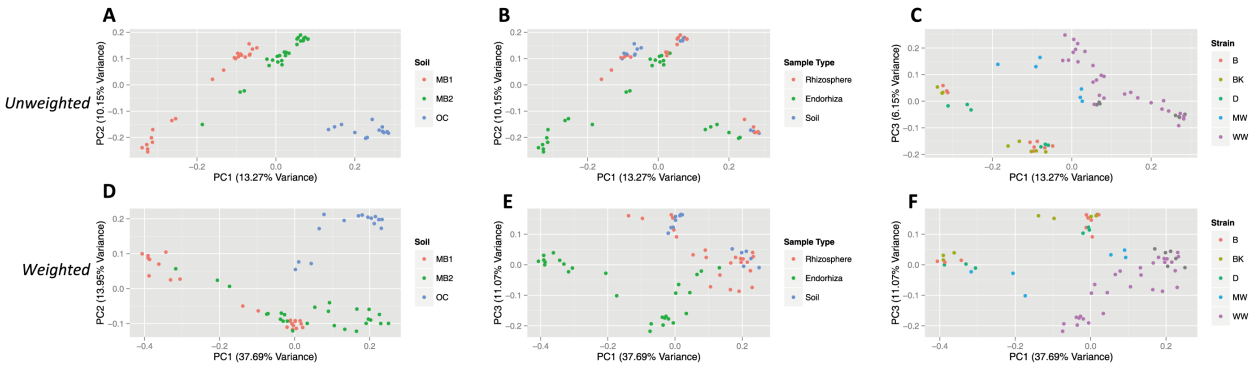

Figure 22: PCoA plots of microbial community similarity in pooled experiments for unweighted analysis (AC) and weighted analysis (DF). Plots for unweighted analysis are based on unweighted UniFrac distance, and demonstrate relationship between soil type (A), sample type (B), strain (C), and the major PC axes (PC 1=13.27% variance, PC 2=10.15% variance, PC 3=6.15% variance). Plots for weighted analysis are based on weighted UniFrac distances, and demonstrate relationship between soil type (D) sample type (E), strain (F), and the major PC axes (PC 1=37.69% variance, PC 2=13.95% variance, PC 3=11.07% variance). Abbreviations for strains are denoted by B (Burmese), BK (BooKoo Kush), D (Sour Diesel), MW (Mauie Wowie) and WW (White Widow). Abbreviations for soil type are denoted by MB1 (Mo-Bio soil from the first experiment), MB2 (Mo-Bio soil from the second experiment) and OC (Orange County soil).

OTU differences, there were no significant unweighted OTU differences between strains, further suggesting the importance of strain in structuring OTU abundances—rather than OTU presence/absence.

As suggested by the two-tier model (Bulgarelli et al., 2013), our results demonstrate a decrease in abundance of *Acidobacteria* and an increase of *Proteobacteria* and *Actinobacteria* relative to the rhizosphere and bulk soil (Fig. 4). Furthermore, the most significant OTU abundance difference between sample types was the decrease in *Acidobacteria* from the order iii1-15 in endorhiza samples (Bonferroni-corrected ANOVA: $p = 1.12e-7$). Of the 51 OTUs significantly differentiating between sample types, the 17 OTUs which increased in abundance within the *Cannabis* endorhiza relative to rhizosphere were predominantly *Proteobacteria*, including several from the *Rhizobiales* order. Mean abundance of the 51 OTUs were highly correlated between bulk soil and rhizosphere samples (Pearson's rho: 0.92), versus a lower correlation between rhizosphere and *Cannabis* endorhiza (Pearson's rho: 0.63), and even lower between bulk soil and *Cannabis* endorhiza (Pearson's rho: 0.42).

Significant OTU abundance differences between strains were composed mostly of differences in *Proteobacteria*, notably *Pseudomonadales*, *Burkholderiales*, *Sphingomonadales*,

	Weighted	Unweighted
Soil Type	690	657
Sample Type	51	11
Strain	71	0

Results of both unweighted (g-test) and weighted (ANOVA) analyses using FDR multiple test correction.
doi:10.1371/journal.pone.0099641.t002

and *Rhizobiales*. Apart from *Proteobacteria*, *Bacteroidetes* orders *Sphingobacteriales* and *Flavobacteriales* were also responsible for several significant OTU differences between *Cannabis* strains. Intriguingly, one of the significant OTUs between strains was the prevalence of *Sphingomonas wittichii* in the Maui Wowie strain, which in some contexts can metabolize phenazine-1-carboxylic acid and has been implicated in increased survival in soil environments.

Bulk soil and rhizosphere microbiomes are more similar to each other than to endorhiza microbiomes. Beta distances between rhizosphere and bulk soil communities were significantly lower than distances between rhizosphere and endorhiza communities for both unweighted and weighted analyses (unweighted: t=4.59, p¡0.001 weighted: t=11.82, p¡0.001). Beta distances between rhizosphere and bulk soil communities were significantly lower than distances between bulk soil and endorhiza communities for both unweighted and weighted analyses (unweighted: t=5.15, p¡0.001; weighted: t=11.56, p¡0.001). Beta distances between rhizosphere and endorhiza communities were not significantly different from distances between bulk soil and endorhiza communities for both unweighted and weighted analyses (unweighted: t=2.10, p=0.109; weighted: t=2.23, p=0.078).

Endorhiza share more OTUs with the soil they are grown in than with another soil in which the same strain is grown. Previously, a two-step process of root colonization, first fueled by rhizodeposition and followed by fine-tuning by host genotype has been posited (Garbeva et al., 2004; Berg & Smalla, 2009; Bulgarelli et al., 2012). This two-step selection model was tested by pooling samples by *Cannabis* strain and analyzing the core microbiome within each strain. As bulk soils are the putative source of microbes for the plant, endorhiza communities would be expected to share more OTUs with their own soil than with another.

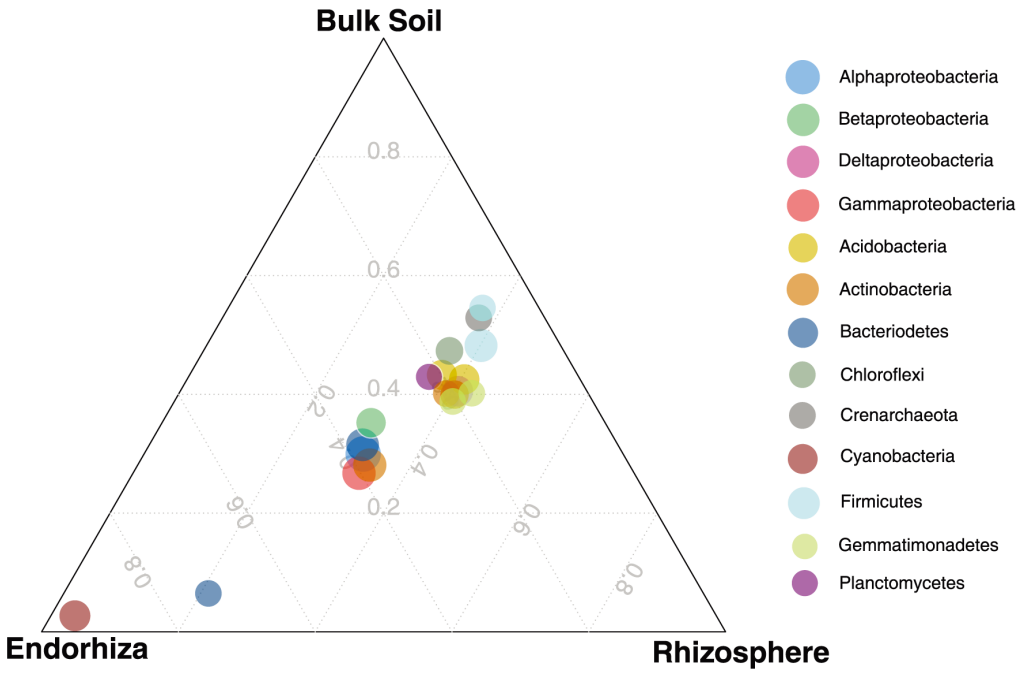

Figure 23: Ternary plot of distribution of bacterial taxonomic groups among sample types in the second experiment. Size of circles proportional to the log of the total abundance, taxonomic groups are all phylum-level, except for Proteobacteria, which is by class.

White Widow was grown in two different soils, and roots shared more OTUs with the soil they were grown in than with the different soil in which the different white widow plant was grown. The number of shared OTUs between endorhiza and their own soil (n=45, mean =2934) was significantly greater (t=10.05, p=1.209e-15) than the number of shared OTUs between endorhiza and the other soil (n=45, mean =2162).

Cannabinoid concentration and composition was significantly correlated to structure of endorhiza communities. Each plant in the second experiment was tested for a variety of cannabinoids, including delta-9-tetrahydrocannibinol. Cannabinoid data associated with the plants was used in Mantel tests to understand the potential biochemical associations with community composition or structure; with significant differences between strains (unweighted; r-stat: 0.863, p-value =0.001). However, due to higher THC composition and concentration in plants from one of the soil types, THC variables were also significantly correlated to the soil edaphic variables, and as such any association between microbiota and THC is very hard to disassociate from soil physicochemical variables.

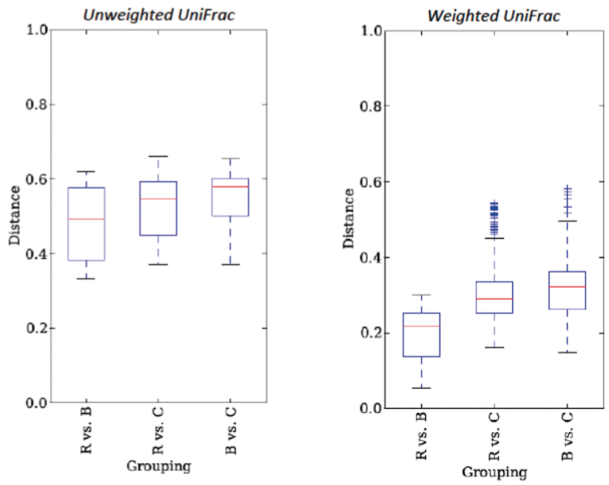

Figure 24: Box plots of beta-diversity distances between communities for both weighted and unweighted analyses. Initials (i.e. B vs. C) stand for comparisons of beta-distances for samples within groups (R = rhizosphere, C = Cannabis endorhiza, B = bulk soil).

Edaphic factors were strongly linked to structure of microbial communities in rhizosphere and endorhiza communities. In both experiments, edaphic data associated with the plants was used in Mantel tests to understand the effect of edaphic factors on structuring bulk soil, rhizosphere, and *Cannabis* endorhiza communities. For all experiments, the soil texture was defined as a sandy loam, with significant differences in clay and other edaphic factors (Table 2) between the two soil types in the second experiment, and the soil types used in the first experiment. For both weighted and unweighted UniFrac distances (all samples pooled in the analysis), all edaphic factors tested were significantly correlated with community beta-diversity (p=0.001). For the weighted analysis, Nitrogen had the strongest effect in structuring the communities (r-stat: 0.465, p-value =0.001), followed by salinity (r-stat: 0.437, p-value =0.001), Carbon (r-stat: 0.330, p-value =0.001), water content (r-stat: 0.281, p-value =0.001), and pH (r-stat: 0.221, p-value =0.001). For the unweighted analysis, the relative importance of the edaphic factors remained the same, with Nitrogen as the most important (r-stat: 0.630, p-value =0.001), followed by salinity (r-stat: 0.620, p-value =0.001), Carbon (r-stat: 0.512, p-value =0.001), water content (r-stat: 0.466, p-value =0.001), and pH (r-stat: 0.292, p-value =0.001). Running a BEST analysis, the variance in community data is optimally explained by three edaphic factors; Nitrogen, Carbon, & Water (rho=0.632).

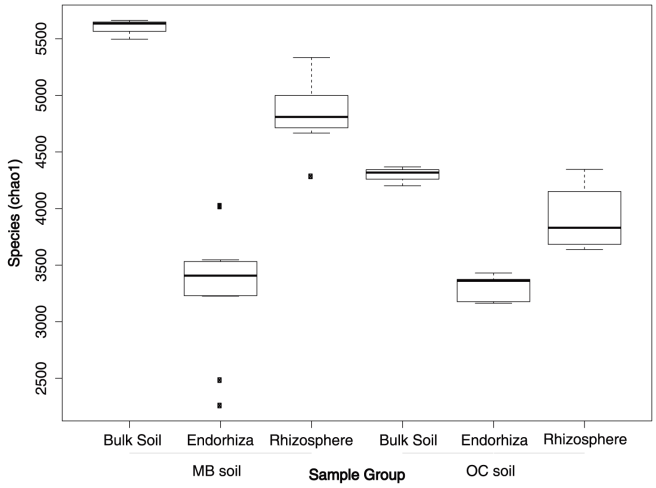

Figure 25: Box plots of alpha diversity (observed species) for endorhiza, rhizosphere, and bulk soil from two separate soil types in the second eperiment. MB = Mo-Bio soil, OC = Orange County soil. Note the significant differences between alpha diversity in the bulk soil and rhizosphere but negligible differences between endorhiza alpha diversity between soil types.

Alpha diversity peaks in bulk soil and declines with the transitions into the rhizosphere and endorhiza microbiomes. Observed species and chao1 alpha-diversity metrics from the second experiment demonstrated a slight reduction in alpha diversity from bulk soil (chao1: $\mu = 4947; \sigma = 717$) to rhizosphere samples (chao1: $\mu = 4525; \sigma = 542$), followed by a dramatic reduction in alpha diversity from rhizosphere to endorhiza (chao1: $\mu = 3321; \sigma = 420$). Although diversity was significantly higher in MB bulk soil (chao1: $\mu = 5597; \sigma = 89$) and rhizosphere (chao1: $\mu = 4859; \sigma = 286$) in comparison to OC bulk soil (chao1: $\mu = 4296; \sigma = 85$) and rhizosphere (chao1: $\mu = 3913; \sigma = 290$), diversity of MB endophytes (chao1: $\mu = 3325; \sigma = 517$) was not significantly different from that of the OC endosphere (chao1: $\mu = 3311; \sigma = 112$). Despite much shallower sequencing in the first experiment, the same pattern was recovered, with both species richness and chao1 diversity index highest in bulk soil (chao1: $\mu = 2010.7, \sigma = 146.2$), slightly lower in the rhizosphere (chao1: $\mu = 1837.2, \sigma = 114.0$), and lowest in the endorhiza (chao1: $\mu = 916.1, \sigma = 161.7$).

Curiously, when samples from both experiments were pooled and rarified to the level of the first experiment, alpha diversity of the endosphere from the first experiment was greatly reduced (chao1: $\mu = 916.1, \sigma = 161.7$) in comparison to the endospheres grown in MB

soil (chao1: $\mu = 1413, \sigma = 280.1$) and OC soil (chao1: $\mu = 1374, \sigma = 64.4$). Although this might be explained by decreased diversity in the MB soil from the first experiment (MB1), comparisons of diversity between rarified samples demonstrate MB1 bulk soil had intermediate diversity (chao1: $\mu = 2010.7, \sigma = 146.2$) relative to the MB bulk soil (chao1: $\mu = 2319.1, \sigma = 124.3$) and the OC bulk soil (chao1: $\mu = 2004.8, \sigma = 118.6$). This reduction in alpha diversity in the endosphere from the first experiment is consistent with the early stages of root decay following the harvesting of the plant.

Composition of endorhiza communities in the first experiment suggest potential root decay. After analysis of the data from the first experiment yielded high abundances (greater than 10% of taxonomy assigned reads) of the known cellulytic bacterium *Cellvibrio*, we sought to investigate the possibility that *Cellvibrio* was an indication of root decay rather than its unexpected presence as a member of the endophytic core community. This was of particular interest because the samples were taken 8 weeks post-harvest. Comparisons of relative abundances of *Cellvibrio* between the first and second experiments yielded rather convincing results demonstrating the early stages of root decay despite significant cultivar-specificity within the samples. Specifically, the relative abundance of *Cellvibrio* within the endosphere of the first experiment was 16.9% ($\sigma = 13.0\%, N = 9$) versus 0.095% ($\sigma = 2.7\%, N = 18$) in the endosphere of the second experiment.

Discussion

Recent literature has suggested a two-step selection model for the endorhiza, where bulk-soil microbial communities are filtered by increased concentration of rhizodeposits, followed by convergent host genotype-dependent selection on endophytic communities (Garbeva et al., 2004; Berg & Smalla, 2009; Bulgarelli et al., 2012). Results from both experiments support many of the expectations produced by this model. Most importantly, the principal coordinate analysis (PCoA) plots for the second experiment demonstrate highly significant clustering patterns. First, soil type is the main determinant of PC1 (32.06%) for the unweighted anal-

ysis of the second experiment, revealing that soil is undoubtedly the most important factor in all samples for determining what microbes are present. Second, communities within both soil types demonstrate a similar community shift from bulk soil to endorhiza samples along PC2 (11.34%), which is dominated by differentiation between sample types. Specifically, endorhiza samples have high, positive values along PC2, rhizosphere samples have intermediate values, and bulk soil samples have more negative values. Third, *Cannabis* strain is the main determinant of PC1 (34.51%) for the weighted analysis of all samples in the second experiment, suggesting that convergent host genotype-dependent selection acts through controlling community structure (abundance) more than composition. PCoA results exhibit how all sample types form significantly differentiated clusters in weighted analyses but that only rhizosphere and endorhiza samples form significantly differentiated clusters in unweighted analyses, suggesting niche-filtering of microbes in rhizosphere and endorhiza samples from bulk soil. Furthermore, there were no significant segregating OTUs based on unweighted analysis between cultivars in endorhiza and rhizosphere samples in the second experiment, however there were 71 when abundance was accounted for. This differs greatly from the 657 OTUs that significantly differ between soil types in the same dataset. Testing of the two-step selection model with pairwise comparisons of shared OTUs between endorhiza and bulk soil samples also validated the hypothesis that a portion of the endophytic microbes are inherited and selected from the surrounding soil, showing significantly more OTU overlap between endorhiza and their own bulk soil compared to endorhiza and foreign bulk soil.

Given the results from the second experiment strongly suggesting that *Cannabis* cultivars have important structuring effects on both rhizosphere and endorhiza samples, it may seem troubling that results from the first experiment do not suggest this for the rhizosphere samples. However, differences in *Cellvibrio* abundance between experiments show that root decay could have diminished the rhizosphere effect, thus diminishing this potential signal. Sampling for the first experiment was done post-harvest, when plant tissues were undergoing senescence and decay, while samples for the second experiment were taken from actively

growing plants. Considering the extensive work demonstrating the importance of plant growth stage on the microbiota (van Overbeek & ven Elsas, 2008; Duineveld et al., 1998), as well as the plant-soil feedbacks identified in structuring belowground microbial communities (Bezemer et al., 2006; Bonanomi et al., 2005), the differences between the first and second experiments are unsurprising. The similarities, however, are surprising. In particular, that cultivar-specificity could be identified in the microbiota within the endorhiza samples in the first experiment without any input of cultivar-specific metabolites from the living plant for weeks.

Although we have presented several highly significant findings supporting expectations of the two-step selection model, some expectations remain to be validated. Specifically, although the mean beta-diversity distances indicate that rhizosphere and endorhiza samples are closer than bulk soil and endorhiza samples, this difference was not significant and thus provides little evidence for the first differentiation step of the two-step selection model (Garbeva et al., 2004; Berg & Smalla, 2009; Bulgarelli et al., 2012).

Future work with the *Cannabis* microbiome should focus on elucidating the role of cultivar on rhizosphere, as well as what aspects of host genotype are producing the structure observed across *Cannabis* strains. Increased testing of cannabinoids and decoupling this variation from edaphic factors will improve our understanding of the importance of cannabinoid production in structuring endorhiza communities. Sampling a time series of endorhiza communities across several plants may help us to understand natural variation in the endorhiza during the reproductive cycles of *Cannabis*. Understanding this natural variation will help direct future mechanistic studies aimed at using microbial communities to increase plant fitness, suppress disease, or augment desired metabolite production.

13 Appendix B: Unpaved roads alter foraging patterns of the leafcutter ant *Atta colombica*

Abstract

Leaf cutting ants are dominant herbivores and influential ecosystem engineers in the Neotropics. It has been suggested that habitat disturbances alter the architecture of foraging trail systems for colonies in their vicinity; however, the evidence remains scarce. In this study we investigated the effect of unpaved roads dissecting tropical lowland forest habitat on the structure of leafcutter foraging trail systems and foraging effort. We mapped trail systems for 16 mature *Atta colombica* colonies located at different distances from unpaved roads. Our results suggest exploitation of unpaved roads by leafcutters provides favorable foraging conditions, causing significant differences in foraging trail structure.

Introduction

Leafcutter ants are dominant herbivores of the Neotropics, responsible for the consumption of 12% of annual leaf-area production (Herz et al. 2007a). Harvested material can represent a significant 10% of the total forest canopy foliage in the foraging area (Wirth et al. 2003). They are also influential ecosystem engineers, concentrating nutrients in the otherwise poor soil of the Neotropics (Fonte & Schowalter 2005; Sternberg et al. 2007; Hudson et al. 2009; Silva et al. 2013), with demonstrated preference for plants with high concentrations of nitrogen and phosphorous supplemented with manganese and aluminum (Berish 1986).

Leaf-cutting ant nests are built underground with a surface area between 50 and 160 m^2, yet their fora- ging area can reach hundreds of meters away from the nests (Farji-Brener & Silva 1996; Wirth et al. 2003). Foraging trails cleared and maintained by the leafcutter majors are prevalent in Neotropical rain forests, and increase the efficiency of resource transport across large distances (Rockwood & Hubbell 1987; Kost et al. 2005; Farji-Brener et al. 2007). A single, large leafcutter colony is capable of gathering hundreds

of kilograms of biomass in a year (Herz et al. 2007a), and is discriminative in the species of plants it chooses to harvest (Rockwood 1976; Berish 1986; Rockwood & Hubbell 1987; Howard 1988; Farji-Brener 2001). Different colonies of the same *Atta* species have been shown to consistently attack the same plant species if available, as well as to forage for certain species according to seasonal preferences (Rockwood 1976). Howard (1988) found that the strength of leafcutter preference for nutrients depends on their availability, increasing as nutrient supply decreases.

Human interactions with leafcutters are frequent, and human development has a variety of important influences on the Neotropical herbivores. Primarily, leafcutters are prevalent in successional forests (Wirth et al. 2007; Silva et al. 2009; Dohm et al. 2011), which directly result from the expansion of human infrastructure (Chazdon 2003; Laurance et al. 2009;Dohm et al. 2011). Leafcutter prevalence in these habitats is likely due to their foraging decisions, which tend to target leaves with high nutrient content and the low level of chemical defenses that are common in successional forests (Shepherd 1985; Farji-Brener 2001). Empirical evidence has supported this concept, as evaluation of diet composition showed pioneer species were harvested three times more than shade-tolerant species, and field assays demonstrated leaves from pioneer species were selected eight times more frequently than shade-tolerant species (Farji-Brener 2001). Furthermore, higher nest density in anthropogenically disturbed areas has been shown to be partly the result of increased colonization effort in the disturbed regions (Vasconcelos 1990;Wirth et al. 2003, 2007).

It has been suggested that disturbed habitat significantly alters the foraging trail structure for nearby colonies (Vasconcelos et al. 2006). In light of research that has estimated trail maintenance as 75% of the total energetic costs of the colony (Lugo et al. 1973), and other work that has shown leafcutters respond to specific environmental conditions to optimize perfor- mance (Lewis et al. 2008; Farji-Brener et al. 2014), it is possible that leafcutter foraging in disturbed habitat differs from that in undisturbed, old growth forest. Conversely, estimation of foraging costs by Howard (2001) suggests the costs of trail maintenance to be

minimal relative to the number of available workers and the rates of mass harvest. Understanding how foraging trail structure is impacted by habitat disturbance is important as it demonstrates the spatial interactions between the colony and the environment (Vasconcelos et al. 2006), where leafcutters play a large role as both an ecosystem engineer (Fonte & Schowalter 2005) and an agricultural pest (Cherrett 1986; Leal et al. 2014).

To investigate the impact of unpaved roads on leafcutter foraging behavior, this study mapped the foraging trails of 16 mature *Atta colombica* colonies that were at varying distance to the roads intersecting otherwise undisturbed habitat. To evaluate the potential impact of this human disturbance, measured variation in foraging trail structure has been plotted against distance from human roads and correlations between relevant parameters have been explored. Due to the preference of leafcutters for disturbed habitat and the community composition of successional forests, we predict significant changes in foraging trail structure near unpaved roads.

Materials and methods

Study sites

The study was conducted at two sites in the lowland moist evergreen forests of Soberania National Park in Central Panama. Both sites were in protected, old secondary forests dissected by unpaved single-track roads with very infrequent traffic. One site was located along Pipeline Road in Gamboa [$9°10'N, 79°45'W$], a gravel road used mostly for birding and access to research sites. The canopy above is mostly open, allowing for high light conditions. The second site, located 11—13 km southeast of Gamboa [$9°05'N, 79°40'W$], was the forest along Plantation Road, a dirt road mostly covered with tree canopy, and currently used mostly for outdoor recreation such as mountain biking and hiking.

For this study, we located 16 mature colonies of the leafcutter ant species *Atta colombica* at various distances from the roads, nine in the Pipeline Road area and seven in the Plantation Road area. *Atta colombica* is the dominant leafcutter ant species occurring within

closed forest in the area. We mapped their foraging trail systems in July—August 2007 to evaluate whether the roads influenced them.

To locate the nests, we surveyed the roads as well as transects at varying distances [50, 100, 150, 200, and 250 m] parallel to the roads for foraging trails, and followed them back to the nests. Leafcutter nest density in the study sites was low, so that interactions between nests did not have an effect on the shape of the foraging area. We included only mature colonies in this study, because immature colonies do not have well-developed trail systems. We used the refuse deposition rate (RDR), which is diurnally constant and highly correlated with daily herbivory rates in Atta colombica colonies (Herz et al. 2007b) to assess maturity of the colonies. Ants carrying a refuse particle leaving the nest on the trail to the dump site were counted for 5 min and only colonies with deposition rates of > 20 refuse particles/min (that corresponds to about 40,000 plant fragments harvested/day) were included in the study.

Mapping ant trails and foraging sources

The distance of each nest center to the closest point on a nearby road (d_{road}) was measured with transect tape. The area within a 510 m perimeter around the nests was searched to locate all radiating foraging trails, including subterranean trails that surface within a few meters of the nest (Burd & Howard 2005). Leafcutter ant trails can take many forms—the typical barren paths cleared from leaf litter by the ants, but also preexisting linear and smooth structures such as fallen logs and branches, lianas and roads. In this study we considered trails any line travelled by more than five ants within 5 min. We mapped the foraging trails as a series of vector segments. Vector directions (θ) and lengths (d_{vector}) were measured with a transect tape starting from the nest out to their termination points at either ground or arboreal foraging sources. A new vector was recorded when change of direction was more than 10 degrees for a distance of more than 0.5 m, as well as at trail junctions, to best approxi- mate the continuous trails.

Analysis

We transferred the vector array of measured foraging trail segments into maps of the foraging network (program written in Java SE 6) and added additional features such as roads, foraging sources, refuse dumps, magnetic north, and relative scale. All foraging sources were plotted on Cartesian coordinates relative to the nest at the origin (in Visual Basic). The mean distance to all the foraging sources ($\bar{d}_{foraging}$) was calculated for each colony using the shortest distance (direct line) between each source and the nest. The total length of foraging trails of each colony was calculated by summing the length of all its foraging trails, and the foraging area of each colony was approximated using a minimum convex polygon (MCP) method for the observed foraging sources. To assess the shape of the foraging area, we calculated the ellipticity of the distribution of foraging sources for each colony, i.e. the ratio of the longest primary axis to the perpendicular secondary axis.

Ellipticity

Ellipticity is defined as the variance (length) of the primary axis (σ^2_{PC1}) found by principal components analysis (PCA) divided by the variance (length) of the secondary axis found by PCA (σ^2_{PC2}). To calculatethe ellipticity of the distribution of foraging sources for each of the individual colonies, PCA was applied to the foraging source plots to define the desired variables (PC1, PC2, σ^2_{PC1}, σ^2_{PC2}). It should be noted,from the definition of PCA, it is always the case that $\sigma^2_{PC1} > \sigma^2_{PC2}$, and that both σ^2_{PC1} & σ^2_{PC2} are non-zero. Thus, an ellipticity value of one indicates a circular shape ($\sigma^2_{PC1} \approx \sigma^2_{PC1}$) and larger values indicate increasingly elongated shapes. The PCA was done in R using the prcomp command in the stats package (Venables & Ripley 2002).

Significance

We examined how the variables (refuse deposition rate, distance to road, total trail length, foraging area, and ellipticity of the foraging area) relate to each other after testing their

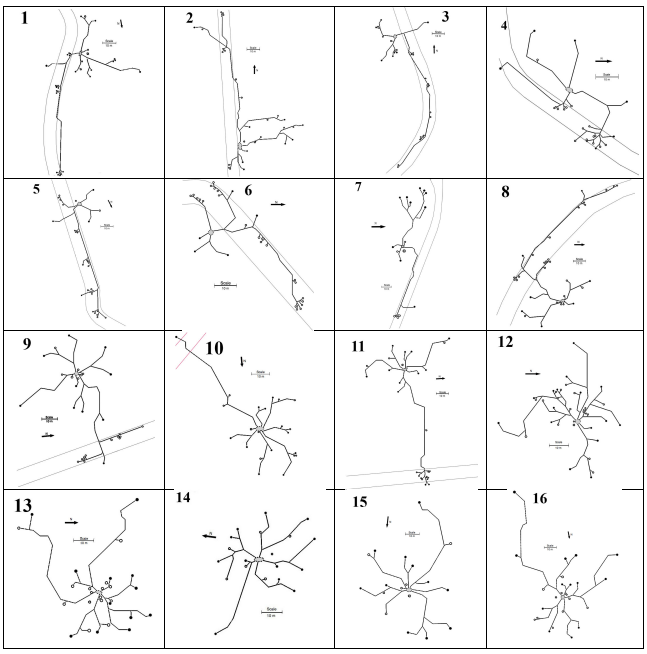

Figure 1

Figure 26: Foraging trail maps of the studied colonies of *Atta colombica* in Panama. Eight out of 16 maps are arranged in order of increasing distance of the nest from the road. The nest region is represented by gray ovals at the nexus of all the foraging trails, circles represent foraging sources, arrows represent directional north, all scale bars are 10m, and roads are based on approximate measurements.

normal distribution with a ShapiroWilk normality test (R *stats* package). For normally distributed data we used Pearsons product-moment correlations, and for non-normally distributed data we used the Spearman-Rank Rho Test (R *stats* package). Multiple test correction was employed on the 15 pairwise comparisons of the six measured variables, resulting in a Bonferroni- corrected significance value ($\alpha_{BF} = 0.0033$) instead of the standard non-corrected significance value ($\alpha = 0.05$).

Results

Colonies near unpaved roads frequently had foraging trails on the roads and there was no indication that roads acted as barriers (Figure 1). The ellipticity of foraging source distribution of the nest decreased sig- nificantly with distance from a road (Spearmans rank correlation rho test: $\rho = 0.71, p = 0.003$), i.e. far from roads foraging effort had near-circular distribu- tions, whereas colonies located near roads tended to have elongated foraging effort (Figure 2A, Table 1).

The mean distance to the foraging sites significantly increased with ellipticity of the

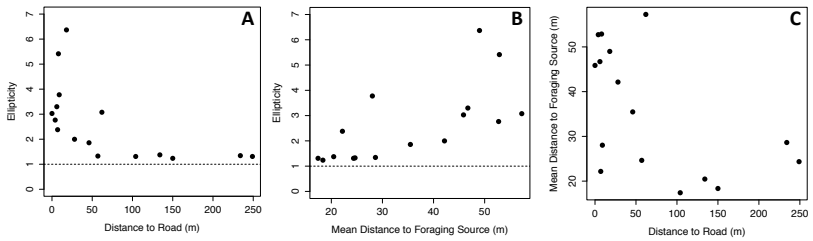

Figure 27: Relations between foraging patterns and distance of nests of *Atta colombica* to the nearest road. Relationships between A, distance to road and the ellipticity of the foraging area; B, ellipticity and the mean distance to the foraging sources; and C, distance to road and the mean distance to the foraging sources. The dotted line represents the theoretical lower limit of ellipticity ($\sigma^2_{PC1}/\sigma^2_{PC2} = 1$).

foraging source distributions ($\rho = 0.78, p = 0.0007$, Figure 2B), indicating that colonies with higher ellipticity traveled farther to reach their foraging sources. Although the mean distance to the foraging sites was not significantly associated with distance to the road after Bonferroni-correction ($\rho = 0.53, p < 0.04$, Figure 2C), there was a strong negative correlation between these variables.

As expected, the foraging area significantly increased with RDR, a proxy for harvesting rate (Pearsons product-moment correlation: $cor = 0.72, p = 0.0016$), meaning that larger colonies had a greater foraging effort. Another measure of foraging effort, the total length of the foraging trails, showed strong correlation with RDR ($cor = 0.62, p = 0.011$), but was not significant under Bonferroni correction. An expected significant correlation was found between mean distance to the foraging sites and the RDR of the colonies ($cor = 0.7344, p = 0.001$), meaning larger colonies travelled farther to their sources than smaller ones. Furthermore, there did seem to be a potential relationship between foraging area and mean distance to the foraging sites given the correla- tion ($cor = 0.494, p = 0.052$), although not significant (Figure 3).

As anticipated, trail length and foraging area were highly correlated ($cor = 0.854, p = 0.00003$) since larger foraging areas contain longer trail systems. However, neither total trail length of the colonies nor their foraging area were significantly associated with ellipticity ($\rho = 0.209, p = 0.436; \rho = 0.062, p = 0.822$, respectively), or distance from the road ($\rho = 0.109, p = 0.689; \rho = 0.05, p = 0.857$, respectively). Additionally, total trail

length of the colonies demonstrated no relationship with mean distance to the foraging sites ($cor = 0.246, p = 0.358$). Lastly, RDR was not significantly correlated with distance from the road ($\rho = 0.171, p = 0.527$) or ellipticity ($\rho = 0.274, p = 0.304$). These correlations indicate that distance from the road and the shape of the foraging territory—as measured by ellipticity—were independent from both measures of foraging effort (total trail length and foraging area) of the colonies, as well as colony size (RDR).

Discussion

The results of this study show that unpaved roads in forests increase the mean distance to foraging sources and alter the distribution of foraging sources in nearby colonies of the leafcutter ant *Atta colombica*. Minimizing colony-level energetic costs usually leads to roughly circular foraging areas (Covich 1976), and this study supports this finding, but only in the undisturbed forest interior. Reduction of energetic costs through the utilization of linear clearings vastly changes the shape of leafcutter foraging trail networks. Through using the roads for their trails, the ants may avoid the considerable costs associated with trail clearing and maintenance, and thus be able to travel further. Far-reaching trails along roads may further facilitate leafcutter ant colony development by allowing access to specific compounds and elements required in their diet (Berish 1986; Howard 1988; Silva et al. 2013) as well as a diverse diet (Shepherd 1985; Rockwood & Hubbell 1987; Traniello 1989), while avoiding the high costs of clearing and maintaining a long foraging trail. These results suggest that man-made roads may be beneficial for leafcutters by facilitating access to preferred plant species.

Preference for pioneer species occurring in the disturbed areas along the roads may also have additionally contributed to the observed prevalence of foraging trails near roads in our study. Recent work by Silva et al. (2013) demonstrating the adjustment of leafcutter foraging trail networks to pioneer plant ability supports this hypothesis; however, we do not have explicit plant composition data from the roads in our study to quantitatively test this

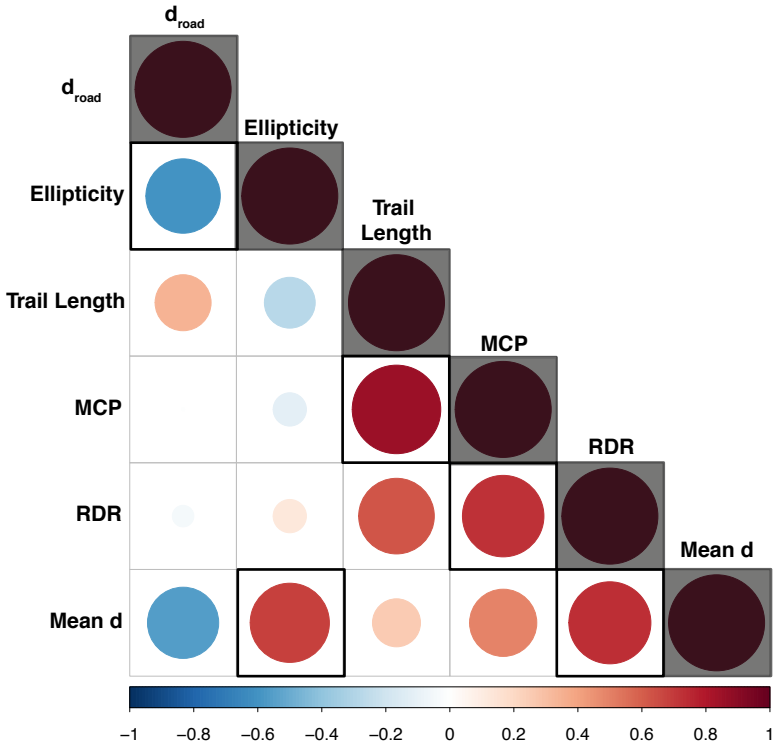

Figure 28: Correlogram of six measured variables in the study. Shade of circle (correlation coefficient, horizontal lines indicate negative relationship) and circle size (significance) describe the relationship between the six measured variables in the study: 1, distance of nest to road (d_{road}); 2, ellipticity; 3, total length of all trails (trail length); 4, foraging area of the colony as measured by minimum-area convex polygon (MCP); 5, refuse deposition rate (RDR); and 6, mean distance to a foraging source (Mean d). Larger circles indicate more significant relationships, and all boxes with a bold border represent significant relationships under the Bonferroni-corrected significance value ($\alpha_{BF} = 0.0033$). Relationships of a variable with itself have been shaded for clarity.

hypothesis. It has been proposed that severe levels of human disturbance are detrimental to leafcutter ants, in that complete transformation of old growth habitat to monocultured agroecosystems limit available nutrients and plant species (Folgarait 1998). Considering that leafcutters may require a diverse diet of plants for fungal growth if preferred species are not present (Shepherd 1985), it is likely that human disturbance could impede this need by reducing ecological diversity. However, while many of the possible impacts of road-building and the expansion of human infrastructure on leafcutters remain unclear, the observed high prevalence of leafcutter ants in and close to disturbed areas suggest that positive effects outweigh the negative effects as long as the intensity of disturbance is intermediate (Vasconcelos et al. 2006; Silva et al. 2009).

For leafcutter ants, trail building and maintenanceare a major energy cost for resource acquisition (Lugo et al. 1973; Lewis et al. 2008; Farji-Brener et al. 2014). The energy invested into resource acquisition is gener- ally balanced against the nutrient value of a resource (optimal diet theory; Rockwood & Hubbell 1987), and thus the trade-off between trail-building costs and resource nutritional value has been hypothesized to partially govern foraging in leafcutter ants (Shepherd 1985; Rockwood & Hubbell 1987). In roadside foraging areas, this trade-off changes, as the costs of trail maintenance are lowered without decreasing the nutritive value of the resource. Reduced costs per foraging distance through the use of roads allow an increase of the mean foraging distance, thus potentially resulting in access to more plants. Simultaneously, roads improve the accessibility to plants directly adjacent, and the elongated shape of the foraging areas along the roads are consistent with hypotheses stating that ants will maximize the resource intake by focusing on the most accessible and nutrient-rich resources (Traniello 1989; Silva et al. 2013). Although the importance of this trade-off to foraging behavior has been questioned on the basis that costs of trail maintenance are not significant enough to constrain foraging trail structure (Howard 2001), results from this study and other described leafcutter behavior (Farji-Brener et al. 2007, 2014) imply that avoiding the costs of trail maintenance is preferable. Specifically, fallen branches, logs,

and exposed roots have been shown to facilitate leaf transport by increasing transport speed, and have been suggested as components of the physical environment that could direct the leafcutters searching effort (Farji-Brener et al. 2007). Our results suggest that roads may have similar effects, but at a far larger scale.

The construction of roads leads to the creation of edge habitats, and the majority of generalist herbivores tend to increase in abundance with edge creation (Wirth et al. 2008). Leafcutter herbivory is no exception to this trend; in a study in Brazil equally sized *Atta* colonies located at the forest edge removed twice as much leaf area from their smaller foraging area than interior colonies (Urbas et al. 2007). The results of this study provide a mechanism for increased edge herbivory, as utilization of human roads in lowland Neotropical forests by *Atta colombica* offers high-quality resources at lower costs than foraging in the forest interior. High consumption rates of leaf-tissue by leafcutter ants—measured at 266 kg biomass/colony/year (median) in late-successional tropical moist forest (Herz et al. 2007b)—suggest that increases of leafcutter herbivory at the forest edge is ecologically significant. It is possible that altered foraging patterns such as increased foraging distance could increase herbivory along roads in forest edge ecosystems, which in turn could strongly influence the demography of their preferred plant species (Vasconcelos et al. 2006), potentially exacerbating negative ecological effects of the roads them- selves. Unpaved roads facilitate leafcutter ant foraging by lowering energetic costs of trail establishment and maintenance, and offering increased concentration of pioneer species, which are likely significant forces underlying the increased colonization and prevalence of leafcutter colonies in areas of human disturbance.

14 Appendix C: Supplementary Material

For all supplementary material, please refer to the supplementary online material (SOM) found on the Proquest ETD website. The organizations of the SOM is outlined below.

C1. Early and dynamic colonization of Central America drives speciation in Neotropical army ants

- **Fig. S1:** *De novo* locus assembly and quantitative modeling
- **Fig. S2:** Full phylogeny inferred from both ML and Bayesian methods with bootstrap support and BPP.
- **Fig. S3:** Tree-dating procedure using nonparametric rate smoothing (NPRS) and absolute calibration and verification using credible intervals from Brady et al. (2014).
- **Fig. S4:** Plots of parameter estimates from converged, independent Bayesian inference MCMC chains.
- **Fig. S5:** Genetic relationships between the Central American and South American army ant lineage pairs.
- **Fig. S6:** Maps of clade assignments and geographic ranges for each Neotropical army ant.
- **Appendix S1:** Supplementary information text with eight subsections (SI. 1-8), supplementary figure legends (Fig. S1-S6), and supplementary table legends. Includes **Table S1:** *In silico* digest results for ApeK1 on eight published ant genomes, and **Table S2:** Partitioning of genetic diversity between parapatric pairs of sister lineages.
- **Table S3:** Sample Information.

C2. Novel approach to heritability detection suggests robustness to paternal genotype in complex morphological trait

- **Supplementary Information:** All figures and supplementary information text for the second chapter.

C3. Colony-specific caste allometry in a top Neotropical predator

- **Supplementary Information:** All figures and supplementary information text for the third chapter.

C4. Emergence from subterranean environment shapes Neotropical army ant allometry

- **Fig. S1:** Map of sampling locations for all colonies.
- **Fig. S2:** Partial warp scores plotted against centroid size for all Neotropical army ant species.
- **Fig. S3:** Stochastic mapping results for ecological variables.
- **Table S1:** Collection information for all samples.